# Development of a comprehensive on-line multidimensional high performance column liquid chromatography system for protein and peptide mapping with integrated size selective sample fractionation

Dissertation

Zur Erlangung des Grades

„Doktor der Naturwissenschaften“

vorgelegt dem Fachbereich Chemie und Pharmazie

der Johannes Gutenberg-Universität Mainz

von

Knut Wagner

geboren am in Wiesbaden

September 2001

Every scientific advance is an advance in method.

M.S. Tswett

# Contents

# 1 General scope

All the information which is characterising the complexity and mystery of life is stored in molecules of deoxyribonucleic acid (DNA). Specific parts of the complete DNA sequence contain the genes that encode the structure of proteins as a master copy. The genetic code is translated into the amino acid sequence of the proteins [1].

Since the Human Genome Project (HGP) was started in 1988 by publicly funded researchers, an enormous amount of labour was spent to sequence the entire human genome with its three billion base pairs. In 1999 the US company Celera Genomics, Rockville, Maryland stepped in and was competing in finalising the human genome sequence using a different strategy. The public project adopted a clone-by-clone approach providing a high-resolution map of the entire genome while Celera used the whole genome shotgun approach. Now that the draft human genome sequence has been published, researchers are turning their attention to identifying the functions and expression patterns of the proteins encoded by the genes. Not only the genome is characteristic for an organism, but in particular the proteins present determine the appearance and state of a phenotype. The proteins are the basic cell constituents conducting the cell functions. It is generally believed that patterns of protein expression and its changes under the influence of biological perturbations will correlate with disease states. Understanding of disease mechanisms will potentially improve or even revolutionise human medicine and health care.

The research described in this thesis is a new approach to develop a separation platform for generating high resolution patterns of protein and peptide expressions.

# 2 Objectives

The objective of this work was to implement novel approaches and system components to significantly improve resolution, speed, repeatability and robustness for the analysis of proteins and peptides of a molecular weight smaller than 20 kDa.

The aim was to introduce a complementary method to 2D-polyacrylamide gel electrophoresis for protein separation based on multidimensional chromatographic techniques. The application of ultra-high-speed separations of biopolymers using n-octadecyl modified non-porous 1.5 µm silica beads was the starting point of developing an on-line system employing different separation speeds in either dimension. The employment of ion exchange chromatography as an orthogonal separation mechanism was considered.

The emphasis was on the construction and investigation of different on-line set-ups using conventional low void volume chromatographic equipment. Extensive employment of new column switching techniques was considered for fully unattended operation avoiding any off-line liquid handling. Highest resolving power and reproducible performance were required. Furthermore the options for on-line coupling to mass spectrometric detection methods were to be addressed.

The challenge was the high-resolution mapping of small sized proteins and peptides from human fetal fibroblast cell-line supernatant, from human hemofiltrate and other samples. Furthermore, the focus was on the evaluation of the potential of restricted access materials with anion- and cation exchange and reversed-phase functionality for size selective sample fractionation and sample enrichment. Finally, the performance of new developed silica based monolithic reversed-phase columns (Chromolith$^{TM}$) were to be compared to non-porous reversed-phase columns for the alternative use in the fast operating second dimension. The influence of column length, flow rate and gradient time were to be investigated and compared to the theoretical models.

# 3 Summary

A comprehensive on-line 2D-HPLC-system with integrated size selective sample fractionation was developed for the analysis of proteins and peptides with a molecular weight below 20 kDa which can not be separated by 2D-gel electrophoresis.

The main idea of the on-line coupled column system was the employment of different separation speeds in either dimension. Ion exchange chromatography was followed by ultra-high-speed reversed-phase (RP) separations using non-porous n-octadecyl modified 1.5 µm silica beads as an orthogonal chromatographic mode. The initial system, using two parallel RP-columns was improved with regard to higher resolution by implementing further parallel RP-columns to extend the gradient time.

The automated on-line system resolved approximately 1000 peaks within the total analysis time of 96 min and avoided sample losses by off-line sample handling. The low molecular weight target analytes were separated from the matrix using novel silica based restricted access materials (RAM) with ion exchange functionality. The size selective sample fractionation step was followed by anion- or cation exchange chromatography as the first dimension. The separation mechanism in the subsequent second dimension employed hydrophobic interactions using short reversed-phase columns. A new column switching technique including four parallel reversed-phase columns was developed and employed in the second dimension for on-line fractionation and separation. Gradient elution and UV-detection of two columns were performed simultaneously while loading the third and regenerating the fourth column. The total integrated workstation was operated in an unattended mode.

Selected peaks were collected and analysed off-line by MALDI-TOF mass spectrometry. The system was applied to protein mapping of biological samples of human hemofiltrate as well as of cell lysates originating from a human fetal fibroblast cell-line, demonstrating it to be a viable alternative to 2D-gel electrophoresis for mapping peptides and small proteins. The applicability for the isolation of target compounds from their by-products was also demonstrated. Validation parameters like repeatability,

linearity and limit of detection were determined proving the stability of the separation platform. Furthermore, the performance of monolithic silica based reversed-phase columns was compared to the performance of non-porous reversed-phase columns and optimum operational parameters like column length, gradient time and flow rate were investigated for the use in the 2D-HPLC system.

# 4 Introduction and theoretical background

## 4.1 Proteomics

The identification, characterisation and quantification of all the proteins expressed by a genome is known as proteomics. The word proteomics derives from the term proteome, a word that was coined by analogy with the term genome, by Marc Wilkins and Keith Williams of Macquarie University, Sydney, Australia in 1994 [2]. The term proteome was first discussed in print by Wasinger *et al.* [3] in 1995, who defined it as the 'total protein complement of a genome'. Similar definitions of the proteome, such as 'the set of proteins encoded by a genome', may frequently be found in the literature. However, all definitions which define the proteome as the protein readout of a genome are inadequate because the genome does not explicitly encode the full structure and diversity of the proteins present in an organism.

The proteome unlike the genome is not a fixed feature of an organism. Instead it changes with the state of development, the tissue or even the environmental conditions under which an organism finds itself. There are therefore many more proteins in a proteome than genes in a genome. This is because there can be various ways a gene is spliced in constructing mRNA and because there can be various ways that the same protein can be post-translationally altered. After the proteins were being synthesised in the ribosome, they undergo covalent modifications like phosphorylations and glycosylations. Finally one of the famous dogmas of biology the "one-gene-one-protein hypothesis" is no longer tenable. This has been recognised in other definitions of the proteome, like 'the protein complement of an organism', in which there is no suggestion of a simplistic linear relationship between an organism's deoxyribonucleic acid (DNA) and its protein profile. Anderson and Seilhamer [4] presented the first multi-gene comparison plot of mRNA versus protein abundances for cellular gene products and found a correlation coefficient of 0.48 between them.

Even though, the recent revelation that humans have only about 30,000 genes instead of 80,000 to 100,000 genes as previously estimated, the task of identifying all the proteins

expressed by genome is immensely more complex compared to DNA sequencing [5]. This is due to the fact that the protein building blocks are 20 amino acids plus a large group of modified amino acids instead of four nucleotides. Additionally, the number of proteins is higher than the number of genes. Furthermore, the proteins differ in concentration over five orders of magnitude, hence high abundant proteins can mask smaller ones [6]. Amplifications like in the nucleic acid world to boost the sensitivity for low abundant proteins are not possible.

Recently, the efforts in mapping the human proteome were focused by a group of top-level proteomics researchers launching a global Human Proteome Organisation (HUPO). The founders see it as a post-genomic analogue of the Human Genome Organisation (HUGO) and its mission will be to increase awareness of and support for large-scale protein mapping [7].

It is evident that proteins are central for the understanding of cellular function and disease processes and without putting effort in proteomics, the bargain of genomics will be unrealised. The focus of proteomics is upon the proteins present in biological systems, whether these systems are embodied within cell extracts, cell cultures, tissues or organisms. Contemporary proteomics is primarily concerned with the distribution of proteins, but there is an increasing emphasis on their functional organisation as well.

Proteomics involves the systematic mass analysis of proteins rather than a focus upon any particular molecule. However, the application of proteomics technique to a specific problem may focus our interest onto one or a handful of specific proteins. In addition to the mapping, identification and characterisation of proteins, proteomics also involves documentation – the organisation of information about protein profiles to create a functional resource for further research. Bioinformatics is one of the key challenges in proteomics.

Above all, what sets proteomics apart from earlier protein studies is its scale and systematic nature. Already in 1975 before modern DNA techniques like sequencing, cloning, recombinant techniques and polymerase chain reaction (PCR) were available, high resolution two-dimensional electrophoretic methods were published [8]. It seemed

to be evident that systematic application of this approach would be the only tractable approach for surveying biological complexity at the molecular level. At that time, the analysis of the proteins from a single biological sample would have involved an entire laboratory team in months of laborious research. Now the protein constituents of a sample can be analysed within days or weeks, by largely automated systems. As a result, biotechnology and pharmaceutical companies, as well as academic research institutions, have embarked proteomics approaches.

Cell regulations by proteins can be monitored by measuring the protein expressions. Over and under expressions of normal profiles will be indicators of a genetic error, faulty regulation, disease or a response to drugs. Proteins associated with specific disease states become targets for high-throughput screening large numbers of potential interacting drug compounds. The search for drug compounds like inhibitors for proteases, kinases and phosphatases as well as agonists/antagonists of growth factors, cytokines and receptors are the driving force for the pharmaceutical industry to spend huge investments and resources into the field of proteomics.

State of the art techniques in proteomics are 2D-gel electrophoresis and mass spectrometry. The qualification and quantification of protein expressions have been enabled by tremendous developments of mass spectroscopic techniques in the last decade.

## 4.2 2D-gel electrophoresis

2D-gel electrophoresis which was established by Klose, O'Farrell and Scheele [9] in 1975 is a core technology of proteomics because it is currently unrivalled in its capacity to separate individual protein constituents from a complex mixture.

The migration velocity *v* of a protein in an electrical field depends on the electrical field strength E, the net charge of the protein *z* and the friction coefficient *f* according to Equation 1.

$$v = \frac{Ez}{f} \qquad \text{(Equation 1)}$$

The electric force *Ez* accelerates the charged molecule to the contrary charged electrode whereas the friction force *fv* hinders the migration. The friction coefficient depends on the size and shape of the molecule and the viscosity of the medium. Gels which mostly consist of polyacrylamide avoid convection currents and improve the separation by dealing as a molecular sieve. Thus, the proteins in a sample are separated from one another according to the speed with which they diffuse through a gel under imposed diffusion gradients.

The separation is first carried out according to the surface charge of the proteins by placing the gel in a charge gradient (isoelectric focusing). The main technique used in modern proteomics is the immobilised pH gradient (IPG) gel [10]. IPG gels were created by incorporating immobilines into the gel matrix. This acrylamide derivatives have buffering properties but are immobilised within the gel. Their use prevents drift of the pH gradient and any gradient in the range of pH 2.5-12 can reproducibly be constructed.

In the second dimension, the proteins are separated in an orthogonal axis according to their molecular mass, usually by sodium dodecyl sulphate-polyacrylamide gel electrophoresis (SDS-PAGE). The protein mixture is dissolved in sodium dodecyl sulfate (SDS), a detergent destroying all non-covalent interactions in native proteins. For

reduction of disulfide bridging, dithiothreitol is added. The SDS binds to the main amino acid chain of the proteins forming a highly negative charged complex. The negative charge is proportional to the molecular weight of the proteins. Thus, migration in the electrical field is governed by the molecular weight of the proteins.

Theoretically, any given protein should migrate to the same point on a gel defined by its charge and mass. Until recently however, differences in the matrix properties and size of gels and differences in separation methodologies meant that the gels gave highly variable data. Standardisation of gel production has been a major advance in the emergence of proteomics, for the first time, proteins can be compared reliably between different samples, and they can be provisionally identified by comparison with the gel position of previously identified proteins.

### 4.2.1 Gel staining

Following the separation by electrophoresis, the proteins within the gels must be stained for subsequent analysis. Although some laboratories still extract proteins onto blots prior to staining, on-gel staining is becoming widespread in high-throughput proteomics. Besides radiolabelling the most used technique is silver staining followed by the less sensitive coomassie-blue staining. To resolve protein spots in which only low femtomolar quantities of protein are present, fluorescent dye approaches are essential.

### 4.2.2 Sample preparation for 2D-gel electrophoresis

Sample preparation is the first stage of proteomic analysis and vital to the success of subsequent steps. Proteins must be effectively disaggregated and solubilised without contaminating the sample or above all degrading or modifying its constituent polypeptides. This is a very challenging task, particularly with regard to membrane proteins.

Protocols for sample preparation vary between different laboratories and may be modified according to the chemical properties of the proteins being targeted and the particular electrophoretic technique to be used. Generally, however, they involve

thorough washing in a low-salt buffer, chemical and/or mechanical disruption to disaggregate and solubilise proteins, and to degrade other cellular components such as nucleic acids and lipids which can affect solubilisation and may affect electrophoresis. Chemical lysis buffers are the optimal means of degrading unwanted components and these also contain a range of additives to preserve the structural and ionic integrity of the polypeptides. Mechanical techniques include ultrasonication or rapid agitation in the presence of zirconium or glass microspheres.

High-speed centrifugation is used to eliminate any non-solubilised material and to concentrate the protein fraction. Effective centrifugation is particularly important in obtaining sufficient quantities of low copy number proteins.

Sample fractionation may also be carried out. It serves two purposes. Firstly, it divides up the frequently vast array of proteins present in a sample into more analytically resolvable subsets. Secondly, it supports crude functional analysis, particularly in eukaryotes where membranes, organelles, or water-soluble proteins may be segregated, or proteins may be selected on the basis of binding affinity to an extraction medium.

### 4.2.3 Limitations of contemporary 2D-gel electrophoresis

Despite of its advantages like unsurpassed separation power, information on isoelectric point and molecular weight and the possibility of running gels in parallel, limitations exist inherently associated with 2D-PAGE.

These are extensive sample handling, non-linear response factors for the most commonly used staining techniques, limited loading capacity, low extraction efficiencies of the gel embedded proteins and a decreasing resolving power for proteins with a molecular mass of less than 15 kDa due to their high mobility in the gel. Furthermore, it is difficult to isolate proteins with a pI at the acidic and basic extremes of the pH gradient, proteins with a molecular weight higher than 200 kDa or membrane-bound proteins and other hydrophobic proteins. In addition, the technique is time consuming, difficult to automate and there is no simple way for on-line coupling to mass spectrometric detection.

## 4.3 Mass spectrometry of proteins and peptides

Mass spectrometers use the difference in mass-to-charge ratio of ionised atoms or molecules to separate them from each other [11]. Molecules have distinctive fragmentation patterns that provide structural information to identify structural components. The general operation of a mass spectrometer is to create gas-phase ions, separate the ions in space or time based on their mass-to-charge ratio and measure the quantity of ions of each mass-to-charge ratio. In general, a mass spectrometer consists of an ion source, a mass selective analyser and an ion detector. However, the magnetic-sector quadrupole and time-of-flight (TOF) designs also require extraction and acceleration ion optics to transfer ions from the source region into the mass analyser.

Historically, ionisation in mass spectrometry (MS) was carried out using electron impact ionisation or chemical ionisation. Unfortunately, the high temperatures required to volatilise the molecules precluded the study of fragile biomolecules. The first attempt to develop biocompatible “soft” ionisation techniques started in the late 1960s, when field desorption was introduced [12]. However, the ionisation produced with this technique was restricted to molecules having a mass of a maximum of 2 kDa. Later, plasma desorption and fast atom bombardment [13] made it possible to routinely determine masses up to 10 kDa and 20 kDa, respectively. The low sensitivity and ion suppression effects of these techniques limited their practical use in protein characterisation.

The breakthrough for mass spectrometric analysis of biomolecules came in the late 1980s when intact proteins of several hundred kDa were successfully ionised by using electrospray ionisation (ESI) [14] and matrix-assisted laser desorption/ionisation (MALDI) [15, 16].

### 4.3.1 Ionisation and detection techniques

In contemporary proteomics there has been particular emphasis on electrospray ionisation (ESI) and on matrix-assisted laser desorption/ionisation (MALDI).

ESI involves ionisation of peptides at atmospheric pressure by nebulising a flowing stream of solvent under a potential difference of several thousand volts between the sample exit and the MS entrance. The technique which is usually coupled with triple quadrupole and ion trap detectors, can determine protein masses in excess of 150 kDa to an accuracy of 0.005 %. ESI has been further developed into nano-electrospray in which the miniaturisation of the electrospray source has increased the sensitivity to the low femtomolar range.

In MALDI, the peptide is embedded in a small organic compound consisting of aromatic acids (*e.g.* α-cyano-4-hydroxycinnamonic acid), the so called matrix. The matrix effectively absorbs the photon energy of the laser light pulse used in the ionisation technique, allowing desorption from the matrix and concurrent soft ionisation to take place. MALDI is most often used in conjunction with TOF mass spectrometers. A TOF mass spectrometer uses the differences in transit time through a drift region to separate ions of different masses. MALDI-TOF MS allows very sensitive and accurate measurements of protein and peptide masses up to and exceeding 500 kDa. A schematic illustration of a MALDI-TOF MS instrument (Voyager DE Pro, Applied Biosystems) is shown in Figure 4.1.

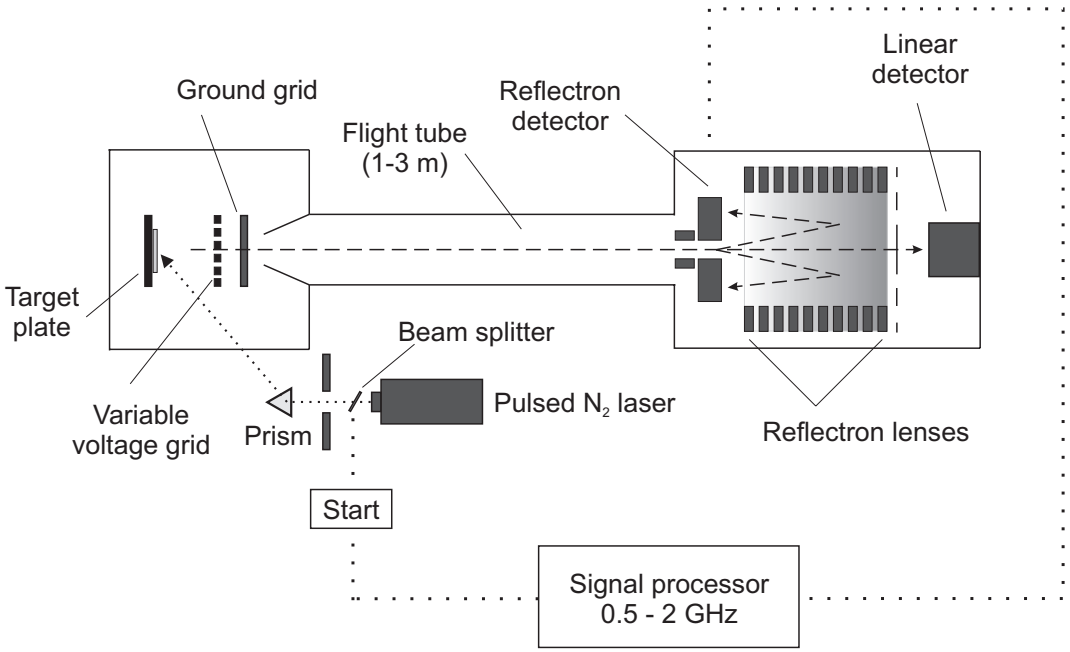


Figure 4.1 Illustration of a MALDI-TOF MS instrument

## 4.4 Antibody based techniques

Antibody based protein extraction can be deployed within affinity chromatography or immunoblotting, and if monoclonal antibodies are used to extract specific proteins, the technique is able to identify as well as to isolate specific proteins [17]. So far, antibody based techniques have played only a marginal role in proteomics because they are poorly suited to mass screening and have tended to focus on specific proteins.

## 4.5 Protein Chips

One of the most interesting and potentially important recent developments in proteomics has been the development of protein microarrays [18,19] analogous to the biochips that have been productive in functional genomics [20]. The microarray contains a matrix of specific molecules that will bind any protein within a biological sample that they match. A pattern recognition system surveys the array after exposure to the sample and reports which markers on the array have bound a protein. The new surface-enhanced laser desorption/ionisation (SELDI) protein chip technology permits integrated “on-chip” protein capture as well as protein structure and function evaluation through integration with technologies for mass-scale detection and characterisation of the proteins bound by the chip.

## 4.6 HPLC

High Performance Liquid Chromatography (HPLC) is an excellent technique for separating and analysing proteins and peptides.

The Italo-Russian botanist Tswett is considered to be the inventor of column liquid chromatography. In the early 1900´s he observed separate coloured bands when a liquid sample of colourful plant pigments were migrating by gravity through a glass column packed with calcium carbonate [21]. For that reason Tswett named the new separation technique chromatography, which is derived from Greek where *chroma* means “colour” and *graphy* means “to write”. In 1941, Martin and Synge [22] invented liquid-liquid partition chromatography, which became the starting signal for the renaissance of chromatography. They presented the first fundamental theory of chromatography occurring both in columnar and in planar format (paper chromatography).

The advent of smaller particle sizes in the mid 1960s allowed liquid chromatography to operate at higher pressures with subsequent shorter analysis time. The commercial availability of liquid chromatographic equipment, commonly referred to as high-performance or high-pressure liquid chromatography (HPLC), and the introduction of silica based bonded phase packings during the 1970s [23] facilitated the exponential growth of applications in this field [24]. Today, HPLC is one of the key technologies in the life science community. Its importance as a separation tool is manifested by the extensive use in the pharmaceutical industry for pharmacokinetics, drug monitoring, metabolism, and toxicological studies.

### 4.6.1 HPLC modes for separating biopolymers

Besides affinity chromatography four different modes of HPLC separations are frequently used for proteins and peptides [25]. These are size exclusion, ion exchange, reversed-phase, and hydrophobic interaction chromatography. Each mode has a different separation mechanism with its own inherent advantages and disadvantages.

Size exclusion chromatography (SEC) separates molecules by size and shape, differentiating them by their ability to enter the pores of the column packing material. SEC is limited primarily to separating mixtures of large molecules (mw > 5000 Da) in which there is a significant size difference between the components of interest. The advantages of SEC for proteins and peptides are that aqueous, nondenaturing eluents can be used, elution times and orders are predictable, and molecular size information can be obtained. A primary disadvantage of SEC is its inability to separate highly complex mixtures due to low efficiency and low peak capacity. A typical SEC column can resolve only a few peaks per run.

Ion exchange chromatography (IEC) separates proteins and peptides by their ionic charge. IEC provides good resolution and high capacity using conditions that are generally nondenaturing [26]. Ion exchange is one of the most frequently used chromatographic techniques for the separation and purification of proteins, polypeptides, nucleic acids, polynucleotides and other charged biomolecules. The main disadvantages of IEC are that it requires gradient elution with salt-containing eluents and that preparative separations will require samples to be desalted.

Hydrophobic interaction chromatography (HIC) separates proteins or peptides according to their surface hydrophobicity. In HIC, a high salt concentration eluent causes the hydrophobic portions of proteins or peptides in their native conformation (nondenatured) to interact with a weakly hydrophobic stationary phase. Proteins and peptides can then be resolved by eluting with a mobile phase gradient of decreasing ionic strength. HIC provides good resolution with nondenaturing conditions. Its main disadvantages are that it requires gradient elution with salt-containing eluents and some samples may have low solubility in the initial highly ionic mobile phase.

Reversed-phase chromatography (RPC), like HIC, separates peptides and proteins according to their hydrophobicity. However, unlike HIC, RPC interactions are not necessarily limited to only hydrophobic groups on the surface of proteins [27]. RPC eluents are usually a mixture of aqueous and organic solvents. The main disadvantage of RPC is that denaturation can occur, depending on the protein and the percentage of organic solvent in the eluent. However, the ability to unfold proteins and peptides also

gives RPC its greatest advantage which is unparalleled resolution. RPC can resolve peptides that differ only by a single amino acid. For the analysis of proteins and peptides, RPC is the most commonly used mode of HPLC. Although the denaturing effects of RPC can make it unfavourable for preparative separations, for peptides and proteins that are not denatured by it, preparative RPC has the advantage of generally providing samples in solvents that are relatively easy to remove.

Typical conditions in RPC of proteins and peptides include using alkyl bonded phase silica supports, with a mobile phase gradient of water/acetonitrile with trifluoroacetic acid (TFA) as ion pair reagent. At low pH conditions, suppression of carbonyl group ionisation occurs and amino groups are essentially fully protonated. Thus competing equilibria are suppressed and the solute can behave as a single, averaged ionised species. The isoelectric point of most polypeptides and proteins is above these low pH values. It was empirically proven, that higher selectivity is obtained in RPC when running below the protein pI value. Many volatile alkanoic and perfluoroalkanoic acids are effective mobile phase additives increasing the solubilisation of polypeptides and lead to advantageous ion-pairing/dynamic ion exchange type retention phenomena.

While standard RPC conditions are a good starting point, there are many variables that can affect these separations, related to both the column and the system.

### 4.6.2 Theory and mechanism in reversed-phase HPLC

As described above, the stationary phases normally employed in RPC are silica-based supports modified with alkyl chains which provide the hydrophobic surface where separation can take place. Thus, in this mode of HPLC the retention of peptides and proteins has traditionally been considered to be a function of their relative hydrophobicities.

There is still debate over the mechanism(s) responsible for separations in RPC; however, most researchers agree that the process can be thought of as either the adsorption of the solute at the stationary phase or, alternatively, as the partition of the solute between the mobile and stationary phases. In the widely used adsorption model by Geng *et al.* [28], the solute and mobile phase compete for binding sites at an interfacial surface on the solid support. Retention is, therefore, a function of the strength of the interaction between the peptide or protein and the hydrophobic groups of the bonded phase. In this model, the polypeptide adsorbs onto the hydrophobic surface and remains bound until a sufficiently high concentration of organic solvent comes along and displaces it from the solid support. After displacement, interaction of the peptide or protein with the hydrophobic stationary phase is negligible. This mechanism accounts well for one of the striking features of RPC, that the elution of solutes from the column is extremely sensitive to minute changes in organic solvent strengths. Thus, shallow gradients represent powerful resolving tools in polypeptide separations. In fact, isocratic elution is almost never used in this RPC since exact solvent conditions for elution are difficult to ascertain, and protein peaks are usually broad with tailing. The adsorption model by Geng *et al.* is illustrated in Figure 4.2.

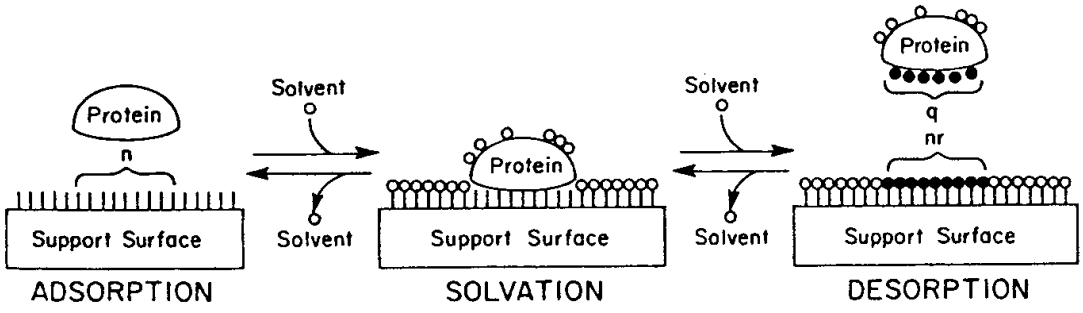


Figure 4.2 The adsorption model of proteins. The illustration shows the process composed of adsorption, solvation and desorption. The lines on the support surface represent alkyl silane ligands, while the small circles on the protein surface represent adsorbed solvent molecules. Unshaded circles designate solvent molecules that make no contribution to the retention when they are adsorbed on either the support or protein. Shaded circles designate solvent molecules that desorb proteins by being adsorbed in the contact area between the RPC support and the protein.

In the partition model of RPC the solute is said to partition between the mobile phase and the solid support.

Most likely, the separation mechanism of RPC probably involves a mixture of the two above processes. Indeed, a third mechanism is sometimes discussed whereby the organic solvent in the mobile phase adsorbs onto the solid support surface, creating a new stationary phase to which solute molecules partition into. Furthermore, one should not presume that the phenomena responsible for the binding of small polypeptides are necessarily the same as those for larger protein structures. Evidence in support of this hypothesis comes from studies that show that the correlation of amino acid hydrophobicity to retention time holds true only for the smaller peptides and is inaccurate above 10-15 residues primarily due to effects of tertiary structure in larger molecules.

## 4.6.3 Basic theory in column liquid chromatography

For efficient use of HPLC to achieve the separation of compounds, it is critical that one possess a basic understanding of physical parameters and theoretical considerations on which the resolving power of the method is based [29].

### 4.6.3.1 Definition of basic chromatographic parameters

The chromatographic $R_s$ resolution is defined as the distance between the peak maxima compared with the average base width of the two peaks. Elution times and peak width should be measured in the same units to give a dimensionless value to the resolution

$$R_s = \frac{\Delta t_R}{4\sigma_i} \qquad \text{(Equation 2)}$$

whereas $\Delta t_R$ is the difference of retention times $t_{Ri}$-$t_R$ (with $t_{Ri} > t_R$) and $\sigma_i$ the standard deviation of the gaussian peaks of the first eluted component in time units.

The resolution parameter $R_S$ for isocratic elution is related to various separation variables as

$$R_s = \frac{1}{4} \sqrt{N_j} (a_{ij} - 1) \left( \frac{k'_j}{k'_j + 1} \right) \quad \text{(Equation 3)}$$

efficiency selectivity capacity

For typical small-molecule samples resolution is achieved by successively optimising these three variables. α is the separation factor, which determines the band spacing within the chromatogram.

$$\alpha_{ij} = \frac{k'_j}{k'_i} \quad \text{(Equation 4)}$$

The separation factor α can be varied by changes in mobile-phase composition, column-packing type, temperature, etc.. It can be used to change band spacing for the entire sample, and specifically to separate adjacent bands of interest.

k' is the retention coefficient (former capacity factor) which can be calculated for each individual peak.

$$k'_j = \frac{t_{Rj} - t_0}{t_0} \quad \text{(Equation 5)}$$

It is desirable for k' to fall within the range $1 \leq k' \leq 10$.
N is defined as the theoretical plate number of the component j. The column length, flow rate, and particle diameter $d_p$ can be adjusted to control the column plate number.

For an optimum packed column and at an optimum flow rate, the plate number can reach a maximum value of

$$N = \frac{L}{2d_p} \qquad \text{(Equation 6)}$$

whereas L is the column length and $d_p$ the average particle diameter of the packing material.

The column efficiency in terms of the number of theoretical plates under specified experimental conditions is related to the band broadening which occurs on the column and can be calculated from the expression

$$N = 5{,}54 \left[ \frac{t_R}{w_{0.5}} \right]^2 \qquad \text{(Equation 7)}$$

where $w_{0.5}$ is the peak width at half peak height. Efficiency is frequently expressed as H (height equivalent to a theoretical plate, HETP), which is the bed length L divided by the plate number.

$$H = \frac{L}{N} \qquad \text{(Equation 8)}$$

The undesirable phenomenon band broadening occurs as the solute experiences dilution during transit through the column. Four major factors contribute to band broadening: Eddy diffusion due to a non ideally packed column bed, longitudinal diffusion from Brownian motion, complications due to mass transfer and extra column effects like excessive dead volume within the system.

The mobile phase linear flow velocity u (cm/s) is defined as

$$u = \frac{L}{t_0} \qquad \text{(Equation 9)}$$

where $t_0$ is the column dead time, the time required for mobile phase molecules to traverse the column.

Plotting H versus u results in the H(u)-curve, which consists of terms for Eddy diffusion, longitudinal diffusion and mass transfer. At an optimum column flow rate, the maximum number of theoretical plates is achieved, which results in a minimum of the van Deemter equation [30].

$$H = A + \frac{B}{u} + Cu \qquad \text{(A, B, C = constantes)} \qquad \text{(Equation 10)}$$

By implementing the dimensionless parameters reduced plate height and reduced velocity in the empirical H(u)-equation, h can be expressed by the Knox equation [31].

$$h = Av^{0.33} + \frac{B}{v} + Cv \qquad \text{(A, B, C = constantes)} \qquad \text{(Equation 11)}$$

The reduced plate height h is given by

$$h = \frac{H}{d_p} \qquad \text{(Equation 12)}$$

and the reduced velocity ν is defined as

$$\nu = \frac{u\, d_p}{D_m} \qquad \text{(Equation 13)}$$

Here $D_m$ is the solute diffusion coefficient in the mobile phase.

#### 4.6.3.2 Gradient elution of proteins and peptides in reversed-phase HPLC

Values of k' in reversed-phase isocratic elution are usually given as a function of organic volume-fraction φ :

$$\log k' = \log k_w - S\varphi \qquad \text{(Equation 14)}$$

$k_w$ is the solute retention factor at the initial mobile phase composition (water). In some systems and especially for peptide solutes, plots of log k' vs. φ are curved rather than linear as predicted by Equation 14. In these cases Equation 14 gives the tangent to this curve at some particular value of φ or k'. Small changes in the organic volume-fraction φ result in high changes in retention time, which underlines the need for gradient elution.

Solute retention time $t_g$ in gradient elution is given as

$$t_g = \left(\frac{t_0}{b}\right)[\log 2.3\, k_0 b + 1] + t_0 + t_D \qquad \text{(Equation 15)}$$

for macromolecular solutes and column-packings of small pore diameter. Here $t_0$ is the column dead time, $t_D$ the dwell-time of the gradient system, $k_0$ is the value of k' for the solute at the start of the gradient in the initial mobile phase and b is a gradient steepness parameter defined by

$$b = S\,\Delta\varphi\, t_0/t_G \qquad \text{(Equation 16)}$$

The quantity $t_G$ is the gradient time and Δφ is the change in φ during the gradient (Δφ = 1 for a 0-100% gradient). A value of $k_w$ can be calculated from

$$\log k_w = \log k_0 + S\varphi_0 \qquad \text{(Equation 17)}$$

where $\varphi_0$ refers to the value of $\varphi$ at the beginning of the gradient. Finally, values of $k_w$ and S thus derived from gradient data define the dependence of k' on $\varphi$ in isocratic systems (Equation 14). Where plots of log k' versus $\varphi$ curve, at a value of $\varphi \equiv \bar{\varphi}$ corresponding to the mobile phase composition at the column midpoint, at the time the solute band is eluted halfway along the column. The corresponding value of k' at this point will be defined as $\bar{k}$. Both $\bar{k}$ and $\bar{\varphi}$ are of fundamental interest in interpreting gradient separation.

#### 4.6.3.3 Peakwidth relationships in gradient elution

Resolution $R_S$ in gradient elution is given as [32,33]

$$R_S = (\tfrac{1}{4})(\alpha - 1)\sqrt{N}\ [\bar{k}/(1+\bar{k})] \qquad \text{(Equation 18)}$$

where $\alpha$ is the separation factor (ratio of $\bar{k}$ values) for a band-pair when the bands are at the column midpoint, N is the column plate number at the same point in time, and $\bar{k}$ is the value of k' at the same point during separation. Thus $\alpha$, N and $\bar{k}$ are each defined in terms of an equivalent isocratic separation. The focus will centre on maximising $R_S$ by maximising the quantity $\sqrt{N}\ [\bar{k}/(1+\bar{k})]$. Changes in $\alpha$ for purposes of increased resolution are not discussed.

Average resolution can also be defined in terms of peak capacity (PC), the number of bands that can fit into a given chromatogram (time equal to $t_G$) with $R_S = 1$ for all band-pairs. Peak capacity is given as

$$\text{PC} = \frac{t_G}{4\sigma_t} = \frac{t_G F}{4\sigma_v} \quad \text{or} \quad \text{PC} = 0.5875\ \frac{t_G}{w_{0.5}} \qquad \text{(Equation 19)}$$

Here $\sigma_t$ is the bandwidth measured in time units, and $\sigma_v$ is the bandwidth measured in volume units, F is the flow rate in volume per time units.

The effective k' value for a gradient separation is equal to $\bar{k}$, so far as resolution is concerned. It is given as

$$\bar{k} = \frac{1}{1.15b} \qquad \text{(Equation 20)}$$

$$\bar{k} = \frac{F\, t_G}{1.15 \Delta\varphi S V_m} \qquad \text{(Equation 21)}$$

$t_0$ is defined as $t_0 = V_m/F$. where $V_m$ is the column dead-volume, given by

$$V_m = \left(\frac{0.4}{x}\right)\left(\frac{\pi}{4}\right) d_c^2\, L \qquad \text{(Equation 22)}$$

The quantity x is the fraction of the mobile phase within the column not contained within the particle pores, $d_c$ is the column inside diameter, and L is the column length.

The peak band width expressed in volume units $\sigma_v$ can be derived as

$$\sigma_v = \frac{t_G\, F}{2.3 S\, \Delta\varphi \sqrt{N}\, [\bar{k}/(1+\bar{k})]} \qquad \text{(Equation 23)}$$

Combination with the definition of the peak capacity yields

$$\text{PC} = \left(\frac{2.3}{4}\right) (\text{S}\ \Delta\varphi)\ \sqrt{N}\, [\bar{k}/(1+\bar{k})] \qquad \text{(Equation 24)}$$

For a given sample (value of S) and gradient range (value of $\Delta\varphi$), Equation 24 predicts that maximising peak capacity also means maximising $R_S$ when $\alpha$ is maintained constant. In gradient elution we can therefore use average resolution and peak capacity interchangeably as measures of 'separation goodness'. The quantity S can be estimated from the approximate relationship

$$S = 0.48\ (mw)^{0.44} \quad \text{(mw: molecular weight)} \qquad \text{(Equation 25)}$$

for reversed-phase HPLC systems and acetonitrile as organic solvent in the mobile phase.

A value of N for the system can be estimated as follows. The first step is to calculate the coefficients A, B and C in the Knox equation. Because values of ν are typically large in peptide separations, the B/ν term can be ignored, similarly values of N are not sensitive to changes in values of A. C can be predicted by the experimental conditions for peptide separations

$$C = \left[\frac{(1-x+\bar{k})}{(1+\bar{k})}\right]^2 \frac{D_m / D_p}{(1-x)30\gamma\rho} \qquad \text{(Equation 26)}$$

$$\text{where} \qquad \left(\frac{D_m}{D_p}\right) = \frac{(1-x)}{[(B/2\gamma)-x]} \qquad \text{(Equation 27)}$$

$$\text{and } B = a' + b'\bar{k} \qquad \text{(Equation 28)}$$

The tortuosity factor γ , the restricted-diffusion parameter ρ, a' and the surface-diffusion parameter b' are determined by fitting experimental data to the equations.

The sample molecular weight can be used to estimate the solute diffusion coefficient in water at 25°C:

$$D_{w,25} = 10^{-5}\ [2.2(mw)^{-1/3} + 62/(mw)] \qquad \text{(Equation 29)}$$

Equation 29 is empirical, but it accurately predicts the $D_m$ values of various proteins in water at 25°C (40-900 kDa), and it mimics the Wilke-Chang equation for molecular weights less than 1,000 Da. Equation 29 is empirically corrected for viscosity η and temperature T (°K) via the Wilke-Chang equation:

$$D_m = D_{w,25}\,(0.9/\eta)\,(T/298) \qquad \text{(Equation 30)}$$

For acetonitrile-water mobile phases, the value of η is empirically related to the η value at 25°C as

$$\eta = \eta_{25}\,(298/T)^6 \qquad \text{(Equation 31)}$$

In gradient elution a change in L or F by itself will also change $\bar{k}$ because $\bar{k}$ depends on F and $V_m$ which is proportional to L. A further difference relates to the values of molecular weight that are typically found for peptide/protein samples compared to other samples. Thus the Knox equation predicts that changes in flow rate (and reduced velocity ν) will have a greater effect on h and N when ν is large. Larger molecules have smaller diffusion coefficients $D_m$ which means that corresponding HPLC separations of these molecules will exhibit larger values of ν. Therefore, reductions in F will generally result in larger increase in N for peptides and proteins. In order to hold $\bar{k}$ constant this can be achieved by increasing $t_G$ in proportion to any decrease in F, *i.e.* by holding the gradient volume $V_G = t_G F$ constant.

When the flow rate is reduced to a sufficiently small value, so that the reduced velocity approaches 3-10, further reduction in F is not advantageous (N approaches a maximum). At this point the best strategy is to increase column length for further increase in N and resolution, however column length has little effect on peak capacity or resolution when $t_G$ is small [34].

If $\bar{k}$ and band spacing are not to maintain unchanged, the peak capacity and resolution can be maximised by changing the gradient steepness parameter ($b = S\,\Delta\varphi\,t_0/t_G$). Both, the peak capacity and resolution will thus show inverse dependencies on the b-term with maximum values of PC and $R_S$ favoured by smaller values of b, that is for given solutes (S-values) and gradient values (Δφ) by larger $t_G$ values. With very long $t_G$ values a compromise arises in the sense that peak height and sensitivity, both inversely proportional to bandwidth, will also decrease.

### 4.6.4 Microcolumn HPLC

The increasing interest in miniaturised liquid chromatography is primarily driven by the demand to handle small sample volumes encountered in bioanalysis, the demand of highest detection sensitivity when using concentration-sensitive detectors and small volumetric flow rates which are appropriate to straightforward interfacing to mass spectrometry [35].

The miniaturisation in chromatography started with the theoretical and experimental development of open tubular capillary columns for gas chromatography in the mid 1950 ´s by Golay [36]. The pioneering work on microcolumn LC began as early as 1967 by Hórvath *et al.* [37], who used 0.5-1.0 mm I.D. x 2 m long columns packed with pellicular particles for the separation of ribonucleotides.

The terminology of miniaturised liquid chromatography used in the literature is inconsistent and confusing. Chervet *et al.* [38] suggested that the chromatographic techniques should be defined according to the volumetric flow rates used, as summarised in Table 4.1.

| COLUMN I.D. | FLOW-RATE | NAME |
|---|---|---|
| 3.2 – 4.6 mm | 0.5 – 2.0 ml/min | Conventional HPLC |
| 1.5 – 3.2 mm | 100 – 500 µl/min | Microbore HPLC |
| 0.5 – 1.5 mm | 10 – 100 µl/min | Micro LC |
| 150 – 500 µm | 1 – 10 µl/min | Capillary LC |
| 10 – 150 µm | 10 – 1000 nl/min | Nano LC |

Table 4.1 Classification of liquid chromatography techniques based on volumetric flow rate

The recent developments in microcolumn liquid chromatography were reviewed by Vissers [39]. The implementation of monolithic silica based columns in capillary format [40] will have a major impact on stability and robustness of the method. In the following the vital theoretical and practical aspects of microcolumn LC are discussed.

#### 4.6.4.1 Chromatographic dilution

The chromatographic process entails that an analyte will be diluted during the separation. The maximum theoretical gain in detection sensitivity can be represented by the downscale factor $f$ that is proportional to the ratio of the two column diameters in square.

$$f = \left( \frac{d_{conv}}{d_{micro}} \right)^2 \qquad \text{(Equation 32)}$$

In this equation $d_{conv}$ and $d_{micro}$ represent the diameters of the conventional and micro scale columns, respectively. Reducing the column I.D. from 4.6 mm to 300 µm would result in a 235-fold gain in mass sensitivity. However, it should be noted that this advantage is valid only in cases when the sample volume is limited, since the sample amount that can be loaded on a column is proportional to the amount of stationary phase in the column.

#### 4.6.4.2 Extracolumn band broadening

Generally, a 5% loss in overall chromatographic resolution is accepted to the overall variance in a HPLC system. Minimising extracolumn band broadening, originating from the various parts of the LC system, becomes critical when employing small I.D. columns. Stringent requirements on minimising all volumetric dispersion associated with the injection device and detection system is also detrimental for maintaining the obtained chromatographic resolution. The dead volume generated by the tubing connecting the chromatographic equipment is important to the extent that this contribute to extracolumn band broadening. The tubing contribution is proportional with the length and raises to the power of two with the radius. Therefore, it is of utmost importance to employ 50 µm I.D. tubing for columns having the dimensions of $\leq 300$ µm I.D. Furthermore, direct connection of the column to the injector and connecting the column outlet to the detector, with virtually zero dead volumes connectors, are imperative for maintaining the chromatographic resolution.

#### 4.6.4.3 Instrumentation

Microcolumn LC was previously difficult to perform which was due to the lack of commercially available instrumentation (columns, pumps, autosamplers, and detectors). Today, dedicated microcolumn instrumentation with the same integration and flexibility as conventional HPLC systems is commercially available.

The pump systems employed for microcolumn LC can be broadly categorised into two types, depending on how the solvent delivery is achieved. One configuration is based on direct pumping of low-µl/min flow rates using either miniaturised reciprocating pumps or syringe pumps. The other option invokes the use of split-flow techniques in which conventional analytical pumps are combined with a split device. Manual injection valves having replaceable internal loops are capable of injecting sample volumes reproducibly down to 20 nl.

Special consideration of UV absorption and fluorescence detection in microcolumn LC is necessary, due to the small peak volumes. The simplest way to minimise band broadening is to perform on-column detection. An optical window serving as the detector cell is obtained by removing the polyimide layer of the packing free part of the fused silica column. The short optical path length limits the concentration sensitivity. This limited sensitivity has been addressed through the development of Z-shaped longitudinal capillary flow cells, having an optical path length of 3-8 mm depending on the column I.D. [41]. Even though the noise level of this flow cell type is to some extent higher, the sensitivity detection is about 25-50 times lower than on-column UV detection.

### 4.6.5 Non-porous silica supports for HPLC

Non-porous 1.5 µm octadecyl modified silica beads [42] proved to have the required characteristics for high-speed and high resolution separations of proteins and peptides [43,44].

Besides the limitation of having a low loadability due to the small surface area and generating a high column back pressure, non-porous silica packings provide a number of advantages. These are the high mechanical stability and a fast mass transfer due to a lack of pore diffusion. This allowed extremely short analysis and reconditioning times.
The non-porous silica beads form an extremely uniform and accessible surface enabling almost quantitative recoveries. The narrow particle size distribution of ± 5 % standard deviation adds to the favourable chromatographic properties. Non-porous silica enable the use of eluents with low eluent strength and the biological activity is often preserved due to short time in the column.
By using small (1.5 µm) non-porous octadecyl modified silica beads a high number of theoretical plates N can be achieved even when short columns are applied. As shown in Equation 32, N is inversely proportional to the average particle diameter. On the other hand, the column pressure-drop Δp increases inversely to the power of two with the average particle diameter, thus limiting the applicability.

$$\Delta p = \frac{\mu u L \Phi}{d_p^2} \qquad \text{(Equation 33)}$$

| | | | |
|---|---|---|---|
| Δp: | column pressure-drop | $d_p$: | average particle diameter |
| µ : | viscosity of the eluent | L: | column length |
| u: | linear flow velocity | | |
| Φ: | column resistance factor | | |

A scanning electron microscopy (SEM) picture of 1.5 µm non-porous silica beads (MICRA ODS I, Eichrom Technologies Inc., Darien, IL, USA) is shown in Figure 4.3.

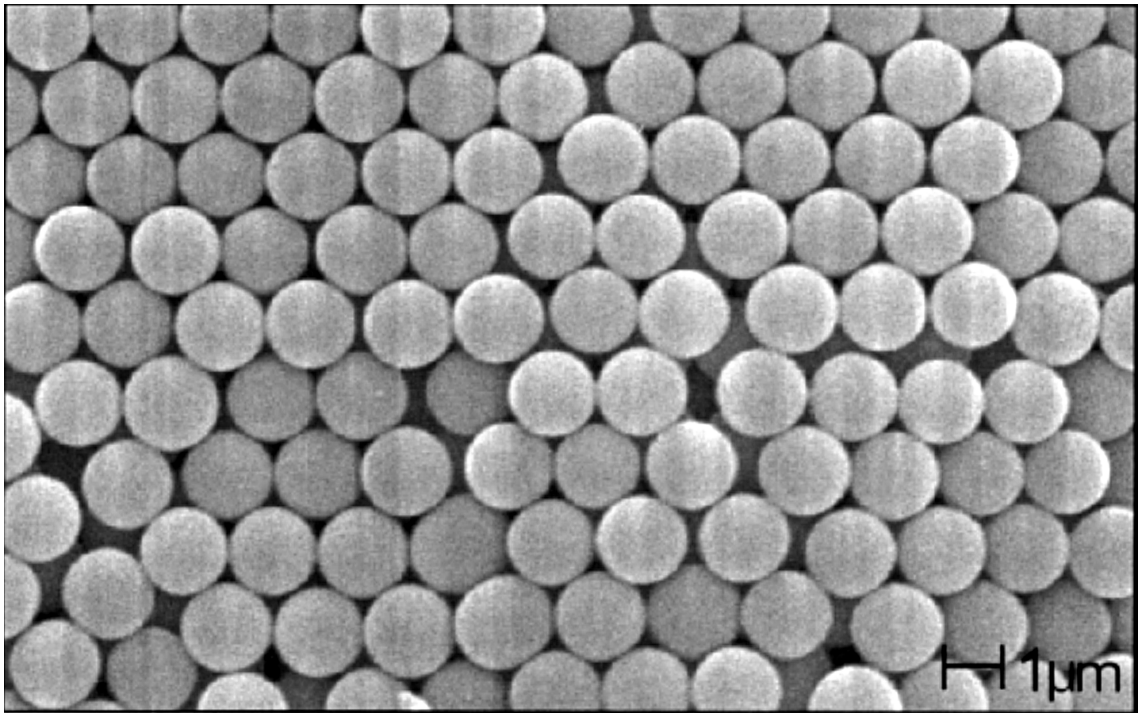


Figure 4.3 SEM picture of 1.5 µm non-porous silica beads

### 4.6.6 Monolithic silica rod columns for HPLC

The very nature of small particulate powdered silica gel, when packed tightly into an HPLC column creates an significant obstacle to the flow of the solvent thus generating a high column back pressure. However, the reduction in particle size $d_p$ leads directly to higher column efficiency, or reduced plate height in the high linear velocity region making the use of small particles preferable. Ultra-high pressure liquid chromatography [45,46] and capillary electrochromatography (CEC) [47] are two techniques to circumvent the difficulties. The limitations can also be overcome by a new sorbent material consisting of monolithic cylindrically shaped rods of highly porous metal free silica [48]. The defined homogeneous bimodal pore structure means that the columns possess a unique combination of large internal surface area over which fast chemical adsorption can take place together with significantly higher total porosity. The synthesis is based on the hydrolysis and polycondensation of alkoxysilanes in the presence of water soluble polymers [49]. The size of the silica skeleton and the throughpores

(macropores) can be controlled independently. Silica rod columns (Chromolith™, Merck KGaA, Darmstadt, Germany) possess a total porosity of about 85 % compared to particulate columns containing only up to 70% total porosity. Therefore, the Chromolith™ columns show a significant higher permeability and much lower column back pressure, respectively. An open network of interstitial channels (macropores), each 2 µm in diameter creates the high porosity. The network of mesopores inside the skeleton, each 13 nm in diameter creates the large internal surface area. The specific surface area is 300 m²/g, the specific pore volume 1.0 ml/g and the content of carbon due to the RP 18 surface modification is 18 % leading to a surface coverage of 3.6 µmol/m².

Furthermore, silica rod columns show very high separation efficiencies. Due to the reduced back-pressure, column length can be extended or columns can be coupled in series. Column clogging of Chromolith™ columns is improbable due to the macropores and the lack of frits. Monolithic columns based on polymers have also been reported [50].

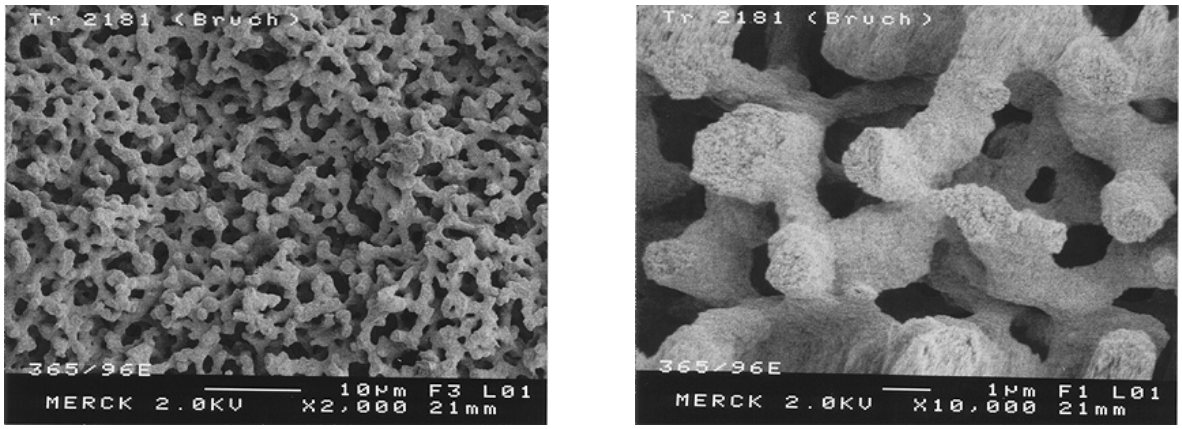


Figure 4.4 SEM images of a cross section of a monolithic silica rod

## 4.7 Sample preparation techniques for biological samples

Sample preparation plays a dominant role in analytical chemistry and is often the single most important step in analysis. Generally more than 50 % of the time for an entire analysis are spent for the sample preparation step [51].

Sample preparation protocols of biological samples often result in samples, that contain complex mixtures of inorganic salts, buffers, chaotropic agents, detergents, preservatives and other solubilising agents and possibly a large number of undesired matrix proteins.
Electrospray ionisation (ESI) and matrix-assisted laser desorption/ionisation (MALDI) are the two most widely used mass spectrometric techniques. The presence of salt or high molarities of non-volatile sample buffer concentrations particularly effect ESI MS. Even though MALDI MS is more tolerant to impure samples [52], there is still a deterioration in resolution and sensitivity due to increased chemical noise in the mass spectrum and suppression of analyte ions.

Furthermore, the direct injection of biofluids as samples such as hemolysed blood, plasma, serum, fermentation broth and supernatants of cell cultures or tissues would contaminate the analytical separation column leading to an irreversible increase in column back-pressure and a decrease in retention and selectivity thus limiting the column lifetime [53].

The sample preparation technique is one of the throughput limiting steps in high sensitivity analysis. The ideal method should preferably provide efficient isolation of the compounds of interest from their matrices with high selectivity and analyte enrichment as well as integrate sample preparation and analysis in an automated mode.

### 4.7.1 Removal of interfering matrix components

Detergents are generally used to keep proteins in solution. Classical methods for the removal of detergents are dialysis or acid precipitation of the detergent (*e.g.* sodium dodecyl sulfate precipitates upon addition of 6 M guanidine hydrochloride). Another method is the precipitation of the protein itself using an organic solvent like acetone or methanol. However, the precipitation methods are not generally applicable and most often linked with severe sample losses.

Common methods for removing buffer salts from protein or peptide samples are typically dialysis, reversed-phase HPLC and gel-filtration HPLC. For separation of a specific molecular weight fraction from a biological protein or peptide sample, ultrafiltration can be applied. Membranes for different molecular weight cut-offs are commercially available. Disadvantages are that there is no possibility to enrich the target analytes by ultrafiltration and sample losses due to non-specific protein binding to the membrane. Liquid-liquid extraction and solid-phase extraction are widely used for selectively extracting low molecular weight target analytes (*e.g.* drugs and its metabolites) from biological matrices. Automated on-line solid phase extraction requires complex instrumentation and the extraction cartridges are dedicated for single use. This limitations can be circumvented by using restricted access materials for HPLC integrated solid phase extraction [54].

### 4.7.2 Size selective sample fractionation and enrichment using Restricted Access Materials (RAM)

Hagestam and Pinkerton [55] introduced the first internal surface reversed-phase (ISRP) support in 1985 Porous silica particles were modified and covered with a hydrophobic bonded phase (glycyl-L-phenylalanyl-L-phenylalanine). They used the enzyme carboxypeptidase A (mw: 35 kDa) to selectively cleave the peptide bond between glycine and phenylalanine at the outer surface, while the pore inside was not affected due to the steric hindrance. The outcome was silica particles with a hydrophobic bonded phase inside the pores, while the outside was coated by a hydrophilic glycyl ligand [56, 57]. Desilets *et al.* [58] introduced the term restricted access media (RAM),

denoting the limited access to the adsorption sites of porous chromatographic supports for macromolecules due to their molecular size.

RAMs combine two chromatographic separation modes in one column, namely size exclusion and adsorption chromatography. Besides a defined pore size the specific feature of RAM is the topochemically bifunctional surface of the particles. The basic principle of RAM is the size-exclusion process due to the physical diffusion barrier determined by the pore diameter. Simultaneously, a selective retention of low molecular mass analytes occurs in the interior of the pore surface by hydrophobic, ion-exchange, or affinity chromatography mechanisms, depending on the bonded ligand functionality. Usually a hydrophilic non-adsorptive outer surface coating is applied on the particles in order to prevent irreversible protein binding and accumulation, hereby enabling the frequent re-use of the RAM columns.

RAMs were recently reviewed by Boos *et al.* [59] who developed restricted access materials known as Alkyl Diol Silica (ADS). The bonded reversed-phase ligand covering the internal pore surface is a $C_4$, $C_8$, or $C_{18}$ moiety whereas the outer surface is covered with a diol functionality. The RAM is based upon LiChrospher 60 which is a spherical ($d_p$: 25 µm) based silica with an average pore size of 6 nm. This provides a molecular weight cut-off of approximately 15 kDa for globular proteins.
This concept is commercialised by Merck KGaA (Darmstadt, Germany) and the phases are available as LiChrospher® ADS, packed in 25 mm x 4 mm I.D. columns.
Ion-EXchange Diol Silica (IEX-DS) which either carries cationic (diethylaminoethyl) or anionic (sulfonic acid) functional groups is available as a research sample from Merck KGaA.

The synthesis is performed adopting Pinkertons principles of tailoring a stationary phase by specific enzymes. First the native silica surface is silanised by 3-glycidoxypropyl-methyldimethoxysilane. Acidic hydrolysis of the epoxy groups leads to the diol-modified silica. In the next synthesis step, this silica is esterified with fatty acid chlorides of different chain length in presence of triethylamine and is therefore covered with alkanoyl ligands on both, external and internal surfaces. The alkanoyl ligands on the external surface are selectively hydrolysed to the diol using the enzymes porcine

pancreas lipase II (mw: 52 kDa) and lipase VII (mw: 120 kDa) from *Candida cylindracea* which are unable to penetrate the internal surface [60].
RAM columns allow the direct and repetitive injection as well as size selective fractionation of untreated biofluids like plasma, serum, urine, fermentation broth and supernatant of tissue homogenates.

High molecular weight sample components *e.g.* matrix proteins cannot penetrate into the pores and thus are eluted quantitatively in the void volume of such columns. Only analytes of low molecular mass have access to the binding centres at the inner pore surface and thus can be retained and extracted selectively. RAM columns with reversed-phase properties are widely used as pre-columns in coupled-column systems for HPLC integrated, extractive, sample clean-up of low-molecular target analytes in raw biofluids. Recently, sample fractionation and extraction of peptides using silica based ion-exchange RAM columns were demonstrated [61].

Grimm *et al.* [62] developed a polymer based RAM with strong cation exchange moiety on the internal surface and diol groups on the external surface which was characterised in the sample clean-up of small proteins. The silica based ion exchange RAM employed in the current study has a narrower pore size distribution and provided superior discrimination properties as compared to polymeric based ion exchange RAM columns. Furthermore, silica based RAMs with cation exchange functionality possess high loading capacities for proteins.

RAM readily implements the inherent advantages of on-line column switching in HPLC schemes, *e.g.* automation and the use of a closed system, for sample clean-up procedures. RAMs allow the discrimination of higher molecular weight proteins like albumin and enables the enrichment of lower molecular weight components.
The schematic illustration of a restricted access material is depicted in Figure 4.5.

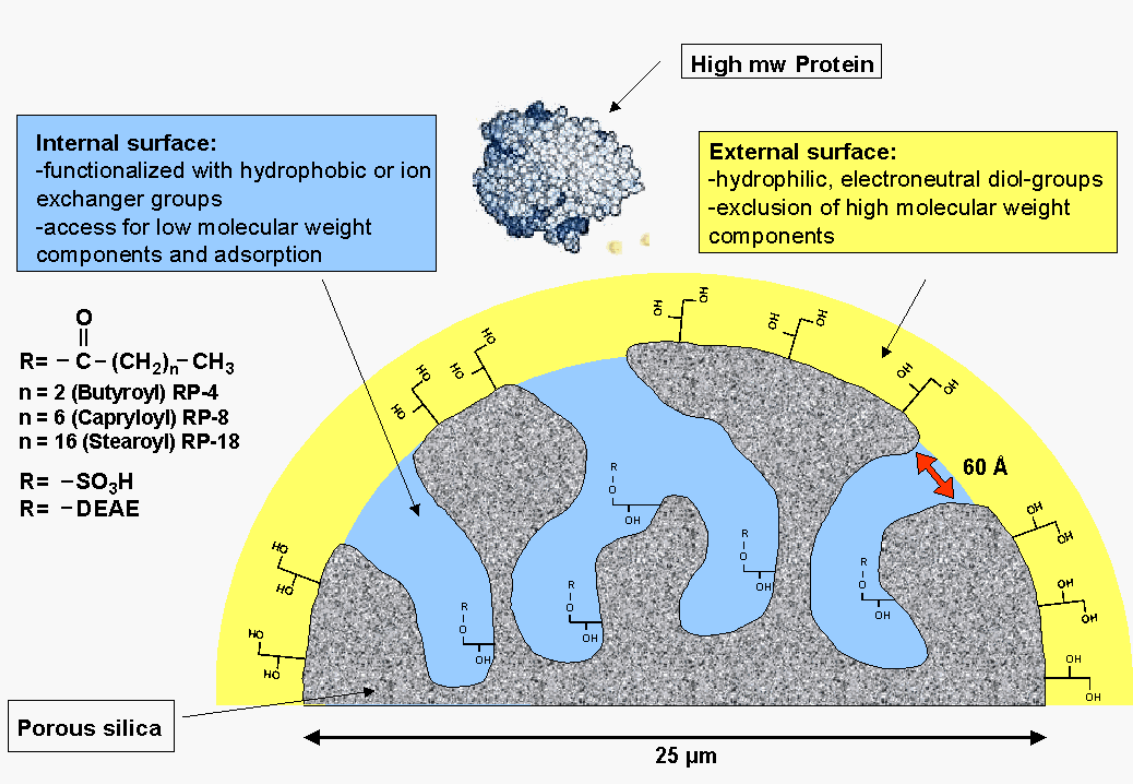


Figure 4.5 Principle of restricted access material (RAM) based on the silica Lichrospher 60

## 4.8 Multidimensional separations

One-dimensional separations have limited resolving power of complex sample mixtures. Increases in resolution can be achieved by variations in the plate number, N, selectivity, α, or the retention factor, k'. However, adjustment of the retention factor has a limited influence on resolution and that only at low values. An increase in the number of plates by extending the column length often yields in marginal increases in resolution and in an unacceptable increase of the analysis time. Since selectivity has the greatest influence on resolution, it is the variable that attracts the most attention [63].

The limitations of single stage separation systems have been recognised for many years, and in order to describe separations of a multicomponent mixture, Giddings [64] introduced the concept of peak capacity, which is defined as the maximum number of components, n, that can be placed side by side in the available separation space with a

given resolution which satisfies the analytical goals, and is given by the following equation for unit resolution:

$$n = (1 + \frac{\sqrt{N}}{r}) \ln (1 + k'_i) \qquad \text{(Equation 34)}$$

where r is the number of standard deviations taken as equaling the peak width (typically 4), and $k'_i$ the retention factor of the last peak in a series.

Modern high-resolution chromatographic systems yield peak capacities which are calculated to be in the range of 100-300. These results would appear adequate to resolve components in a mixture where the number of components, m, is less than the peak capacity of the system; however, components in a complex mixture are usually not uniformly distributed, and appear randomly, overlapping each other. Giddings and Davis [65] developed the statistical model of overlap to study the seriousness of said component overlap, which becomes apparent when the number of visible peaks, V, in a chromatogram is estimated by the following equation:

$$V = m\, e^{-m/n} \qquad \text{(Equation 35)}$$

providing that n is chosen as the value corresponding to a resolution of 0.5. Assuming that the number of components in a mixture can be estimated (and in many cases, this cannot be done), and in the case in which the number of components equals the peak capacity of the system used, the maximum number of visible peaks will be equivalent to 37% of the system's peak capacity. Further, the number of peaks in a chromatogram which represent a single component, S, is given by:

$$S = m\, e^{-2m/n} \qquad \text{(Equation 36)}$$

which yields a value of only 18% of the peak capacity, using the conditions described above.

These calculations help us to understand the limitations encountered in the separation of components in a complex matrix, even in cases where single column (linear) chromatographic systems are operated close to the theoretical limits.

A practical means of effecting changes in resolution is the introduction of a different fundamental mechanism of interaction by the use of two (or more) separation stages (multidimensional chromatography, or coupled column chromatography). In order to obtain the maximum benefit from multidimensional chromatographic systems, the basic mechanisms controlling separation in each dimension should be different (orthogonal). That is, the system should be non-redundant, otherwise, for a column chromatographic system the total peak capacity is given by:

$$n_{tot} = x^{½} n \qquad \text{(Equation 37)}$$

where x = number of identical columns used, yielding a coupled system which is only equivalent to a longer linear system. In addition to coupling separation systems with different separation mechanisms, Giddings suggested the additional requirement that two components, which are resolved in the first separation step, remain separated throughout the process.

A representation of the peak capacity of a planar two-dimensional system is presented in Figure 4.6. The maximum peak capacity attainable in a system of this type is given by the product of the peak capacities of each dimension (discounting the additional band broadening of the migration components in the second dimension).

$$n_{tot} = n_a \times n_b \qquad \text{(Equation 38)}$$

In column chromatography, utilisation of the total available separation space requires a large number of secondary column separations, so that all sample cuts taken in the first dimension can be transferred for subsequent separations.

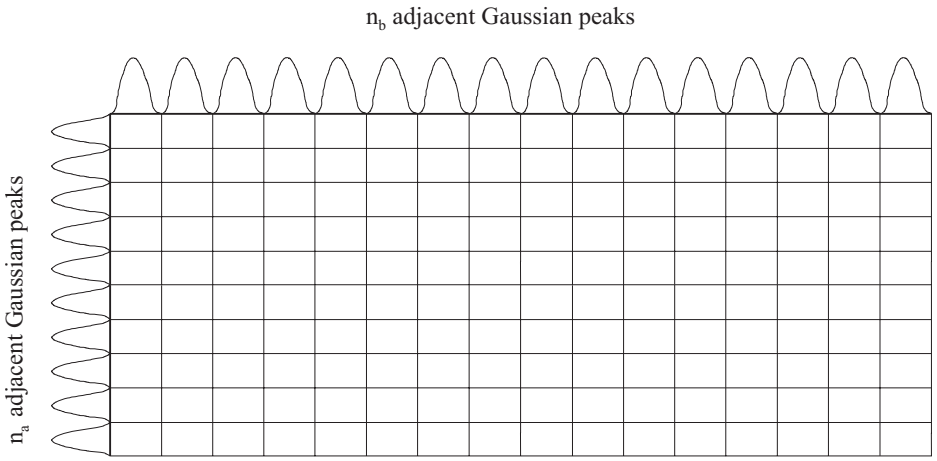


Figure 4.6 Theoretical peak capacity of a 2D system with Gaussian distribution. The rectangular boxes of the gridwork correspond to the peak capacity, in this case $n_c$ equals approximately 160 ($n_a$ x $n_b$).

### 4.8.1 Technical approaches in multidimensional separations

Two distinct multidimensional approaches can be carried out. The first is a two-dimensional separation using the two right-angle dimensions of a continuos planar surface or thin-film bed (*e.g.* 2D-PAGE).

The second approach is coupled column separation, often referred to as multidimensional chromatography. In such systems, the effluent from the primary column is fractionated onto a second column with an orthogonal separation mechanism. The time interval ($\Delta t_r$) of the separation in the first dimension is decisive in determining to what degree coupled column systems comply with Gidding's second criterion. As $\Delta t_r$ increases the more the system approaches simple tandem coupling of chromatographic columns, severely diminishing the overall peak capacity, since components separated in the first column may remerge in the second column [66]. The resolving power will improve with decreasing $\Delta t_r$ until the value of $\Delta t_r$ approaches the width of a single peak. Thus, smaller $\Delta t_r$ will generate more fractionation into the second dimension. Murphy *et al.* [67] investigated the effect of sampling rate on resolution in comprehensive two-dimensional gel-permeation/RP-chromatography of copolymers. In this paper, the authors claim that each peak in the first dimension should be sampled at least three times into the second dimension to achieve the highest resolution.

Different combinations of chromatographic separations were described in the literature, *e.g.* gas chromatography-gas chromatography (GC-GC) [68], LC-GC [69], LC-CE [70] and LC-LC [71].

In the following, the focus will be on the features of two-dimensional liquid chromatography in different coupled column systems. This approach is particularly attractive because of the straightforward automation and on-line detection possibilities by mass spectrometry.

#### 4.8.1.1 Comprehensive and non-comprehensive set-up

According the Gidding's criteria, the maximum peak capacity can only be achieved when the entire analyte is subjected to the various separation dimensions. The fractionation and reinjection of the effluent fractions from the first dimension can be made using either "heart-cutting" or by using the "comprehensive" concept as defined by Bushey and Jorgenson [72].

Heart-cutting techniques require that the retention properties of the analytes in the first dimension are known in advance, since only the components of interest from the first column effluent are subjected to separation on the second column. This technique is appropriate when only one or a few components shall be isolated. In a comprehensive approach, the entire first dimension column effluent (not only an interesting region) is reanalysed as discrete fractions on regular intervals by the second dimension.

#### 4.8.1.2 On-line and off-line techniques in two-dimensional HPLC

The transfer of a discrete fraction onto the second dimension can be done in two different modes:

The first is the off-line mode were fractions are collected and later reinjected into the second dimension. This can either be done manually or in an automated mode. This approach puts low demands on the instrumental set-up and there are no limitations in separation speeds of each dimension.

Off-line techniques are prone to sample losses by vial contamination, low reproducibility and long analysis times [73]. Furthermore, sample dilution and eluent incompatibilities might have a negative impact. However, many off-line experimental approaches have been described throughout the literature [74, 75, 76, 77, 78, 79] and fully automated equipment is now commercially available. Figure 4.7 displays the principle of fractionation and reinjection in 2D-HPLC.

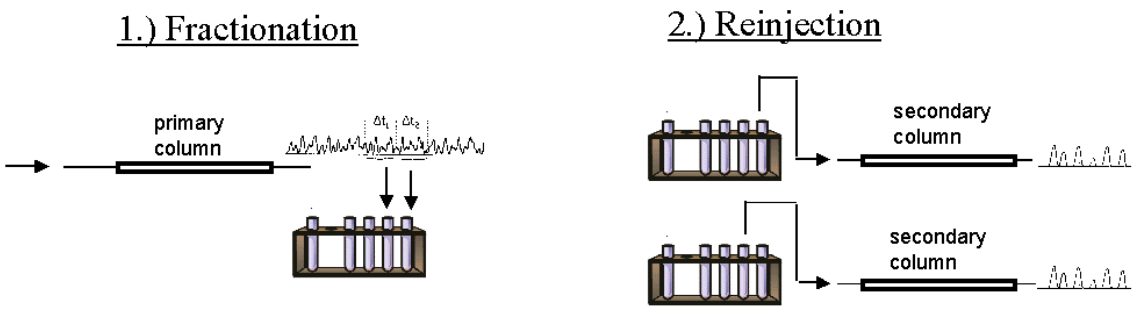


Figure 4.7 Off-line approach in multidimensional HPLC

The most elegant technique is the on-line coupling of different separation modes where two variations are common. One technique uses a continuos flow in the first dimension and different separation speeds in either dimension. To preserve a high sampling rate after the first dimension, the separation in the second dimension should be very fast compared to the first dimension in order to on-line analyse enough samples across each peak without any fraction storage. To compromise this demand, two or more parallel columns in the second dimension can be applied, albeit placing stringent demands on the high-speed separation. The advantages are no sample losses, excellent reproducibility, highest resolution power and fast 2D-separations.

The second technique uses an interrupted flow and step-gradient elution in the first dimension. Discrete fractions are transferred to a single secondary column in intervals, which are sufficient for a separation cycle in the second dimension [80, 81]. Advantages are low demands on instrumental set-up and no restrictions in separation speeds, whereas resolution is sacrificed. The two different on-line techniques are demonstrated in Figure 4.8.

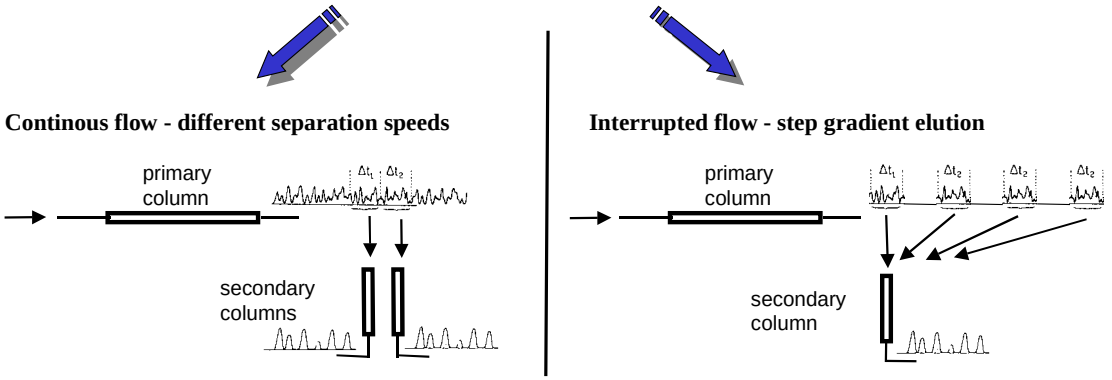


Figure 4.8 Two different on-line approaches in multidimensional HPLC

The interfacing between the first and second dimension in an on-line system is crucial. This can be done by filling storage loops connected to automated switching valves for transferring the fraction onto the next column [82, 83], putting stringent demands on adjusting loop-size, flow rate and column dimensions in either dimension [84].

Alternatively, the fractions eluting from the first dimension can be enriched on the column head of a secondary column (on-column focusing). During the loading time of one column, a second parallel column can be eluted. Automated switching valves are used for alternative linking the first dimension effluent to the parallel columns [85, 86]. The latter interface construction is preferred since it is more flexible to use, is more rugged and sample desalting and enrichment is automatically performed.

In this work, the comprehensive on-line approach using two parallel columns in the second dimension was improved by a four parallel column set-up and a new sophisticated column switching technique.

## 4.9 State of the art in multidimensional HPLC of proteins and peptides

Besides the classical protein mapping approach using 2D-gels electrophoresis, multidimensional liquid phase separations are becoming to have a major impact on the proteome analysis.

Gygy *et al.* [87] and Wall *et al.* [78] demonstrated limitations of analysing protein expressions by 2D-PAGE and mass spectrometry especially for proteins of low abundance. The advantages and limitations of 2D-PAGE and 2D-HPLC are summarised in Table 4.2.

| Properties of method | 2D-PAGE | 2D-HPLC |
|---|---|---|
| Molecular weight information | + | – |
| Isoelectric point information | + | – |
| Fast, not labour intensive | – | + |
| High resolution for mw < 15 kDa | – | + |
| High resolution for mw > 15 kDa and < 200 kDa | + | – |
| High resolution for mw > 200 kDa | – | + |
| Runs in parallel | + | – |
| Concentrate sample to boost sensitivity | – | + |
| Straightforward automation | – | + |
| Integrated size selective sample fractionation | – | + |
| On-line coupling to ESI-MS | – | + |
| Handles any type of proteins (membrane bound, phosporylated, glycosylated) | – | + |
| No limitation in sample load | – | + |

Table 4.2 Advantages and limitations of 2D-PAGE and 2D-HPLC

Protein mapping by multidimensional separations have been performed on intact proteins in solution as well as on digested proteins utilising peptide mapping. In either case the multidimensional liquid phase separation is followed by tandem mass spectrometry and a database search. The later approach, analysing tryptic peptides leads to a tremendous increase of sample complexity. On the other hand, the separation power in terms of peak capacity in reversed-phase chromatography is significant higher for peptides than for proteins. As known, the chromatographic resolution and sensitivity are inversely proportional to the molecular weight of the protein while, for a gel, resolution and sensitivity are proportional to the molecular weight of the protein [78]. Most applications use the digestion of proteins in solution (shotgun approach) in conjunction with multidimensional chromatography and MS-MS techniques for protein identification. Principally, protein identification can be done by peptide mass fingerprinting [88], where the pattern of tryptic peptides is analysed by MALDI-TOF MS and compared to theoretically calculated peptide masses of proteins present in the database. Identification of proteins using peptide sequence information uses tandem mass spectrometry for generating peptide ion fragments by cleavage of the amide bonds [89]. Identification is made by submitting the peptide mass and the peptide fragmentation pattern to database search. The so-called “shotgun identification” approach for the analysis of proteins in mixtures has recently been developed [90]. This technique uses proteases to digest a protein mixture in solution, followed by HPLC-MS/MS analysis in conjunction with database searching of peptide tandem mass spectra.

The three main approaches for separation and identification of proteins are summarised in Figure 4.9.

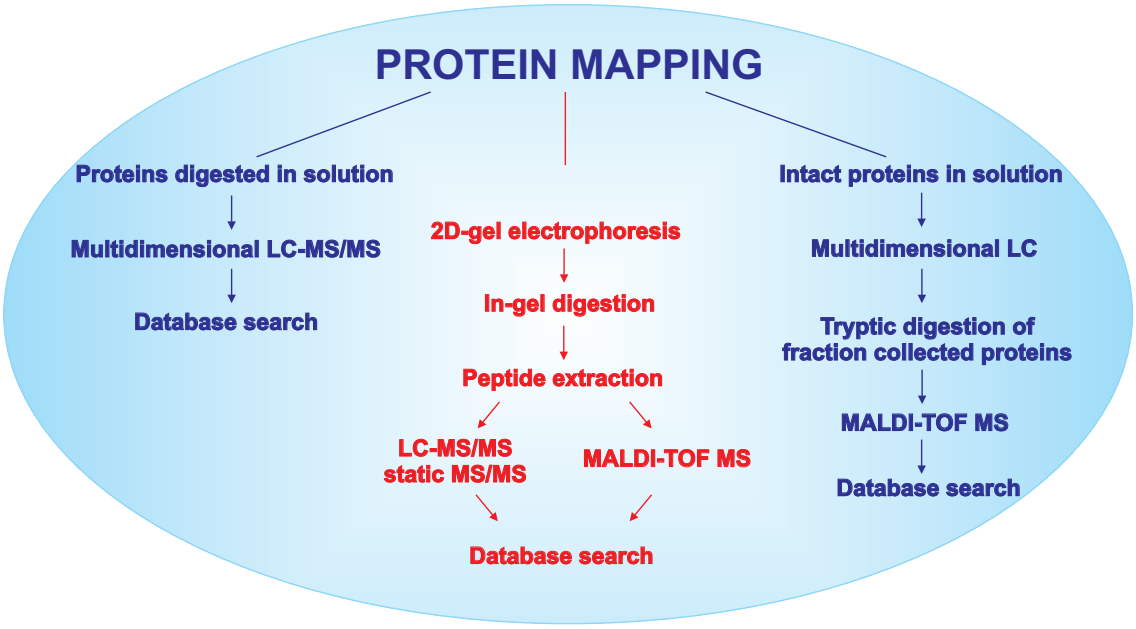


Figure 4.9 Three main approaches for separation and identification of proteins

Different on- and off-line experimental approaches have been described throughout the literature. Several powerful combinations of linear liquid chromatographic techniques based on miscellaneous displacement mechanisms, *e.g.* ion-exchange, reversed-phase, hydrophobic interaction, and affinity chromatography are available. The judicious choice of separation combination is not only restricted by their orthogonality, but also chromatographic parameters like selectivity, resolution, peak capacity, load capacity, bio recovery and speed of separation have to be taken into consideration in accordance to attain a comprehensive multidimensional separation. Using affinity chromatography for selectively separating analytes of interest from complex mixtures is a powerful approach in target oriented analysis where only interesting compounds are subjected to analysis [91, 92, 93].

Cation exchange followed by reversed-phase chromatography in an off-line mode was extensively used for separation of proteins and peptides [74, 75, 76], while an optimisation strategy for two-dimensional peptide partitioning was presented by Lundell *et al.* [94]. Udiavar *et al.* [77] described an off-line combination of reversed-phase HPLC, capillary electrophoresis and MALDI-TOF mass spectrometry. The applicability was demonstrated characterising the heterogeneity of posttranslatorial modifications present in glycoproteins.

Wall *et al.* [95] published an off-line two-dimensional liquid-phase separation method where proteins in cell lysates were separated using isoelectric focusing in the first dimension, followed by fast reversed-phase HPLC using non-porous particles in the second dimension. The protein screening obtained by the 2D-system as compared to 2D-PAGE was complementary and improved results were obtained for lower mass and basic proteins. Vissers *et al.* [79] presented an automated off-line capillary liquid chromatography approach using either strong anion exchange coupled to reversed-phase columns or two different reversed-phase columns for tryptic peptide mapping.

Bushey and Jorgenson [72] pioneered in the comprehensive on-line coupling in 2D-HPLC. A new comprehensive on-line column coupling technique was introduced by Opiteck *et al.*[73] using two parallel reversed-phase columns, rather than storage loops, for sample transfer from the size exclusion mode into the reversed-phase mode. A similar design by Opiteck *et al.*[96] was used for the separation of proteins from a *Escherichia coli* cells. A miniaturised version using microcolumns coupled to a single quadrupole mass spectrometer for peptide mapping experiments was also presented by Opiteck *et al.*[97].

Step gradient elution in the cation exchange mode for an interrupted sample transfer onto a single secondary reversed-phase column in the second dimension was presented by Link *et al.* [80] and Davis *et al.* [81]. In both cases peptide digest mixtures were separated and further analysed by MS-MS. Link *et al.* [80] used a biphasic microcapillary column consisting of strong cation exchange and reversed-phase packing material. The metal microcapillary column was directly used to produce an electrospray during the reversed-phase gradients for on-line MS-MS detection.

### 4.9.1 Protein quantification

Quantification of 2D-gel separated proteins typically relies on image analysis and silver staining methods. More accurate quantification is achieved by metabolic radioactive labelling followed by scintillation counting. New methods based on the use of stable isotopically labelled internal standards ($^{15}N$ or $^{13}C$) followed by 2D-gel separation and

quantitative analysis of the separated proteins by MS enable accurate protein quantification, regardless of the reproducibility of the 2D-gel system [98].

Gygi *et al.* [99] describe an approach for the quantification and concurrent sequence identification of the individual proteins within complex mixtures. The principles of the isotope-code affinity tag (ICAT) approach described are based on selective chemical labelling of cysteinyl residues of proteins. The ICAT tag comprises a specific chemical reactivity towards thiol groups, an isotopic linker (either heavy and contains eight deuteriums or light, containing no deuteriums), and a biotin affinity tag. The ICAT strategy for quantification and identification of differential protein expressions starts with derivatisation of proteins representing two cell states with the isotopically light and heavy ICAT tags, respectively. The two protein samples are then combined and proteolysed to peptide fragments. The ICAT labelled peptides are isolated by two-dimensional chromatography, using avidin affinity chromatography in the first dimension and then separated and analysed by a reversed-phase microcolumn HPLC-MS/MS system in the second dimension. The mass spectrometer is alternating between the MS and MS/MS mode in successive scans, automatically measuring the relative quantities of peptides in the column effluent in the MS mode and obtaining sequence information in the MS/MS mode. In contrast to 2D-gels, the ICAT method can be used for low abundance protein mapping by preparing and injecting large amounts of sample.

Regnier and co-workers presented a concept of identifying proteins in complex mixtures called the “signature-peptide approach” [100]. In the first steps complex protein mixtures are digested in solution and only the tryptic peptides unique to a protein are biospecifically selected for further analysis. The method employed 2D-HPLC, using affinity chromatography as the first dimension to select peptides with unique structural features. Reversed-phase chromatography was then used as the second dimension, followed by MALDI mass spectrometry of the fractionated peptides. In addition, quantification was obtained by derivatisation of the peptides with an isotopically labelled reagent on the $\epsilon$-amino group of all lysines.

# 5 Experimental, discussion and results

## 5.1 Comprehensive on-line 2D-HPLC system for protein separation using a single column in each dimension

The first aim was to set up a 2D-HPLC system composed of anion- and cation exchange chromatography, respectively, in the first dimension and ultra-high-speed reversed-phase chromatography in the second dimension. Therefore, MICRA ODS I columns, consisting of non-porous C-18 modified 1.5 µm silica beads of 14 mm x 4.6 mm I.D. dimension were used. The reversed-phase columns were operated much faster compared to the 2D-systems described in the literature.

The requirements for sample transfer into the second dimension were to be independent from adjusting the volumetric flow rates and column dimensions for interfacing the individual separation modes. To avoid sample dilution and for desalting the fractions, enrichment of the analytes is mandatory prior to the analysis in the second dimension. For that reason, storage loops can not be applied. The initial comprehensive 2D-HPLC system used pre-columns, which allowed to deposit fractions of the analyte leaving the first dimension in an alternating way on small cartridges before they were eluted in series with the analytical reversed-phase column. This technique offers the advantage that only one analytical RP-column in the second dimension is needed. Additionally, the cartridges used produce a pressure drop of only 8 bar at a flow rate of 1 ml/min. Therefore, it was possible to use a commercial UV-detector flow-cell to monitor the separation in the first dimension. Usually, UV-detector flow-cells can stand a maximum pressure of 50 bar which would be exceeded by loading the fractions on a MICRA ODS I column. An illustration of the set-up is given in Figure 5.1.

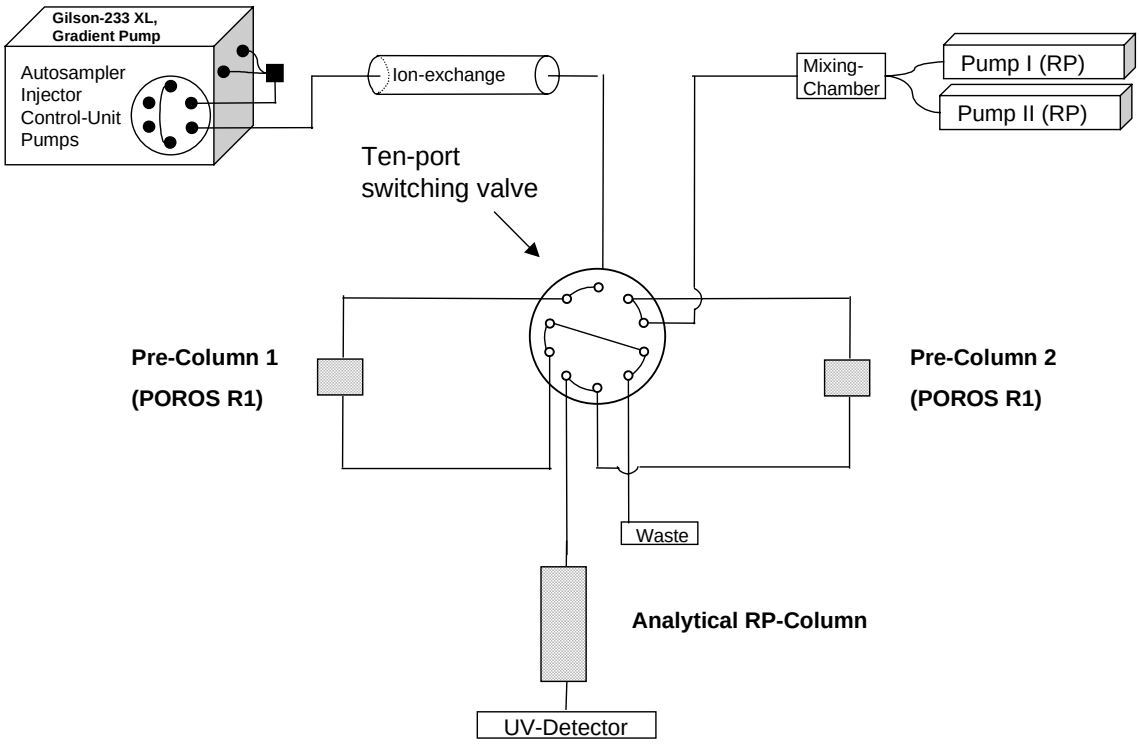


Figure 5.1 Schematic of the on-line comprehensive 2D-HPLC system using pre-columns for fraction transfer

The comprehensive 2D-HPLC-system consists of an autosampler Model 233 XL, Gilson, Villiers-le-Bel, France, working as an autosampler, control-unit for valve switching and gradient start and for control of the data acquisition units. Each of the two individual high pressure binary gradient systems consisted of two HPLC pumps model 2200 and an HPLC-Central Processor model 7110 for gradient control. Eluent mixing was performed by dynamic low void volume mixing chambers. UV-detection was operated at 215 nm using a Lambda 1000 device, equipped with a 0.8 µl flow cell, all supplied by Bischoff Analysentechnik, Leonberg, Germany.

The effluent from the ion exchange column, was alternately enriched on one of two pre-columns switched by an electrically driven ten-port valve (Valco Instruments Co. Inc, Houston, TX, USA). The second gradient system then elutes the pre-column in series with the MICRA ODS I column. The pre-column cartridges of 4 mm x 2 mm I.D. were in house packed with the polymeric perfusion chromatography support POROS R1 from Applied Biosystems, Framingham, MA, USA. The hydrophobicity of POROS R1 can be compared to C-8 modified silica supports, thus being less hydrophobic than the

analytical RP-column. This is a prerequisite for the in series coupling of the two columns. In contrary to that, the pre-columns hydrophobicity and loadability must be high enough, that the entire analyt from the first dimension is trapped on the cartridge under the aqueous elution conditions of the ion exchange column. Although being a polymeric material it was stable up to 250 bar back pressure, which is essential for the high-speed elution in the reversed-phase mode.

Fractions were collected every 45 s which corresponds to the switching interval of the ten-port valve and the gradient cycle in the RP-mode including column regeneration. Anion exchange- as well as cation exchange- was coupled to RP-chromatography separating standard protein mixtures.

### 5.1.1 Anion exchange / reversed-phase separation

The anion exchange column was a in house made poly (p-trimethyl-ammoniumchloride-methylen) styrene-coated 1.5 µm non-porous silica packed into a 33 mm x 4.6 mm I.D. column [101]. Eluents for anion exchange separations consisted of A = 0.01 M $KH_2PO_4$ in water, pH = 6.0 and B = 0.7 M $KH_2PO_4$ in water, pH = 6.0. The flow rate was 0.5 ml/min. The gradient ran from 10 mM $KH_2PO_4$ to 0.7 M $KH_2PO_4$ within 10 min. This was followed by 5 min column washing with 0.7 M $KH_2PO_4$ and 15 min column regeneration using buffer A.
The eluents for RP separations were A = 0.1 % trifluoroacetic acid (TFA) in water and B = 0.1 % TFA in acetonitrile. The gradient cycle for the reversed-phase columns started with 18 % B, which was increased to 70 % B within 25 s, than reduced to the initial conditions (18 % B) which was maintained for 20 s for column regeneration. The gradient cycle time corresponds to the valve switching and fractionation interval of 45 s.

The standard protein mixture for the anion exchange / RP separations contained the following nine proteins: Ribonuclease A from bovine pancreas (rib), cytochrom C from bovine heart (cyt), myoglobin from horse heart (myo), albumin from chicken egg (ov), conalbumin from chicken egg white (con), catalase from bovine liver (cat), β-lactoglobulin B from bovine milk (β-lac B), β-lactoglobulin A from bovine milk (β-lac A) and trypsin-inhibitor from soy bean (try-I). The concentration for each protein

was 1 mg/ml. The separation was performed at pH = 6.0 injecting 10 µl. All protein mixtures were filtered through a 0.45 µm filter unit Milliex-HV (Millipore, Bedford, MA, USA).

The results of the 2D-separation are displayed as the anion exchange chromatogram after the first dimension in Figure 5.2 and the corresponding RP separations are displayed in Figure 5.3.

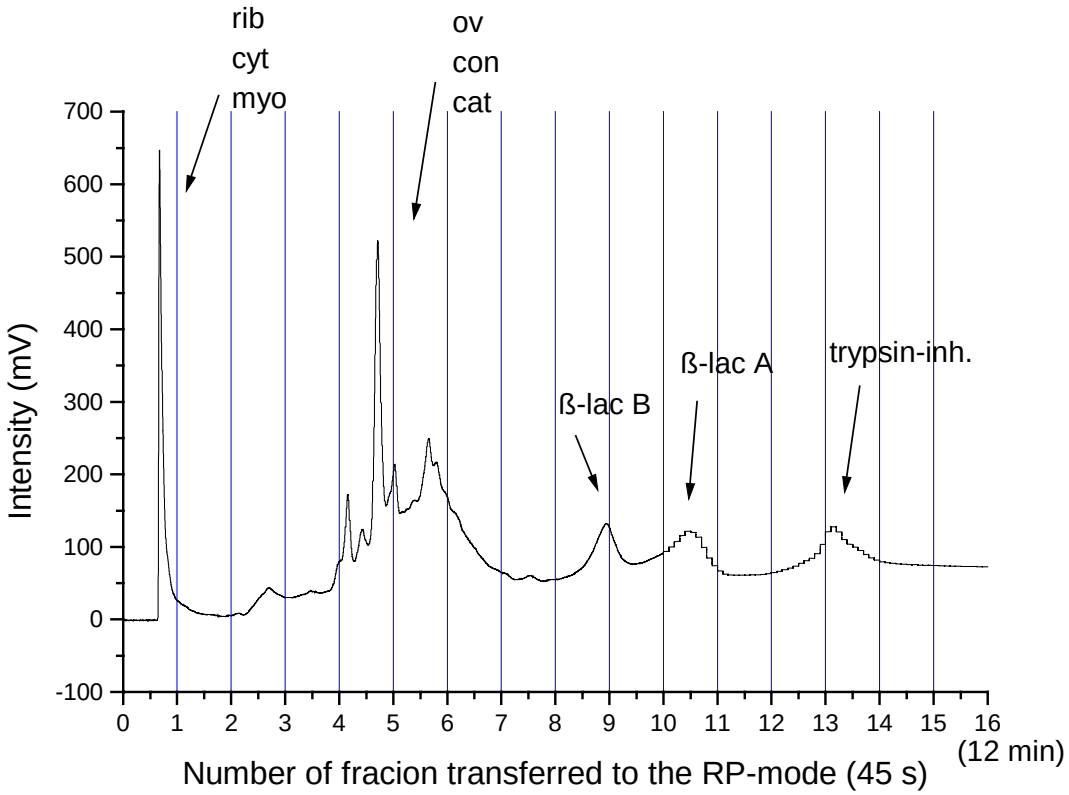


Figure 5.2 Anion exchange / reversed-phase separation after the first dimension, every 45 s a fraction was transferred into the second dimension

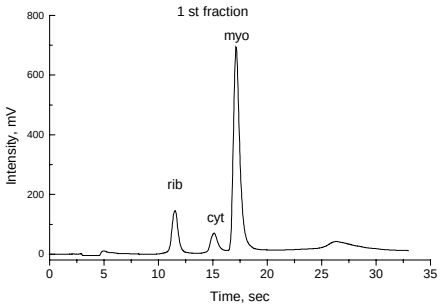
1 st fraction
myo
rib
cyt
Intensity, mV
Time, sec

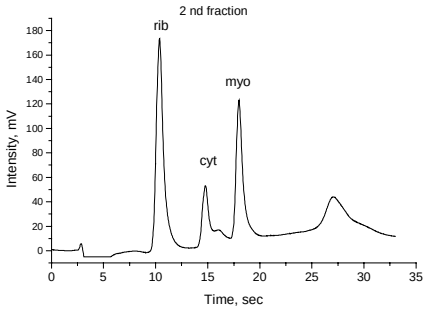
2 nd fraction
rib
myo
cyt
Intensity, mV
Time, sec

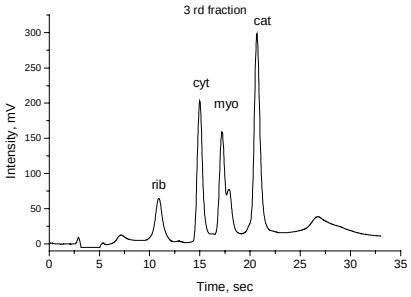
3 rd fraction
cat
cyt
myo
rib
Intensity, mV
Time, sec

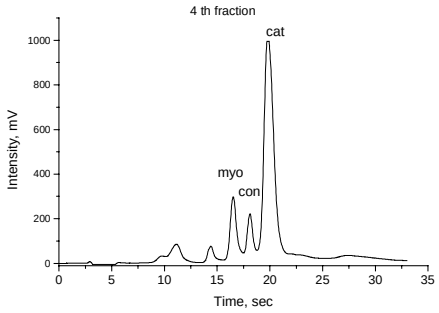
4 th fraction
cat
myo
con
Intensity, mV
Time, sec

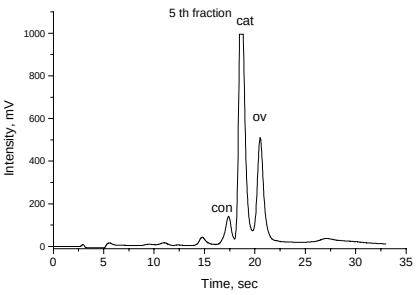
5 th fraction
cat
ov
con
Intensity, mV
Time, sec

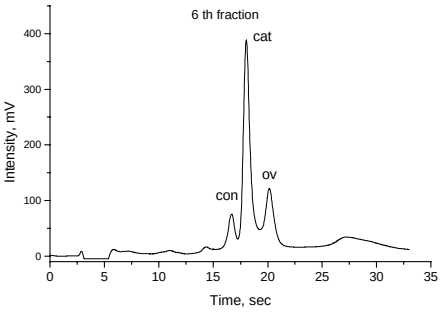
6 th fraction
cat
con
ov
Intensity, mV
Time, sec

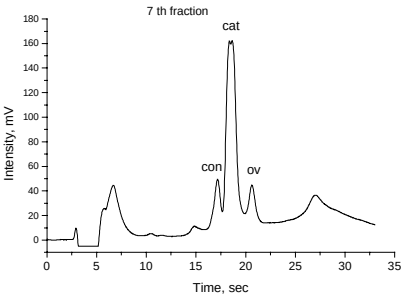
7 th fraction
cat
con
ov
Intensity, mV
Time, sec

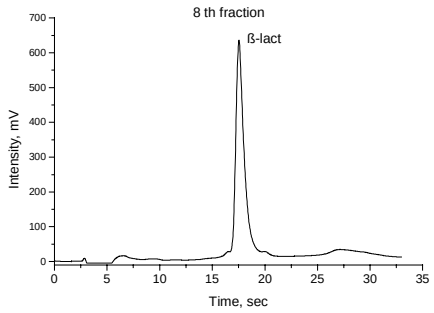
8 th fraction
ß-lact
Intensity, mV
Time, sec

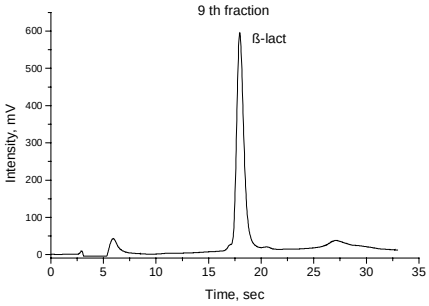
9 th fraction
ß-lact
Intensity, mV
Time, sec

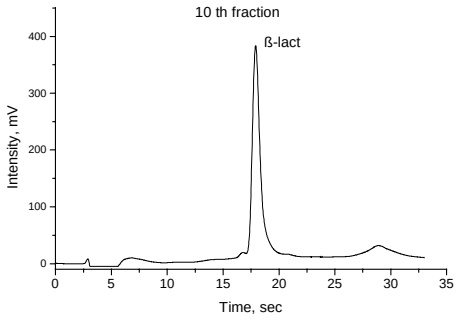
10 th fraction
ß-lact
Intensity, mV
Time, sec

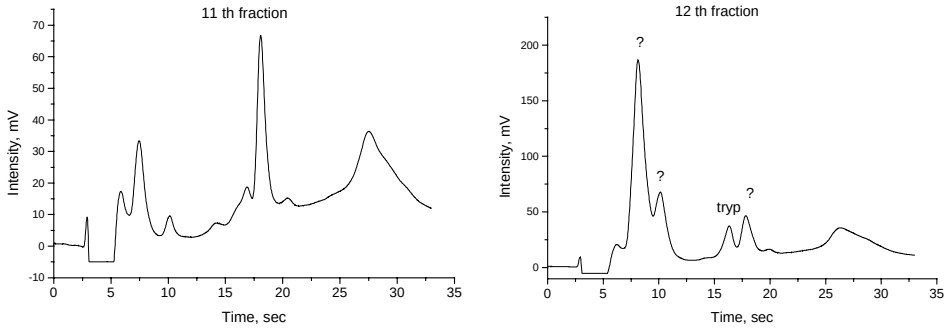


Figure 5.3 Reversed-phase chromatograms of consecutive 45 s fractions taken from the anion exchange column

Figure 5.2 shows the partial separation of the standard proteins in the anion exchange mode. Some proteins are baseline separated while others are co-eluting in one peak, *e.g.* ribonuclease, cytochrome and myoglobin in the void volume of the column.

The RP-separations displayed in Figure 5.3 indicates a baseline separation of the proteins within the analysis time of 25 s in the second dimension. Two adjacent fractions of the consecutive runs often show similarities in the chromatographic pattern. One reason for that is the high sampling rate from the first dimension, which cuts first dimension peaks into several fractions to avoid re-assembly of already isolated compounds. The second reason is suspected to be a memory effect on the pre-columns due to insufficient time for regenerating the small but porous cartridges. For that reason, the system set-up was changed. The new version used two RP-columns in parallel and therefore sacrifices real-time monitoring of the UV-signal after the first dimension.

### 5.1.2 Cation exchange / reversed-phase separation

The coupling of cation exchange with reversed-phase HPLC was done using a VYDAC SCX column of 50 mm x 7.5 mm I.D. dimensions, provided by Vydac, Hisperia, CA, USA. The same eluents, operational parameters, second dimension and interfacing was used as before. Similar results compared to the use of anion exchange chromatography in the first dimension were achieved.

## 5.2 Comprehensive on-line 2D-HPLC system for protein separation using two parallel reversed-phase columns in the second dimension

The results of the protein mapping on a comprehensive 2D-HPLC system using pre-columns were compared to a system where the analyte is directly deposited alternately on the top of the two analytical reversed-phase columns. Improvements were expected in reproducibility, robustness and the ability for system expansion. UV detection after the first dimension is not indispensable, since the entire analyte is automatically transferred to the second dimension. The chromatograms generated in the first dimension were made in an additional single column run without using the second dimension.

For extensive studies on the reproducibility and repeatability, the new system using two parallel analytical RP-columns was rebuilt in an fully automated manner for unattended operation. The 2D-system consists of either an anion- or cation-exchanger in the first dimension and used two equivalent non-porous MICRA ODS I RP-columns in the second dimension. While the first RP-column was loaded with a fraction of the effluent from the ion exchanger, the analytes on the second column were eluted. The two RP-columns were alternately loaded by enriching the analytes on top of the column under ion exchange conditions. Column switching was performed using a ten-port two-position valve. The gradient cycle in the second dimension was extended from 45 s to 60 s, thus one RP-chromatogram per minute was generated. The new column arrangement is illustrated in Figure 5.4.

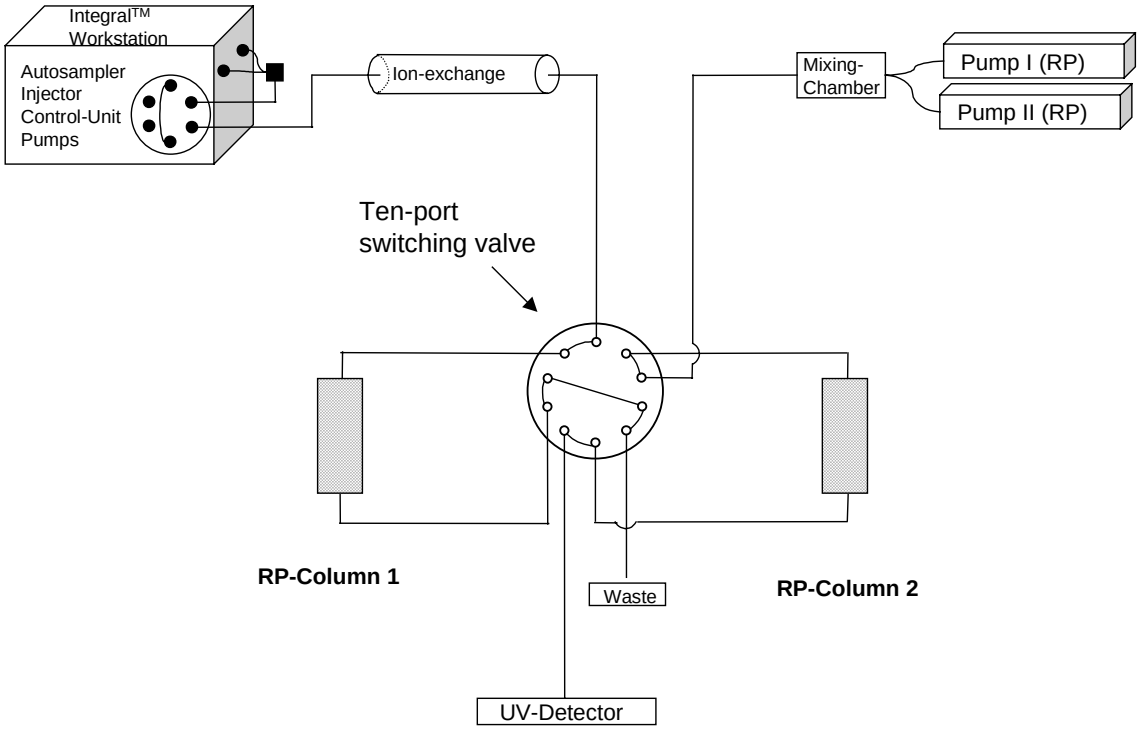


Figure 5.4 Schematic of the on-line comprehensive 2D-HPLC system using two parallel RP-columns for fraction transfer

### 5.2.1 Instrumentation

The fully automated 2D-HPLC device consisted of an Integral™ 100Q workstation (Applied Biosystems, Framingham, MA, USA), equipped with an autosampler with sample cooling device and three pneumatically driven ten-port two position switching valves (Rheodyne, Rohnert Park, CA, USA). One of those was serving as injector and one was used for column switching. The workstation was equipped with one high pressure binary gradient pump system, an UV detector with a 1.2 µl flow cell and a control unit for data acquisition and system management. The second high pressure binary gradient system used in the high-speed second dimension consisted of two HPLC pumps model 2200 and an HPLC-Central Processor model 7110 for gradient control. Eluent mixing was performed using a dynamic low void volume mixing chamber, all supplied by Bischoff Analysentechnik, Leonberg, Germany.

To minimise void volume, tubing lengths were kept to a minimum and an inner diameter of 0.127 mm was used. For biocompatibility PEEK (polyether ether ketone) tubing provided by Upchurch Scientific, Oak Harbor, WA, USA was applied.

### 5.2.2 System operation

The samples were stored in 1200 µl vials at 3 °C in the temperature controlled tray of the autosampler. Injections were automatically performed by filling a 10 or 100 µl sample loop attached to the injection valve. The first dimension high pressure gradient pump eluted the ion-exchange column continuously with an increasing gradient of phosphate buffer, resulting in a partial separation of proteins.

Each 60 s the analyte leaving the first dimension was transferred alternatively to one of the two reversed-phase columns to be enriched on top of the columns (on-column-focusing). Column switching was performed using the pneumatically driven ten-port valve controlled by the method editor software. At the same time a 150 ms electrical contact closure pulse was sent to the central processor device of the second gradient system in order to start the gradient and the column reconditioning procedure. During the time when one of the reversed-phase columns was eluted, all of the analytes corresponding to 1 min (1 ml in volume) ion-exchange effluent were deposited on the other RP-column. By the use of this technique, desalting of the proteins was performed automatically. The RP-column undergoing elution was attached via the valve to the UV detector which was equipped with a 1.2 µl flow-cell and operated at a wavelength of 215 nm.

In order to simplify the data acquisition and handling, just one chromatogram in the second dimension which contained all the 20 RP-chromatograms was generated. Interpretation of the chromatograms is straight forward, since the gradient of each RP-chromatogram starts every full minute. In this way relative retention times can easily be compared.

### 5.2.3 Columns and operational conditions

Ion-exchange columns were based on non-porous 2.5 µm polymeric beads (TSK-gel NP), commercially available with DEAE and $SO_3H$ functionality, respectively packed into 35 mm x 4.6 mm I.D. stainless steel columns (TosoHaas, Stuttgart, Germany). Reversed-phase columns were MICRA ODS I columns of 14 mm x 4.6 mm I.D. dimension similar to the previous set-up.

Eluents for ion-exchange separations consisted of A = 0.01 M $KH_2PO_4$ in water, pH = 6.0 and B = 0.5 M $KH_2PO_4$ in water, pH = 6.0. The flow rate was 1 ml/min. The gradient ran from 10 mM $KH_2PO_4$ to 0.3 M $KH_2PO_4$ (60 % B) within 20 min. This was followed by 5 min column washing with 0.5 M $KH_2PO_4$ and 15 min column regeneration using buffer A.

The eluents for RP separations were A = 0.1% trifluoroacetic acid (TFA) in water and B = 0.1% TFA in acetonitrile. A typical gradient cycle for the RP-columns started with 18 % B, which was increased to 70 % B within 25 s and further increased to 100 % B within 5 s, which was maintained for 5 s before being reduced to the initial conditions (18 % B) within a further 5 s followed by 20 s column regeneration.

### 5.2.4 Comparison of RP-column performance

In the previous column arrangement where two individual RP columns are used alternatively, the columns shall provide similar separations to achieve reasonable results. In order to proof it, a mixture of 8 standard proteins was applied containing ribonuclease A, insulin, cytochrome C, lysozyme, myoglobin, conalbumin, catalase and ovalbumin each at a concentration of 1 mg/ml. 10 µl of the sample were deposited onto the RP-column applying ion exchange eluent A at a flow rate of 1 ml/min but without using any column. After one minute loading, the column was eluted applying the same conditions as compared to the 2D-system. The separation power of the two columns is shown in Figure 5.5.

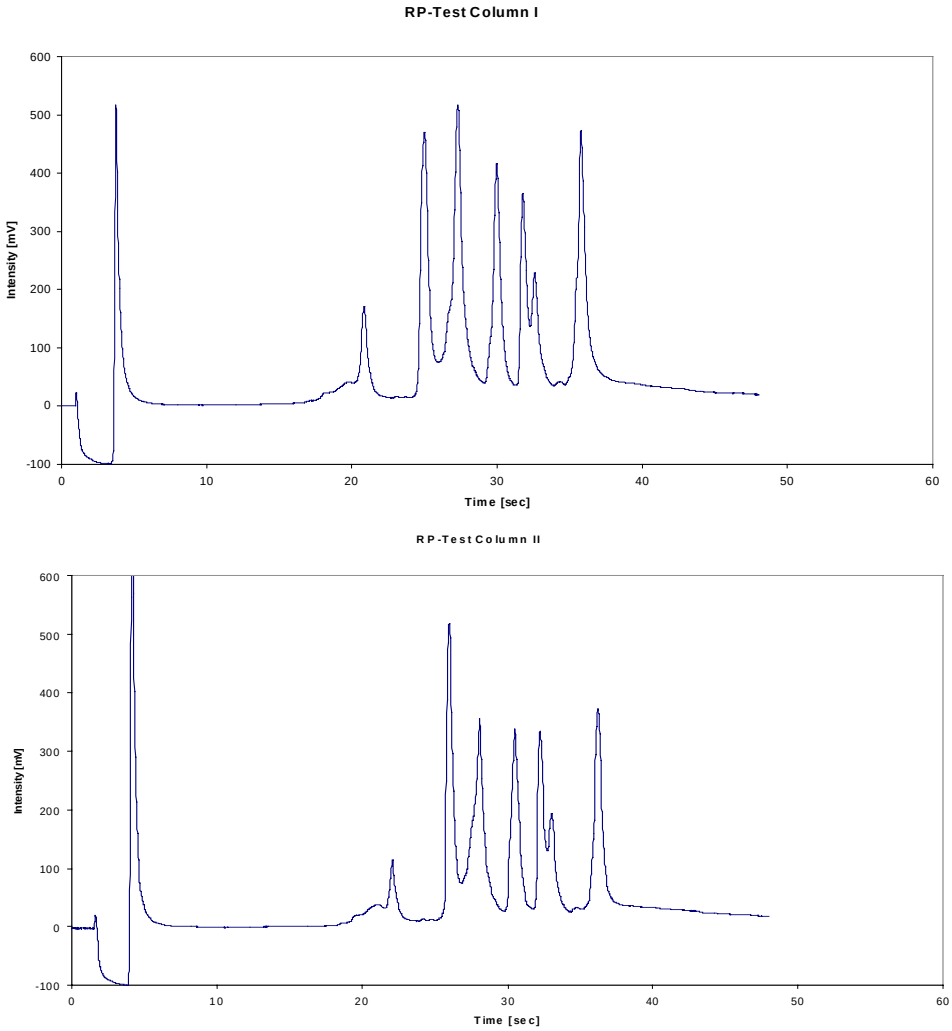


Figure 5.5 Separation of 8 proteins using two similar RP-columns under the same conditions

Both second dimension RP columns were compared showing only a slight difference in the separation performance which proves the concept of the parallel column approach.

### 5.2.5 Anion exchange / reversed-phase separation using two parallel RP-columns

The standard protein mixture for anion-exchange / RP-separations contained the following eleven proteins: Ribonuclease from bovine pancreas (rib.), insulin from bovine pancreas (ins.), cytochrom C from bovine heart (cyt.), lysozyme from chicken egg white (lys.), myoglobin from horse heart (myo.), conalbumin from chicken egg

white (con.), ovalbumin (ova.), trypsin-inhibitor from soy bean (try.-I), β-lactoglobulin A from bovine milk (β-lac. A), β-lactoglobulin B from bovine milk (β-lac. B), and bovine serum albumin (BSA). This separation was performed at pH = 6.0 injecting 100 µl of the test mixture at a total protein concentration of 10.2 mg/ml. All protein mixtures were filtered through a 0.45 µm filter unit Milliex-HV (Millipore, Bedford, MA, USA).

Figure 5.6 shows the anion-exchange chromatogram of 11 standard proteins after the first dimension leading to an incomplete separation roughly according to their respective isoelectric points.

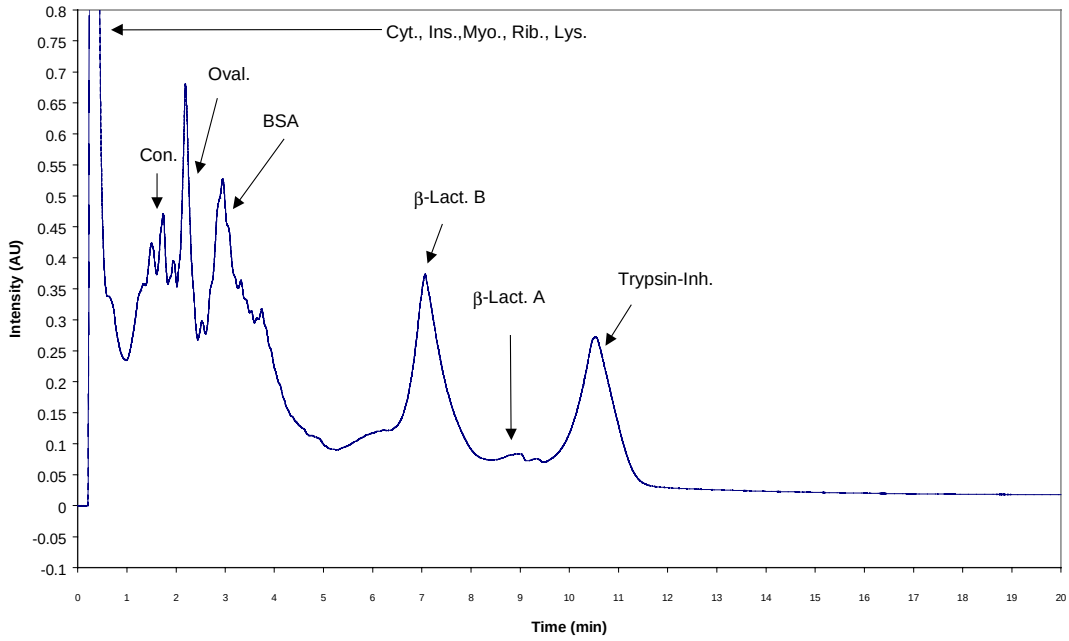


Figure 5.6 Incomplete separation of a 11 protein mixture after the first dimension using anion exchange chromatography

Sixteen out of 20 chromatograms generated in the second dimension applying reversed-phase chromatography are shown in Figure 5.7.

**AX/RP-Separation Fractions 1 - 3**

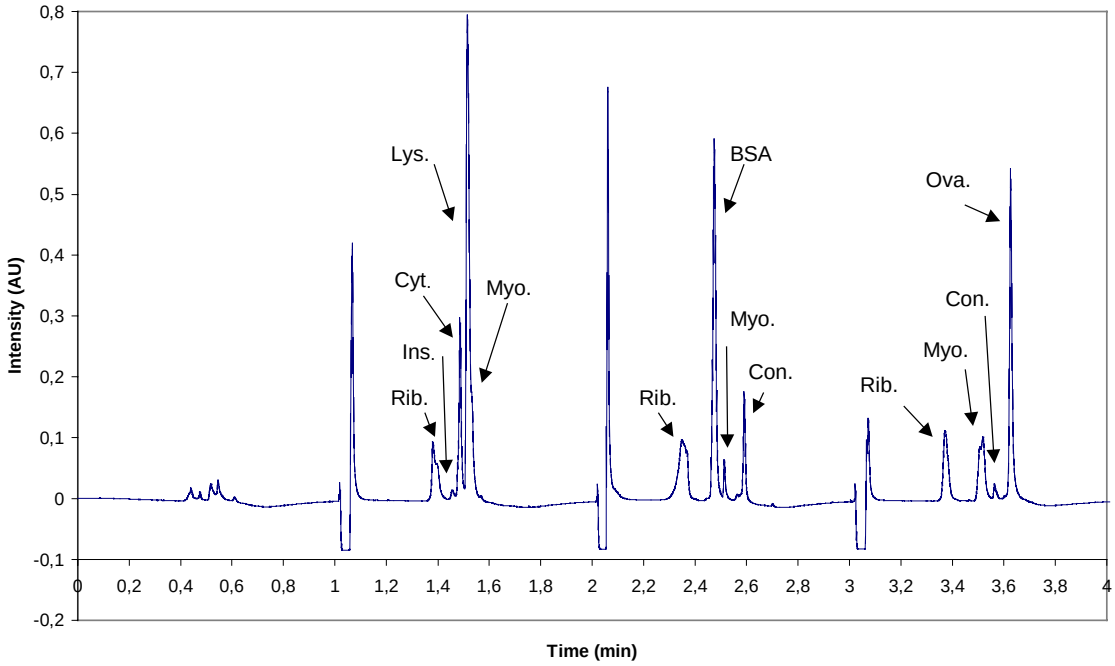


**AX/RP-Separation Fractions 4-7**

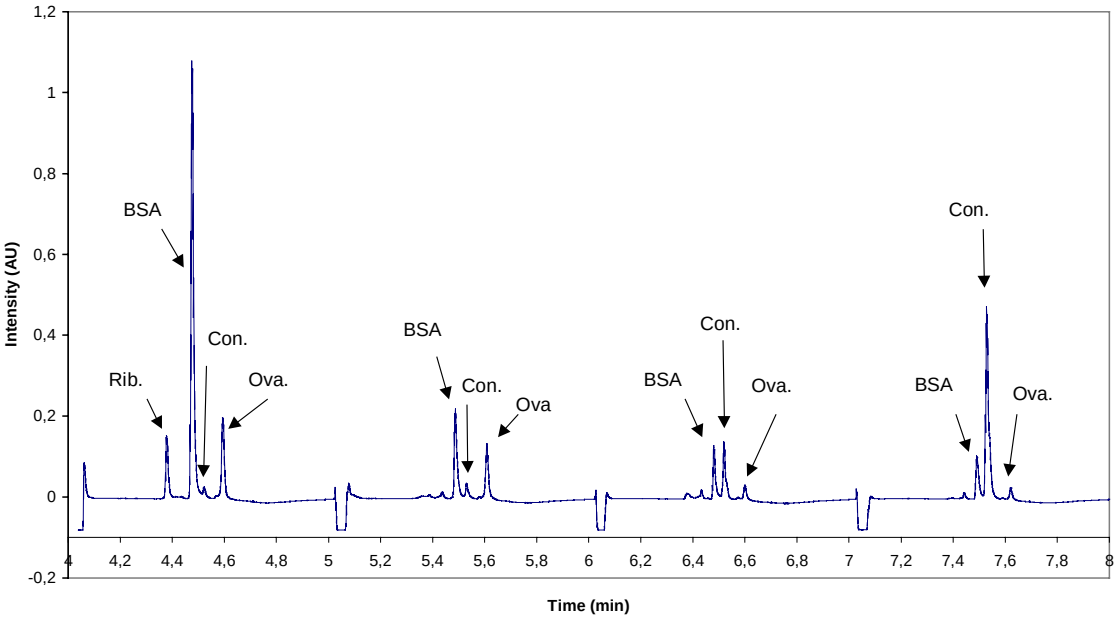

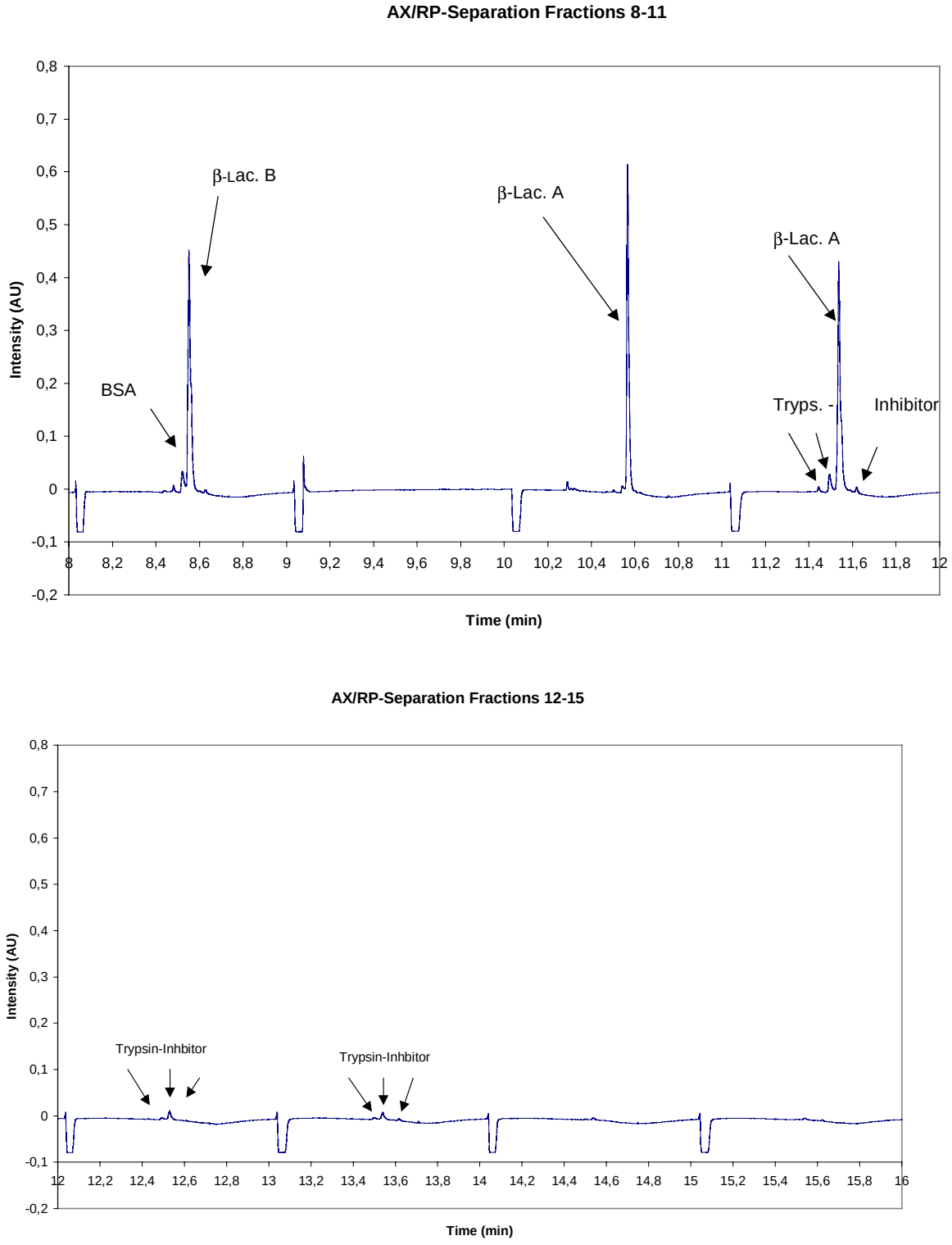


Figure 5.7 Reversed-phase chromatograms of the one-minute analyte fractions taken from the anion-exchange column

Those proteins which have not been successfully separated based on electrostatic interactions can mostly be separated in the reversed-phase mode due to differences in

hydrophobicity. The proteins eluted in the void volume of the anion-exchanger are successfully separated on the RP-column and appear mainly in the RP chromatogram of fractions eluting between 1 min to 2 min. These non-retained analytes are, however, successfully resolved by the cation-exchange column and *vice versa*. Figure 5.7 shows that the proteins eluted from the ion-exchange column appear in approximately three fractions of the reversed-phase chromatogram but in different amounts which allows to follow the ion-exchange separation. Despite the fact that the peak in the ion exchange chromatogram seems to reach the baseline again, there are still small amounts of protein eluting from the column. This seems to be a specific problem in ion exchange chromatography limiting the resolution. For the separation of the specific standard protein mixture the ion-exchange separation might be too slow or the sampling rate too high. But in an unknown more complex sample it might be useful to keep the high sampling rate to get maximal resolution.

The total amount of proteins loaded onto the coupled column system was 1.020 mg, which is close to the maximum loadability of the RP-columns. The separation of the same test mixture at a concentration level which was 100 times lower compared to Figure 5.7 is shown in Figure 5.8. The test mixture was diluted by a factor of ten and 10 µl were loaded corresponding to a total protein amount of 10.20 µg.

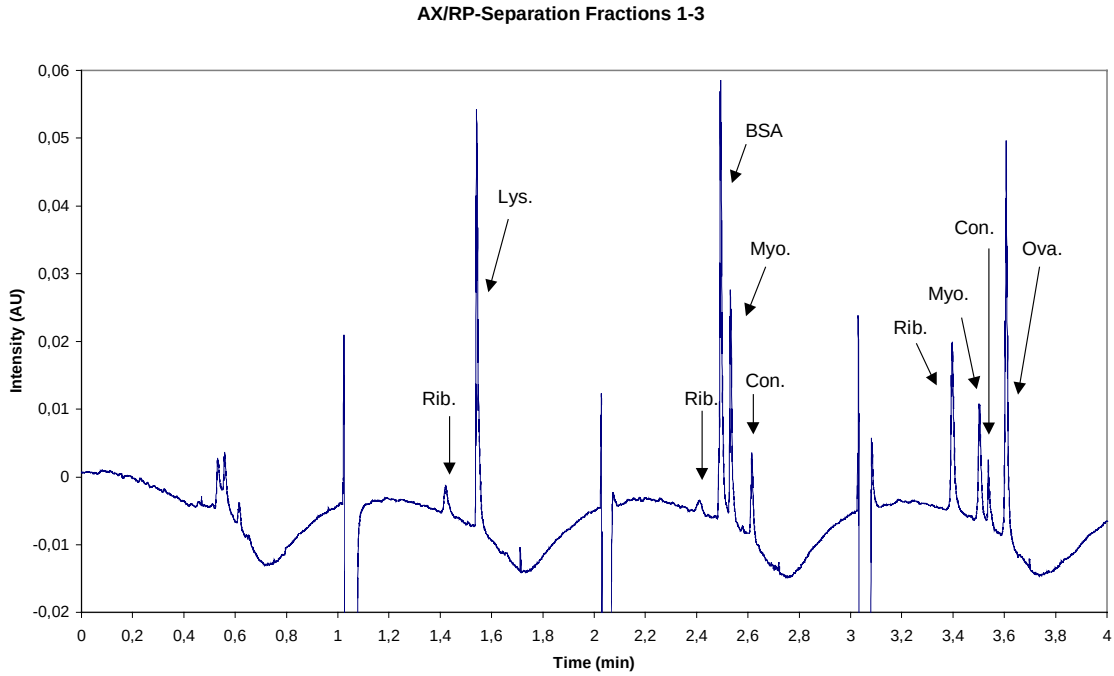


Figure 5.8 Reversed-phase chromatograms of fractions 1-3 from the anion-exchange column at a concentration level which is 100 times lower than the previous run (Figure 5.7)

Despite of the appearance of a baseline slope, the chromatograms at a low concentration level demonstrated that proteins were still detectable and were well separated showing a symmetric peak shape.

### 5.2.6 Cation exchange / reversed-phase separation using two parallel RP-columns

The standard protein mixture for cation-exchange / RP separations contained the following 10 proteins: ribonuclease from bovine pancreas (rib.), insulin from bovine pancreas (ins.), cytochrom C from bovine heart (cyt.), lysozyme from chicken egg white (lys.), myoglobin from horse heart (myo.), conalbumin from chicken egg white (con), ovalbumin (ova.), concanavalin from jack bean (coc.), γ-chymotrypsin from bovine pancreas (γ-chy) and human albumin (alb.H). Separations were performed at pH = 6 injecting 100 µl of the protein mixture at a total protein concentration of 6.8 mg/ml.

The partition of the 10 protein test mixture after the cation exchange column is displayed in Figure 5.9, showing a partial separation especially in the first 5 min retention time.

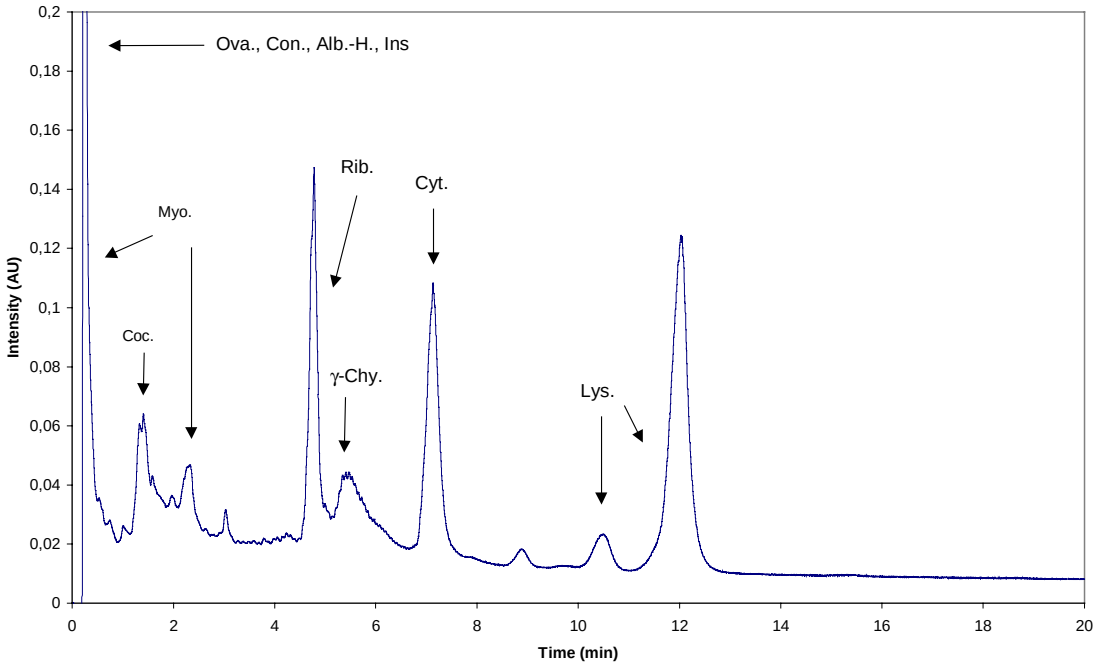


Figure 5.9 Incomplete separation of a 10 protein mixture after the first dimension using cation exchange chromatography

The first 12 RP chromatograms corresponding to the fractions transferred from the cation exchange column are displayed in Figure 5.10.

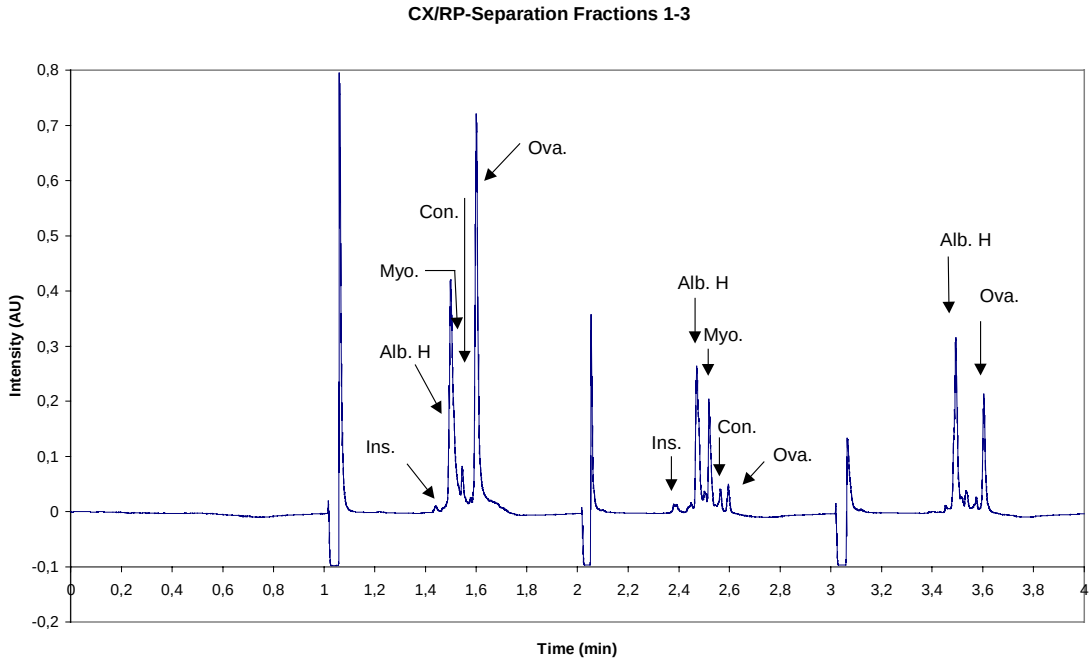


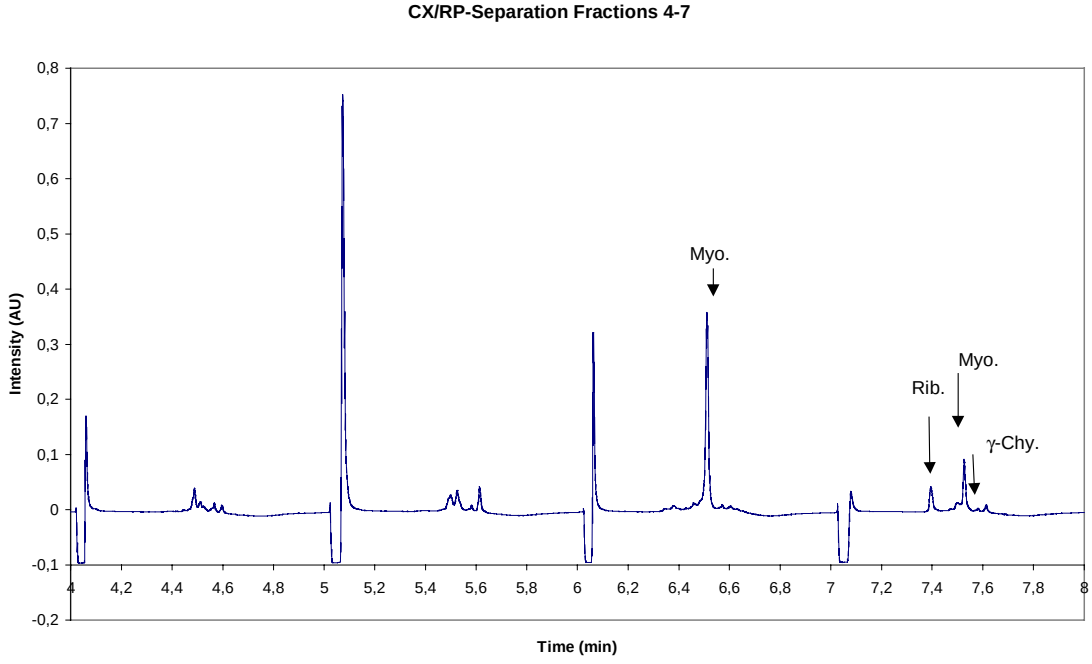

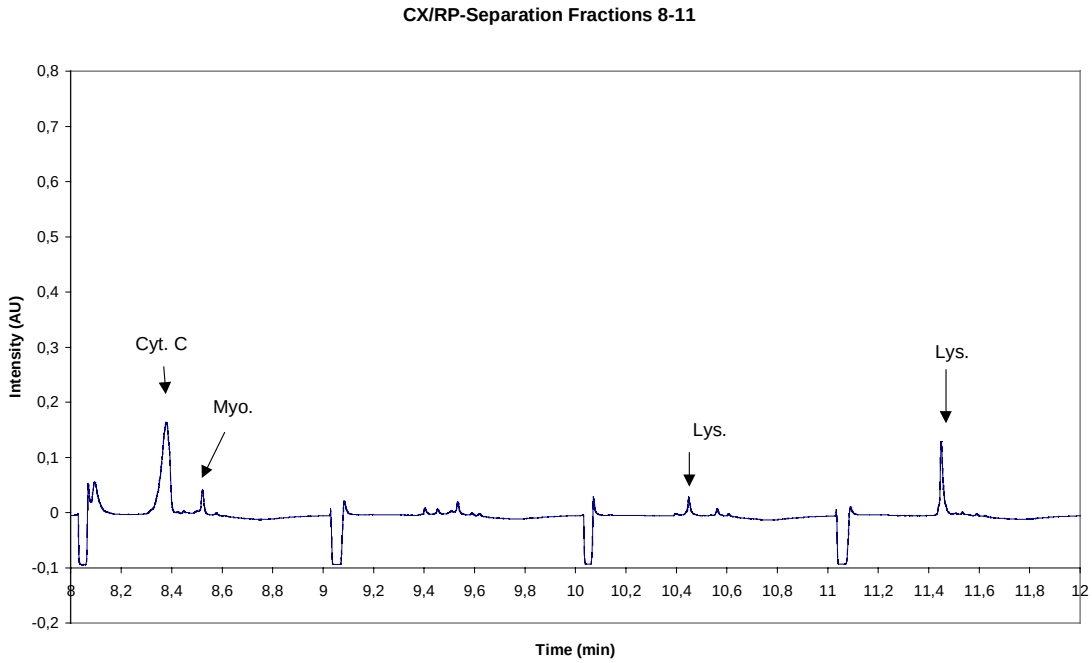


Figure 5.10 Reversed-phase chromatograms of the one-minute analyte fractions taken from the cation exchange column

In the cation exchange / RP-mode, principally the same findings were achieved compared to anion exchange chromatography in the first dimension. For the separation of the standard protein mixture, the peak capacity in the ion-exchange mode is the limiting factor, since proteins appear in adjacent fractions and are mostly baseline resolved in the RP-mode.

### 5.2.7 Repeatability of 2D-HPLC separations

Repeatability of the anion-exchange / RP-system in terms of retention time, peak height and peak area was based on determinations from all 31 peaks generated from the 11 proteins (some proteins appeared in several fractions from the ion-exchange column). The peaks were dedicated to a protein by their retention time generated in blank runs of each protein in the RP mode and their retention time in the single ion-exchange chromatogram.

Parameters derived from 15 chromatograms (n=15) generated in different runs under the same conditions resulted in a relative standard deviation (RSD) of the retention time of less than 1 % in average. The peak areas and peak heights determined by manual integration of each peak showed RSD values ranging from 10 to 20 % on the average. The repeatability data derived from 15 individual 2D runs are displayed in Table 5.1.

| Protein:<br>PI-value: | Rib.<br>9.6 | Ins.<br>5.7 | Cyt. C<br>10.6 | Lys.<br>11.0 | BSA<br>4.6 | Con.<br>5.9 |
|---|---|---|---|---|---|---|
| Average Retention Time [min] | 1.393 | 1.469 | 1.498 | 1.526 | 2.486 | 2.601 |
| Standard Deviation [min] | 0.018 | 0.011 | 0.010 | 0.010 | 0.014 | 0.011 |
| Percentage RSD [%] n=15 | 1.3 | 0.8 | 0.7 | 0.7 | 0.6 | 0.4 |
| Average Peak Area [µAU] | 175493 | 14242 | 210618 | 771973 | 452984 | 165335 |
| Standard Deviation [µAU] | 25619 | 4777 | 24191 | 58427 | 32021 | 17878 |
| Percentage RSD [%] n=15 | 14.6 | 33.5 | 11.5 | 7.6 | 7.1 | 10.8 |
| Average Peak Height [µAU] | 131979 | 13527 | 274981 | 749737 | 584525 | 217655 |
| Standard Deviation [µAU] | 24693 | 3214 | 26402 | 43845 | 50213 | 14485 |
| Percentage RSD [%] n=15 | 18.7 | 23.8 | 9.6 | 5.8 | 8.6 | 6.7 |

| Protein:<br>PI-value: | Myo.<br>7.6 | Ova.<br>4.7 | β-Lac. B<br>5.2 | β-Lac. A<br>5.1 | Try.-I.<br>4.6 |
|---|---|---|---|---|---|
| Average Retention Time [min] | 3.493 | 3.614 | 9.553 | 10.539 | 12.546 |
| Standard Deviation [min] | 0.015 | 0.018 | 0.010 | 0.017 | 0.014 |
| Percentage RSD [%] n=15 | 0.4 | 0.5 | 0.1 | 0.2 | 0.1 |
| Average Peak Area [µAU] | 179619 | 443174 | 222346 | 437714 | 8962 |
| Standard Deviation [µAU] | 19163 | 18780 | 21112 | 12568 | 1665 |
| Percentage RSD [%] n=15 | 10.7 | 4.2 | 9.5 | 2.9 | 18.53 |
| Average Peak Height [µAU] | 160624 | 478140 | 230810 | 542094 | 8204 |
| Standard Deviation [µAU] | 28958 | 59698 | 15460 | 54203 | 911 |
| Percentage RSD [%] n=15 | 18.0 | 12.5 | 6.7 | 10.0 | 11.1 |

Table 5.1 Repeatability data of selected peaks generated with the anion-exchange / reversed-phase HPLC-system (102.0 µg total protein amount)

The repeatability data for the cation-exchange / reversed-phase separations, also derived from 15 different runs, are displayed in Table 5.2.

| Protein:<br>PI-value: | Insulin<br>5.7 | Alb.-H.<br>5.9 | Ova.<br>4.7 | Myo.<br>7.6 | Rib.<br>9.6 | Cyt.<br>10.6 | Lys.<br>11.0 |
|---|---|---|---|---|---|---|---|
| Average Retention Time [min] | 1.433 | 1.495 | 1.620 | 2.537 | 7.411 | 8.385 | 11.467 |
| Standard Deviation [min] | 0.014 | 0.011 | 0.021 | 0.015 | 0.023 | 0.011 | 0.016 |
| Percentage RSD [%] n=15 | 1.0 | 0.7 | 1.303 | 0.6 | 0.3 | 0.1 | 0.1 |
| Average Peak Area [µAU] | 14611 | 431919 | 682538 | 133673 | 71748 | 439368 | 106825 |
| Standard Deviation [µAU] | 6345 | 52271 | 41508 | 17151 | 18877 | 76486 | 4199 |
| Percentage RSD [%] n=15 | 43.4 | 12.1 | 6.1 | 12.8 | 26.3 | 17.4 | 3.9 |
| Average Peak Height [µAU] | 10945 | 379397 | 619659 | 160606 | 89538 | 274920 | 131088 |
| Standard Deviation [µAU] | 1704 | 39630 | 74406 | 23406 | 45226 | 143205 | 6148 |
| Percentage RSD [%] n=15 | 15.6 | 10.4 | 12.0 | 14.6 | 50.5 | 52.1 | 4.69 |

Table 5.2 Repeatability data of selected peaks generated with the cation-exchange / reversed-phase HPLC-system (67.8 µg total protein amount)

The reproducibility data for the cation-exchange / reversed-phase chromatograms also derived from 15 different runs were in the same range compared to the use of anion exchange in the first dimension. The “within days variations” were similar to the “between days variations”, which proves the operational stability of the 2D-HPLC system.

### 5.2.8 Reproducibility

The reproducibility was checked according to ICH guidelines by setting up the device in two different laboratories in Mainz (Germany) and Lund (Sweden) showing the same results and performance. As described before, different types of HPLC-equipment were applied.

### 5.2.9 Recovery

The overall recovery of proteins on the cation-exchange / reversed-phase 2D-HPLC system was determined by comparing the total peak areas generated by a mixture of 6 standard proteins using either the cation-exchange / RP-column configuration or no column at all. The test mixture contained the proteins ribonuclease from bovine pancreas, cytochrom C from bovine heart, lysozyme from chicken egg white, myoglobin from horse heart, ovalbumin and albumin bovine at a total concentration of 6.621 mg/ml. 10 µl of the mixture diluted by a factor of 10 were injected and pumped through the tubing and detector, using 50 % acetonitrile (0.1 % TFA) in water (0.1 % TFA) approximating the reversed-phase elution conditions. The area of the resulting single peak multiplied by a factor of ten was compared to the total peak area of the non-diluted separated mixture. The peak area was calculated as the sum over all single peak areas determined by manual integration. The observed recovery depends on the total amount of proteins loaded and decreases with lower concentrations. At an intermediate amount of injected proteins (66.4 µg total amount) recovery was 70 % while decreasing to 22 % (6.6 µg total amount), which is close to the limit of detection. However, the limit of detection was out of the linear range of the system. It has to be mentioned, that the probability of systematic errors rises with decreasing peak areas.

### 5.2.10 Detection limits

At a wavelength of 215 nm proteins are detected by absorption in the peptide bonds, which is approximately four times more sensitive than detecting aromatic amino acids at a wavelength of 254 nm. The limit of detection depends on the extinction coefficient of the proteins. It was evaluated for a wavelength of 215 nm by injecting 10 µl of a six-protein mixture. The stock mixture was diluted by a factor of two until the limit of detection in the 2D-HPLC runs for all proteins was reached. This resulted in a detection limit of approximately 300 ng per protein, for some proteins (*e.g.* ovalbumin) 50 ng were still detectable. The limit of detection was considered to be at a peak height, which is three times higher than the average baseline fluctuation. The values for the detection limit (LOD), the linear range for quantification and the linear regression coefficient are shown in Table 5.3.

| Protein: | BSA | Ova. | Myo. | Rib. | Cyt. | Lys. |
|---|---|---|---|---|---|---|
| Average Retention Time [min] | 1.483 | 1.601 | 4.526 | 7.385 | 8.375 | 13.478 |
| Limit of Detection (LOD) [ng] | 178 | 53 | 324 | 325 | 152 | 168 |
| Lower Limit of Linearity [ng] | 356 | 213 | 648 | 650 | 305 | 336 |
| Upper Limit of Linearity [µg] | 11.4 | 13.7 | 10.4 | 20.8 | 9.8 | 10.8 |
| Linear Regression Coefficient ($R^2$): | 0.9982 | 0.9909 | 0.9925 | 0.9362 | 0.9928 | 0.9922 |

Table 5.3 Detection limits, and linear regression parameters for a 6-protein mixture at different concentrations applied to cation exchange / reversed-phase chromatography

### 5.2.11 Loadability

Column packing materials for ion exchange chromatography generally provide a higher loadability for proteins and peptides compared to reversed-phase supports. Therefore, the loadability of the 2D-HPLC system is limited by the small surface area of the non-porous 1.5 µm particles in the high-speed reversed-phase columns. Signs of column overloading appear at amounts above 1 mg total protein injected.

### 5.2.12 Linearity of peak area/peak height and protein amount

The linearity of peak height, peak area and the amount of each protein were checked evaluating six selected peaks from a cation exchange / RP-run at nine different concentration levels using a mixture of six standard proteins. This resulted in a linear correlation for average concentration levels. At higher protein amounts, the curve became more shallow until the maximum loadability of the system at approximately 100 µg per protein was reached. Deviations from the linear correlation also occurred at a concentration level close to the detection limit where the peak areas were smaller than expected assuming a linear correlation. The regression coefficient ($R^2$) for the linear part of the curve for each protein is shown in Table 5.3. An example for the linearity of

protein amount and peak area are given in Figure 5.11, where the data is shown for a specific ovalbumin peak, derived from the cation exchange / RP-runs.

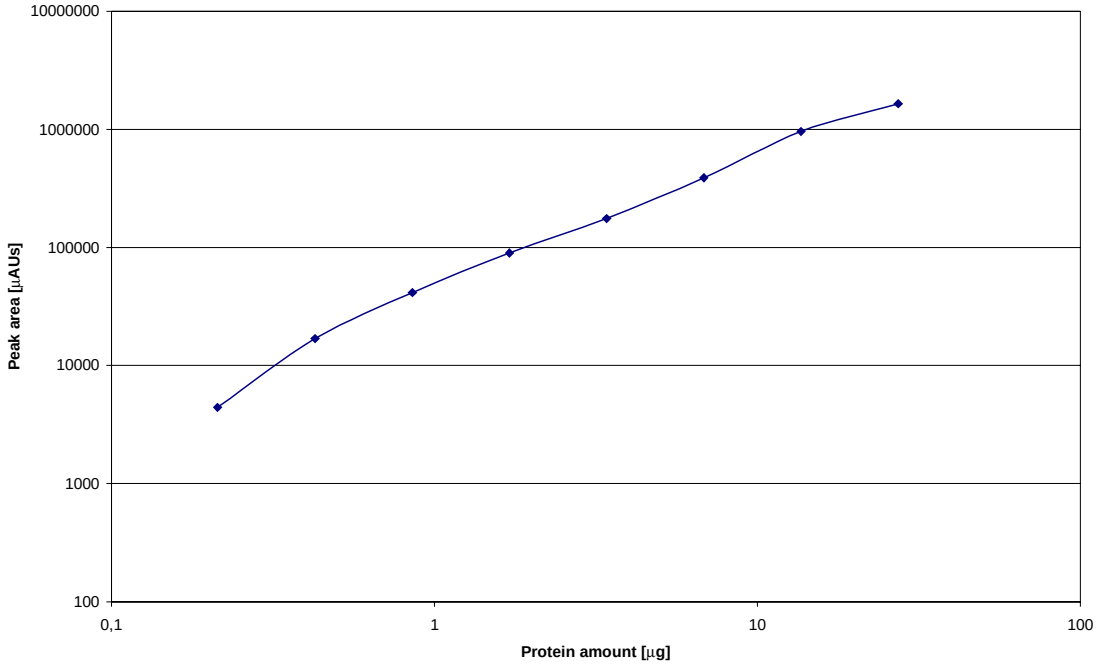


Figure 5.11 Correlation between protein amount and the peak area for ovalbumin

## 5.2.13 Stability test using cell-line supernatant as a matrix

In order to evaluate the applicability and stability of the system, a soluble extract from human fibroblasts grown in culture was used. The samples were spiked with a mixture of six standard proteins at a total concentration of 3.3 µg/µl. The human fibroblast cell model supernatant was made using human lung fibroblast cultures from ATCC (CCL-153) provided by American Type Culture Collection, Rockville, MD, USA. The cultures were permitted to grow to confluence for 48 h in T 75 flasks and harvested by scraping the cells. The cell layer was washed three times with 3 ml cold PBS (phosphate buffered saline), thereafter centrifuged at 40,000 g (4 °C, 20 min). The pellet was resuspended in PBS buffer and sonicated for 40 s. A second centrifugation was performed again at 40,000 g (4 °C, 30 min), after this, the supernatant was subjected to ultrafiltration using a 30 kDa cut-off membrane (YM30, Amicon Inc., Beverly, MA, USA). The total protein content of the sample was measured by Bradford principle based photometric determination using the protein assay reagent Coomassie Plus provided by Pierca,

Rockford, IL, USA. The protein concentration was measured at a wavelength of 595 nm to be less than 0.25 mg/ml using albumin bovine as a standard.

10 µl of the spiked sample was applied to the cation exchange / reversed-phase 2D-HPLC. The repeatability data for 13 consecutive fully automated runs are shown in Table 5.4.

| Protein: | BSA | Ova. | Myo. | Rib. | Cyt | Lys. |
|---|---|---|---|---|---|---|
| Average Retention Time [min] | 1.483 | 1.601 | 4.526 | 7.385 | 8.375 | 12.439 |
| Standard Deviation [min] | 0.0073 | 0.0040 | 0.0162 | 0.0090 | 0.0105 | 0.0046 |
| Percentage RSD [%] n=13 | 0.5 | 0.3 | 0.4 | 0.1 | 0.1 | 0.1 |
| Average Peak Area [µAU] | 355870 | 431554 | 65081 | 120547 | 312462 | 223021 |
| Standard Deviation [µAU] | 19474 | 28987 | 5705 | 1697 | 31828 | 24358 |
| Percentage RSD [%] n=13 | 5.5 | 6.7 | 8.8 | 14.1 | 10.2 | 10.9 |
| Average Peak Height [µAU] | 433433 | 474348 | 113259 | 107968 | 264440 | 310409 |
| Standard Deviation [µAU] | 28331 | 17841 | 25209 | 29860 | 133148 | 39458 |
| Percentage RSD [%] n=13 | 6.5 | 3.8 | 22.3 | 27.7 | 50.4 | 12.7 |

Table 5.4 Repeatability data (n = 13) of cation exchange / reversed-phase chromatography of fibroblast cell culture supernatant spiked with six standard proteins

The data for selected peaks corresponding to a specific spiked protein indicates that even after 13 runs deterioration of chromatographic resolution was not observed and no column clogging or increase of the pressure drop occurred. Unattended operation was applied overnight running these cell samples. The RSD in retention times was less than 0.5 %, (n=13) in the same range as we found for standard samples. The quantitative data in terms of peak height were found to vary in between 5 % and 15 %. The data demonstrated that the 2D-HPLC set-up worked reliable even in the presence of a diluted biological matrix.

The protein concentration of the human lung fibroblast sample was too low to monitor at any separation after the reversed-phase dimension, using UV-detection. However, the lack of higher concentrated samples of the target analytes requires an enrichment step, *e.g.* using restricted access materials.

## 5.3 Size-selective sample fractionation using novel restricted access columns

Two novel restricted access materials (RAM) were applied as column packings being research products of Merck KGaA. IEX-DS (Ion-EXchange Diol Silica) is a spherical LiChrospher 60 based silica. The outer surface is modified exclusively with electroneutral diol-groups whereas the inner particle surface either carries cationic (diethylaminoethyl) or anionic (sulfonic acid) functional groups. The average pore size of the IEX-DS material is 6 nm and the column dimensions are 25 mm x 4 mm I.D.

For comparative experiments an analogue reversed-phase material namely ADS (Alkyl Diol Silica) which is commercially available from Merck KGaA, Darmstadt, Germany as a LiChrospher ADS RP-18 column (25 mm x 4 mm I.D.) was used.

### 5.3.1 Operation of RAM columns for sample fractionation

The starting condition for the reversed-phase RAM column was A = water (0.1 % TFA) while the elution was made with B = acetonitrile (0.1 % TFA). The eluents for the cation exchange RAM column and the analytical cation exchanger were A = 10 mM phosphate buffer at pH = 3.0 and B = 1 M phosphate buffer at pH = 3.0. The corresponding eluents for the anion exchange RAM column and the analytical anion exchanger consisted of A = 10 mM phosphate buffer at pH = 7.0 and B = 1 M phosphate buffer at pH = 7.0.

### 5.3.2 Assessment of RAM column performance by standard proteins

The basic performance of the two different ion exchange RAM types were assessed by injecting standard proteins of different molecular weights applying pH conditions that are appropriate for adsorption of the analytes on the inner surface.

40 µl albumin bovine (BSA) with a molecular weight of approximately 66 kDa were loaded onto the $SO_3H$-RAM column applying buffer A at a flow rate of 0.6 ml/min. After 15 min column washing time for BSA and 20 min washing time for aprotinin, a gradient from 100 % A to 100 % B within 20 min was started. The elution profile is displayed in Figure 5.12, indicating that the albumin bovine (66 kDa) was almost completely eluted in the void volume of the column as expected by theory.

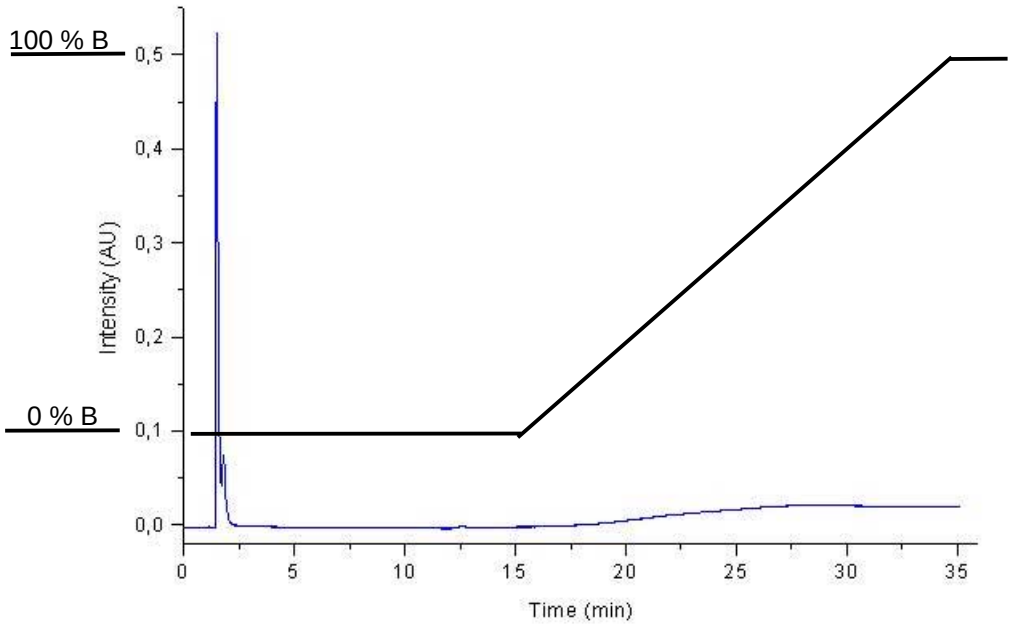


Figure 5.12 Albumin bovine (BSA) with a molecular weight of approximately 66 kDa applied to a $SO_3H$-RAM column, albumin is almost completely eluted in the void volume of the RAM column

The opposite case is shown in Figure 5.13, where aprotinin with a molecular weight of approximately 7.8 kDa was loaded onto the $SO_3H$-RAM column. For evaluation of the column loadability, 500 µg were injected under the same conditions as previously. The aprotinin was almost completely adsorbed at a low ion strength and desorbed while increasing the ionic strength.

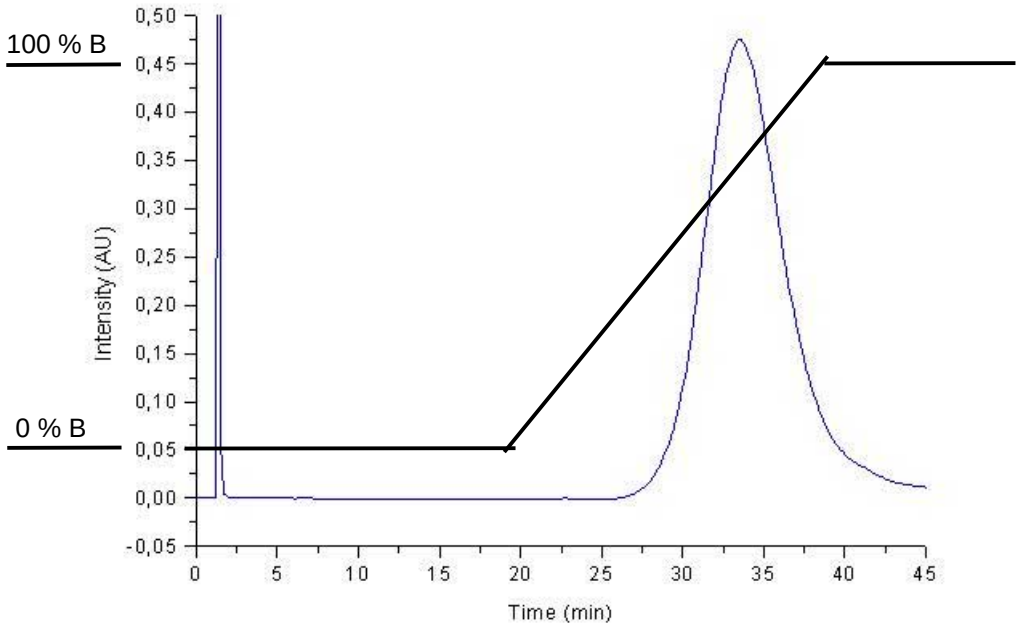


Figure 5.13 Aprotinin with a molecular weight of approximately 7.8 kDa applied to a $SO_3H$-RAM column, aprotinin was almost completely retained on the column

Experiments using cytochrome C (12.3 kDa), lysozyme (14.3 kDa) and ribonuclease A (13.7 kDa) confirm the molecular weight cut-off to be around 15 kDa since the reference substances appear in the void volume of the column as well as in the retained fraction.

The same findings proving the principal applicability of ion exchange RAM for size selective fractionation of proteins where achieved for the DEAE-RAM column using insulin α-chain (2.53 kDa) as the low and ovalbumin (43.5 kDa) as the high molecular weight standard protein.

### 5.3.3 Assessment of RAM column performance by SDS-PAGE and comparison to ultrafiltration

Human hemofiltrate was used as a reference sample for the characterisation of the 2D-HPLC-system and the size-selective sample fractionation step. It was obtained as a lyophilised powder from IPF PharmaCeuticals GmbH, Hannover, Germany. The human blood ultrafiltrate was produced during the dialysis of patients suffering from chronic renal disease using a 30 kDa membrane. Proteins and peptides were isolated in a single step of preparative cation exchange chromatography.

#### 5.3.3.1 Sample fractionation by ultrafiltration

3 ml human hemofiltrate at a concentration of 50 µg/µl were subjected to ultrafiltration through a 10 kDa membrane (YM-10, Amicon, Inc., Beverly, MA, USA) using a 3 ml chamber equipped with a magnetic stirrer while applying an air pressure of 3 bar. 20 µl of the filtrate was analysed by SDS-PAGE for comparison.

#### 5.3.3.2 Sample fractionation by RAM columns

A typical chromatogram of the elution profile from the $SO_3H$-RAM column is shown in Figure 5.14. After 6 min run time, the RAM column was loaded with 100 µl (50 µg protein/µl) of human hemofiltrate at a flow rate of 0.2 ml/min applying buffer A. After 12 min elution of the matrix a linear gradient from 0 to 100 % B within 16 min was started to elute the low molecular weight target analytes from the RAM column.

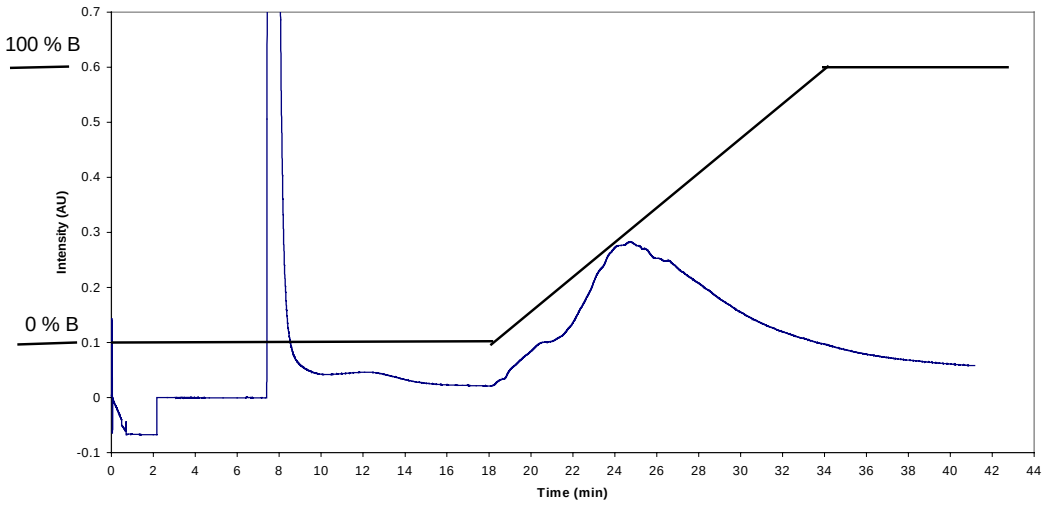


Figure 5.14 Elution profile of the human hemofiltrate sample from the $SO_3H$-RAM column

The two peaks achieved are characteristic for the high molecular weight fraction in the intraparticle volume of the column and the low molecular weight fraction retained on the inner surface of the RAM particles.

Human hemofiltrate contains amounts of remaining ammonium acetate from the production process. To investigate the influence of salt on the retention behaviour, the sample was desalted using a disposable gel filtration desalting column PD-10 containing Sephadex G-25 M from Pharmacia Biotech, Uppsala, Sweden. The gravity operated cartridges have a bed volume of 9.1 ml and a bed height of 5 cm. After equilibrating the column with water, 2.5 ml hemofiltrate (50 mg/ml in 0.01 M $KH_2PO_4$, pH = 3.0) were loaded. The protein fraction was eluted between 2.5 and 6 ml elution volume while the salt eluted afterwards. However, no difference between crude and desalted sample was obvious in retention on the RAM column.

#### 5.3.3.3 SDS-PAGE analysis of fractions generated by RAM columns

The column flow rate for loading the RAM column and elution of high molecular weight components (matrix) was 0.2 ml/min applying buffer A. The column was washed for 12 min to elute the matrix quantitatively. Elution of the retained fraction from the RAM column was performed at a flow rate of 0.2 ml/min using a step elution applying 100% eluent B.

The RAM columns (RP-18, DEAE, and $SO_3H$) investigated, were loaded with 100 µl (50 µg protein/µl) of human hemofiltrate. The sample was dissolved in the initial eluent and the pH was adjusted accordingly prior to loading onto the RAM column. After injection, the matrix was eluted with the void volume and the column was washed for 12 min by applying the appropriate initial eluent A conditions. Elution was performed with 100 % B until the 215 nm UV-signal approached the baseline again. The eluted peaks were collected and subjected to SDS-PAGE analysis. To increase the sample concentration in the lower molecular weight fractions eluted from the RAM column, an enrichment step was applied.

The eluted RP-18 RAM fraction was enriched by evaporating the acetonitrile and TFA by vacuum centrifugation (SpeedVac Plus SC210A, Savant Instruments Inc., Farmingdale, NY, USA). The residue was redissolved in 100 µl 10 mM phosphate buffer of pH 3. The enrichment and desalting of the ion exchange RAM fractions were performed using StrataClean$^{TM}$ resin (Stratagene Cloning Systems, La Jolla, CA, USA). The solid phase silica-based resin modified with a hydrophobic surface reversibly adsorbed the proteins. 40 µl StrataClean$^{TM}$ resin slurry was suspended in each of the retained ion exchange RAM fractions (approximately 2.5 ml) for 30 min.

The suspensions were centrifuged at 12,000 g for 10 min. The supernatant was discarded and the complete pellet was resuspended in 25 µl sample buffer for protein desorption. 20 µl of the ultrafiltrated fraction and 20 µl of the crude human hemofiltrate sample were mixed with 25 µl sample buffer. 5 µl 0.5 M DL-dithiothreitol (DTT) were added to all the samples, which were heated in a water bath (70 °C) for 10 min prior to loading (28 µl) on a 16 % tricine gel (Novex, Frankfurt, Germany). This gel provided a

high resolving power for the molecular weight range from 2 kDa to 20 kDa. The sample buffer was 25 % 0.5 M tris-HCl buffer at pH = 6.8, 20 % glycerol, 40 % SDS, 5 % bromophenol blue. The running buffer was 2.9 % tris base, 14.4 % glycine and 1 % SDS. The samples were analysed at 125 V for 1 h and 40 min until the dye front reached the lower end of the gel. The electrophoresis equipment was from Novex. The molecular weight markers were Novex Mark 12 and Kaleidoscope Prestained Standard (Bio-Rad, Krefeld-Oppum, Germany).

The resolved proteins were visualised by silver staining. After 60 min fixation (50 % ethanol, 50 % acetic acid) the gel was washed in 50 % ethanol for 30 min and for further 30 min in water. The gel was incubated in sensitiser (0.02 % sodium thiosulfate) for 1 min. After rinsing with two changes of water (1 min each) the gel was incubated in staining solution (0.1 % silver nitrate) for 30 min. After rinsing in water the gel was developed in 0.04 % formaldehyde, 2 % sodium carbonate for 30 s. The first solution was discarded and replaced by a fresh one. 8 min were chosen as an appropriate developing time. To stop the development the gel was placed in 5 % acetic acid for 15 min and rinsed two times with water.

Figure 5.15 shows an image of the slightly overstained SDS-gel where different RAM extracts, the crude hemofiltrate sample and the ultrafiltrated sample were analysed.

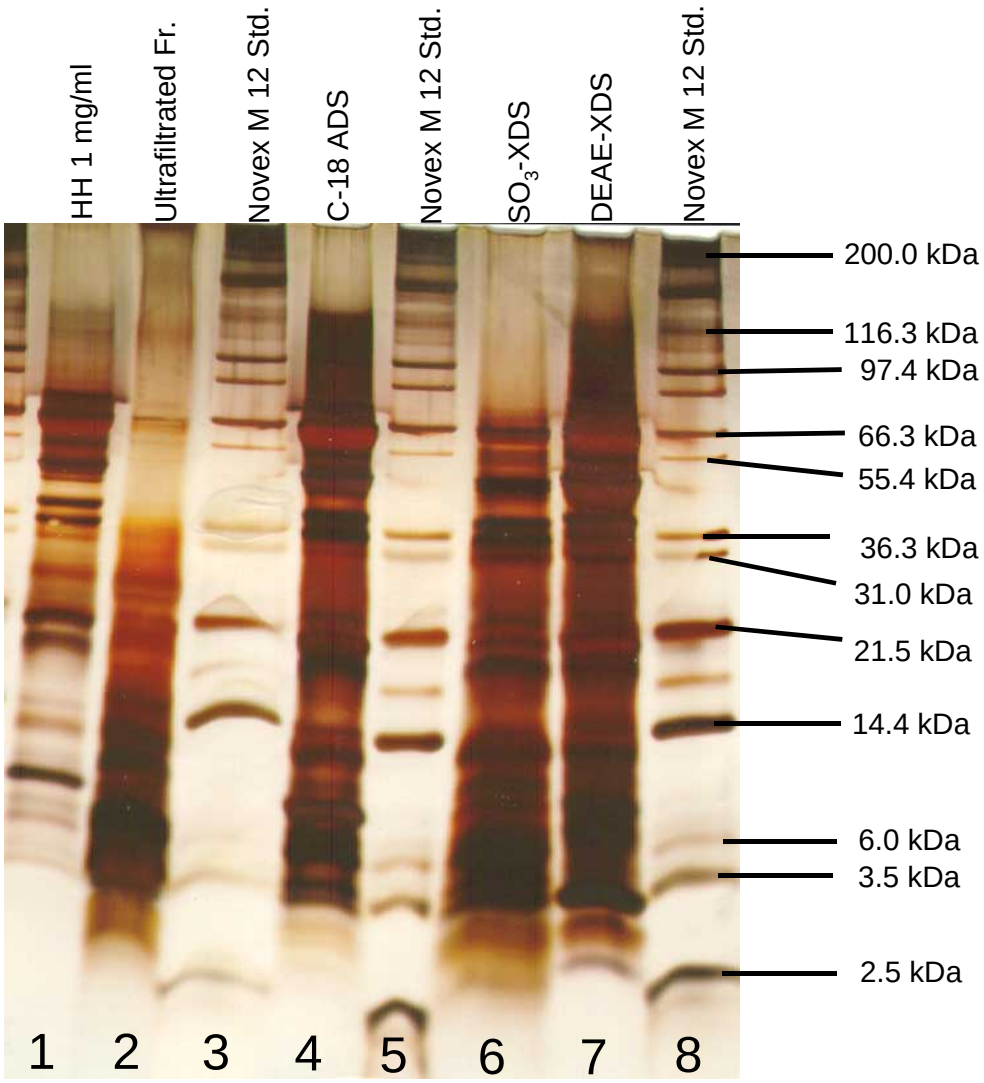


Figure 5.15 Characterisation of RAM performance by SDS-PAGE – different amounts were loaded onto the gel

Track 1 was loaded with the human hemofiltrate sample at a concentration of 1 mg/ml (11 µg protein). Even though silver staining is only quantitative over a limited range, human serum albumin is visible as the most intensive band. Compounds below 15 kDa are in low abundance and appear as low intensity silver stained bands. Track 2 displays a 50 times higher concentrated hemofiltrate sample after ultrafiltration using a 10 kDa membrane (low mw fraction out of 550 µg protein). Human serum albumin was almost completely eliminated, while proteins and peptides below approximately 30 kDa were enriched. Track 4, 6 and 7 show the separation of the retained fraction on different RAM columns. All columns showed an enrichment of lower molecular mass

components and a reduction in the high molecular mass fraction of the sample. Comparable amounts of retained proteins from the $SO_3H$-RAM column and DEAE-RAM column were loaded onto the gel (low mw fraction out of 5,000 µg protein). The low molecular weight fractions eluted from the anion- and cation exchange RAM columns show less binding of human serum albumin compared to the LiChrospher RP-18 ADS column (low mw fraction out of 1,000 µg protein). Non-specific binding of human serum albumin can be explained by interactions between the albumin and remaining silanol groups on the outer RAM surface carrying the biocompatible diol moiety. However, inspection of the gel clearly demonstrated the enrichment of components with a molecular weight lower than approximately 15 kDa, a continuous molecular weight cut-off and some non-specific binding of higher molecular weight components. It should be noted that the protein load onto the gel from the RAM fractions was a 100 times higher compared to the crude hemofiltrate sample.

### 5.3.4 Quantification of the non-specific binding of high molecular weight proteins and recovery from $SO_3H$-RAM columns by UV-detection

The total recovery and the share of non-specifically bound high molecular weight proteins to the RAM-columns was investigated injecting albumin bovine (66 kDa), alcoholdehydrogenase (150 kDa) and β-amylase (200 kDa) at different amounts onto the $SO_3H$-RAM columns. The eluents were A = 10 mM $KH_2PO_4$, at pH = 3.0 and B = 1 M $KH_2PO_4$, at pH = 3.0. The column flow rate was 0.4 ml/min. The gradient profile started after the injection with 100 % A which was maintained for 12 min. From 12-17 min a linear gradient ran to 100 % B which was maintained for 5 min before applying the initial conditions for regeneration. UV-detection was performed at 254 nm. The values for recovery and non-specifically bound proteins were calculated by integrating the peak areas of the non-retained fraction, the retained fraction and the peak generated without using any column.

The data of the total recovery and the share of the non-retained fraction for three standard proteins at different protein amounts are shown in Figure 5.16.

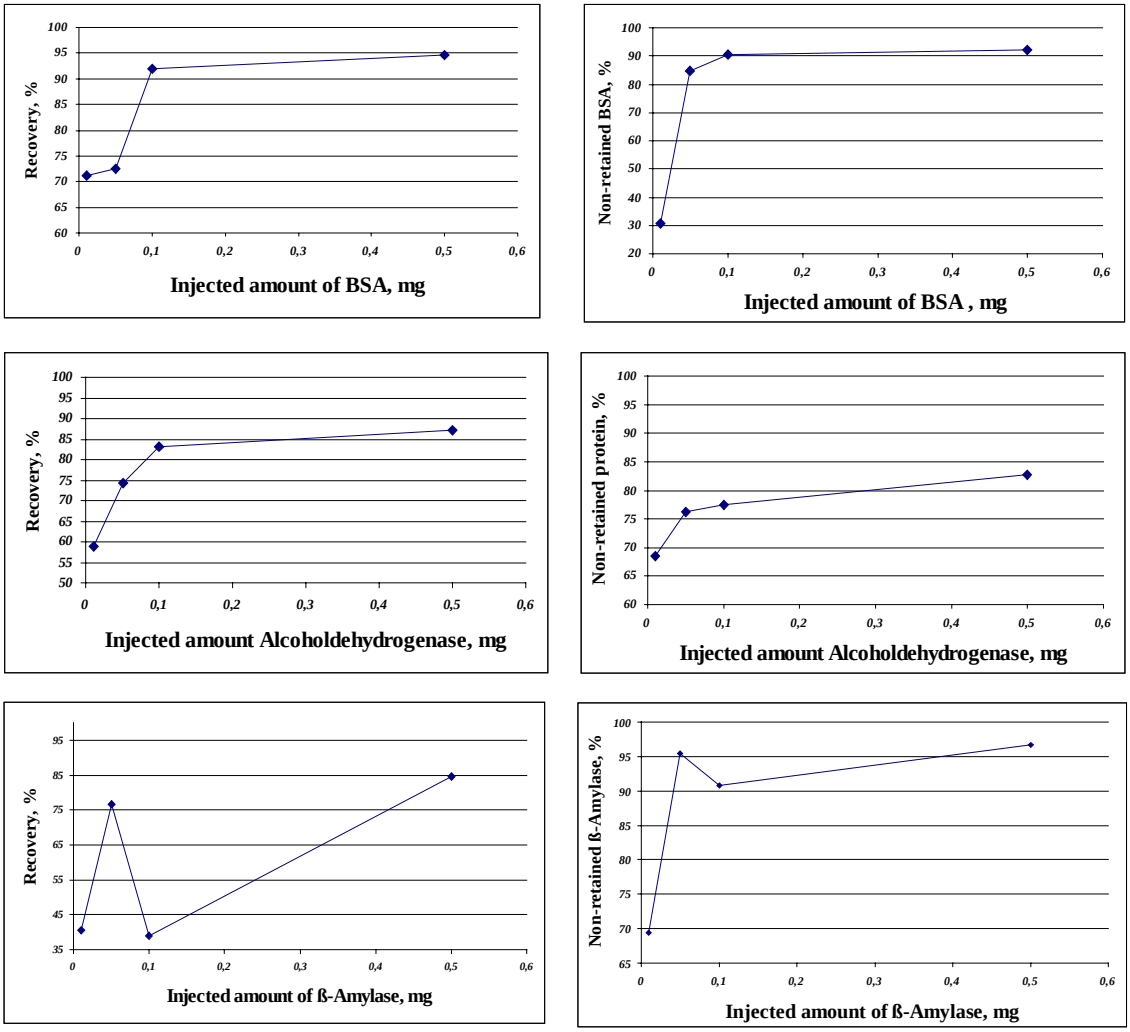


Figure 5.16 Total recovery and the share of non-retained protein for albumin bovine (66 kDa), alcoholdehydrogenase (150 kDa) and β-amylase (200 kDa) at different amounts loaded onto the $SO_3H$-RAM column

The data clearly confirm that there is no influence of the molecular weight on the non-specific binding to the RAM phase. This indicates that the proteins are bound to the outer surface of the RAM possibly due to remaining free silanol groups. The same access to the pore structure for different sized proteins is improbable. The percentage of non-specifically bound proteins decreases with the total amount of protein injected onto the column. This also indicates that there is a certain amount of binding sites available on the outside surface of the RAM-columns. At protein load of 500 µg, the non-specific protein binding is less than 8 % for BSA and β-amylase. For the injection of low protein amounts, the RAM column dimensions should be decreased to achieve high recoveries whereas the loadability will decrease. A new batch of $SO_3H$-RAM columns with a

higher diol group concentration will be investigated in the future to avoid non-specific binding. The recovery for aprotinin (7.8 kDa) which was quantitatively bound on the column was determined to be 97 % at a column load of 100 µg.

### 5.3.5 Quantification of non-specific bound albumin bovine using $^{14}$C-methylated BSA

A second approach for quantification is the use of radio-labelled proteins like $^{14}$C-methylated BSA for exact evaluation without using UV-detection. Albumin bovine at a concentration of 1 mg/ml was spiked with $^{14}$C-methylated BSA leading to a total concentration of 1.022 mg/ml. 1 ml of $^{14}$C-methylated BSA provided an activity of 5 µCi and contained 56 µg BSA. The sample was diluted by a factor of 100 and 100 µl were loaded onto the $SO_3H$-RAM column applying eluent A at a flow rate of 0.4 ml/min. After 12 min 4.8 ml eluent were collected containing the non-retained fraction. Thereafter, eluent B was applied for 12 min at the same flow rate and 4.8 ml were collected containing the retained fraction. In each case 0.5 ml of the sample were mixed with 5 ml of Ultima-Gold scintillation liquid from Packard BioScience, Meriden, CT, USA. The activity in both samples was measured in counts per minute over a time of 10 min. The percentage of non-specifically bound BSA was determined to 33 % for an injection of 1.022 µg $^{14}$C-methylated BSA. It has to be pointed out that those measurements showed a bad repeatability.

## 5.4 Sample transfer from the RAM to the analytical ion exchange column

The RAM columns are generally eluted in a backflush-mode, in-line with the analytical column. This in-series column coupling is susceptible to band broadening due to extra column volume and longitudinal diffusion. Band broadening can be avoided if the binding affinity to the second column is stronger than to the first column and gradient elution is applied.

The effect of band broadening was evaluated with aprotinin (7.8 kDa) as a standard protein. 100 µl aprotinin at a concentration of 1 mg/ml were loaded onto the $SO_3H$-RAM column at a flow rate of 0.2 ml/min applying 100 % eluent A = 0.01 M $KH_2PO_4$ , pH = 3.0. After 6 min column washing, the RAM column was back-flush eluted in-line with the cation exchange column at a flow rate of 0.8 ml/min. The gradient ran from 0 %-100 % B = 1.00 M $KH_2PO_4$, pH = 3.0 within 30 min. The elution profile of the coupled columns was compared to the elution profiles where the protein was directly injected onto the analytical or RAM column applying the same conditions. Figure 5.17 shows the elution profile from the RAM column, the elution profile after direct injection onto the analytical ion exchange column and the elution profile of the coupled column approach.

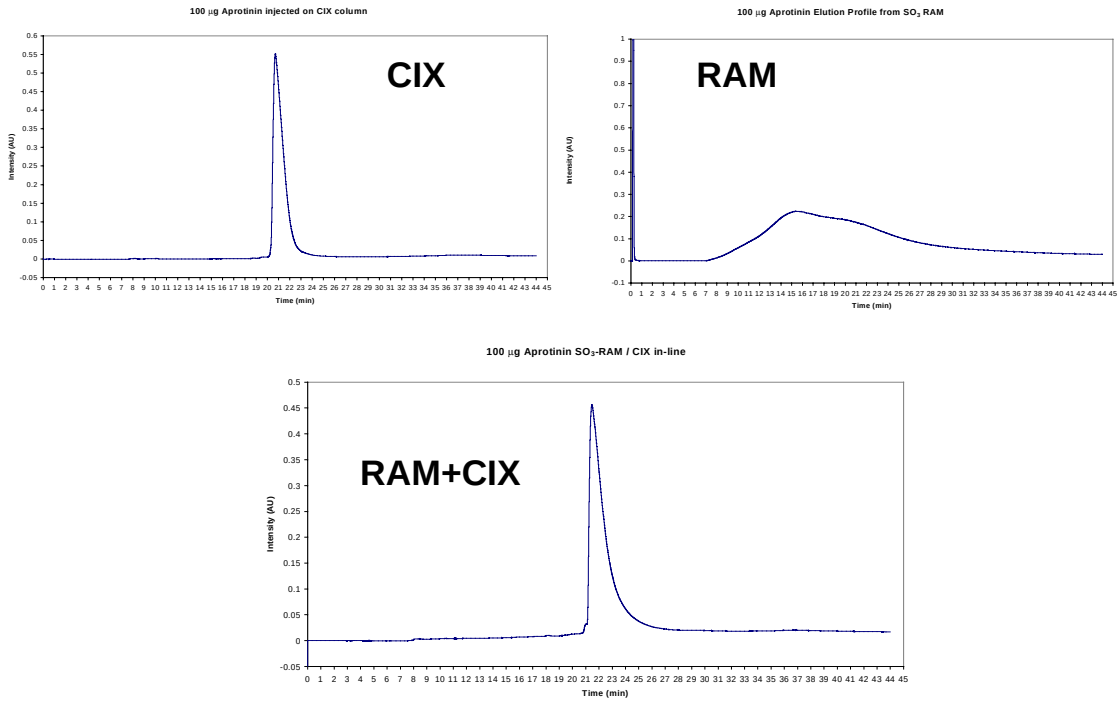


Figure 5.17 Assessment of band broadening due to sample transfer from RAM to the analytical ion exchange column

The comparison of the above described methods proved that band broadening was negligible. However, alternative concepts for sample transfer were investigated. Aprotinin as a standard protein was eluted from the RAM column in a back-flush mode applying a salt pulse of 100 % eluent B at a flow rate of 0.02 ml/min. This was applied for 160 min corresponding to a volume of 3.2 ml which was proven to be sufficient to elute the protein quantitatively. The effluent from the RAM column was mixed with water using a tee-piece which was coupled to the analytical ion exchange column. The water was pumped at a flow rate of 1.6 ml/min, thus the ratio for this dilution was 1:80 which should be adequate to enrich the protein onto the column head of the analytical ion exchange column. However, this post-column dilution technique proved to be not applicable due to severe sample losses. Only very small amounts of aprotinin were found on the analytical cation exchange column. Tuning of the dilution ratio did not result in any improvements.

## 5.5 Requirement for system modification analysing complex samples

Figure 5.18 shows a two-dimensional separation after the reversed-phase column using human hemofiltrate as a complex sample and the fast 2D-HPLC system comprising of two parallel RP-columns. Even though the fractionation interval was extended from one to two minutes, the gradient time is not sufficient to separate complex mixtures. Additionally, the time for adequate regeneration of the RP-columns limits the maximum gradient time. Furthermore, proteins in a high abundance (*e.g.* human albumin) mask other proteins. Higher resolving power is expected for peptides rather than for proteins. The limitations described can be overcome by integrating a size selective fractionation step and a 2D-HPLC system using significant longer gradient times in the second dimension by separate column regeneration and parallel gradient elution.

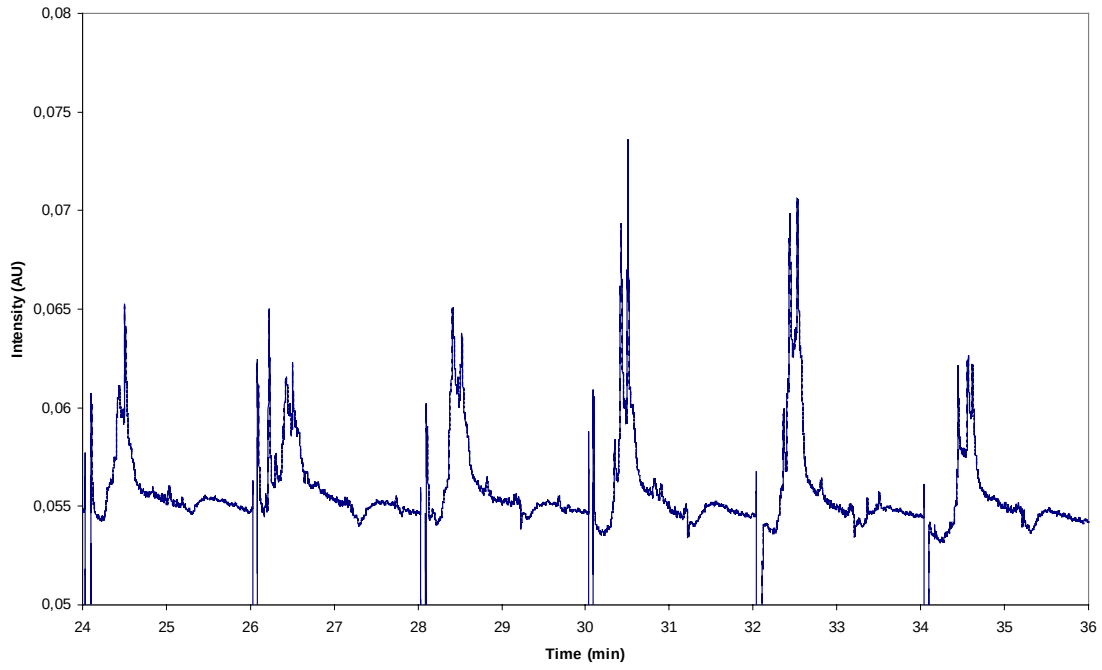


Figure 5.18 Selected RP-chromatograms from a cation exchange / RP-separation of human hemofiltrate using fractionation intervals of 2 min

## 5.6 Comprehensive on-line 2D-HPLC system for protein separation using four parallel reversed-phase columns and integrated size selective sample fractionation

The new coupled column system integrated a size selective sample fractionation step and the second dimension was doubled applying four parallel RP-columns. Thereby the gradient duration was doubled and time for column regeneration was saved. A schematic of the comprehensive on-line 2D-HPLC set-up including size selective sample fractionation is shown in Figure 5.19.

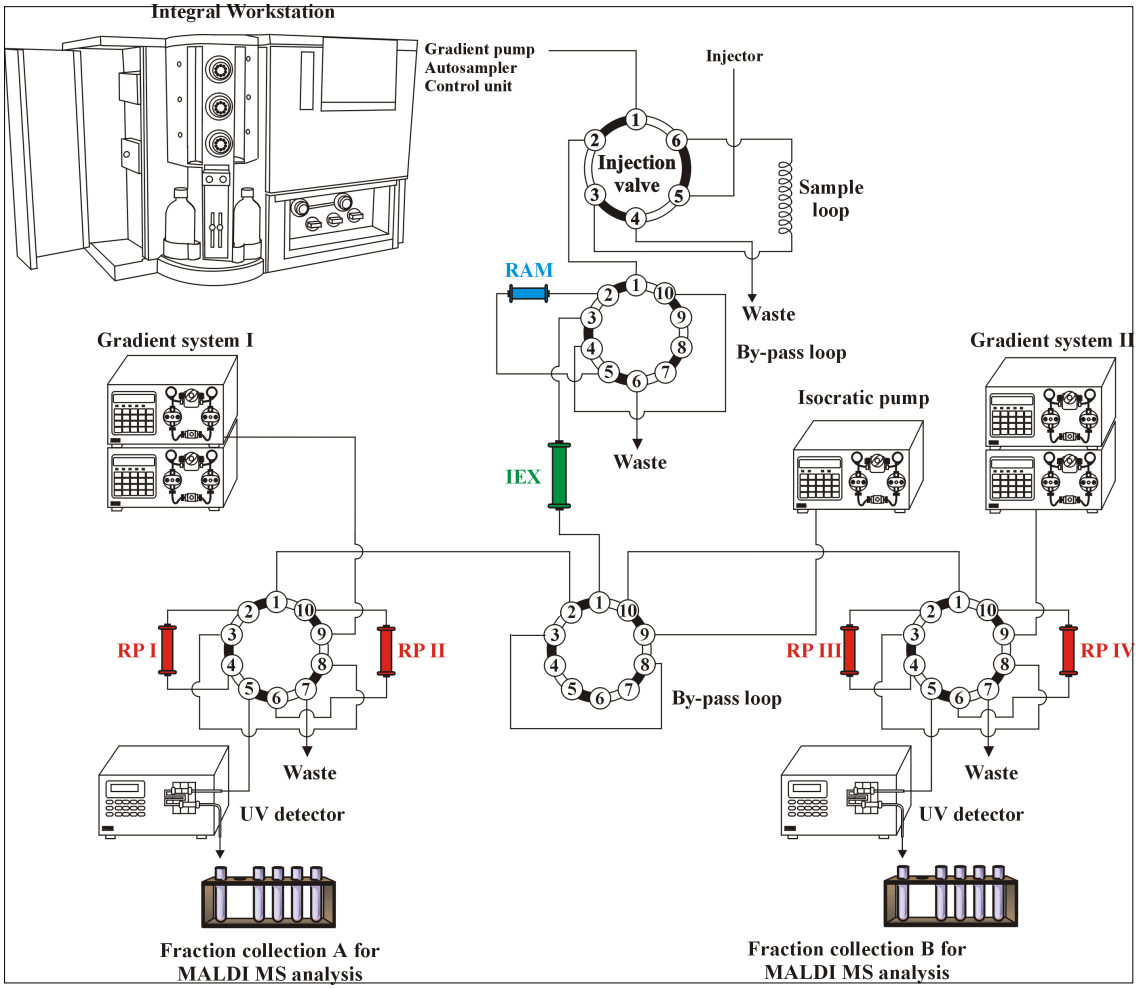


Figure 5.19 Schematic of the comprehensive on-line 2D-HPLC set-up including size selective sample fractionation

### 5.6.1 Operation of the 2D-HPLC system

The column arrangement was fully automated and controlled by the Integral™ 100Q Workstation. The workstation provides a high pressure gradient HPLC system comprising of an UV detector, a refrigerated autosampler and three ten-port valves. Two HPLC gradient systems, a pump and two more ten-port valves were added to build up the total system. The first ten-port valve served as an injector while the second ten-port valve was used for column switching in the sample fractionation step. In valve position A, the lower molecular weight target analytes were enriched on the internal surface of the RAM packing while the matrix and larger proteins were eluted directly to waste.

After valve switching, the RAM column was connected in a backflush mode in-series with the ion exchange column. During the 96 min gradient time of the ion exchange column a total number of 24 fractions were further analysed. Each fractionation occurred over 4 min (corresponding to 2 ml effluent per fraction) and was subsequently transferred to the second dimension. The fractions eluting from the first dimension were enriched on top of one reversed-phase column and desalted, while the aqueous elution buffer was directed to waste. At the same time the second column was regenerated with water while the two other columns were eluted in parallel by the two separate gradient systems. Each column was subjected to cyclic sample enrichment (sample loading), elution and regeneration. The lower three ten-port valves in Figure 5.19 were used for column iteration. Table 5.5 shows the valve positions for the reversed-phase column iteration and the column operating modes over the complete run time.

| Time [min] | Valve 1 position | Valve 2 position | Valve 3 position | Column 1 function | Column 2 function | Column 3 function | Column 4 function |
|---|---|---|---|---|---|---|---|
| 4 | A | A | A | deposit | elute II | regenerate | elute I |
| 8 | B | A | B | elute I | regenerate | deposit | elute II |
| 12 | A | B | B | elute II | deposit | elute I | regenerate |
| 16 | B | B | A | regenerate | elute I | elute II | deposit |
| 20 | A | A | A | deposit | elute II | regenerate | elute I |
| 24 | B | A | B | elute I | regenerate | deposit | elute II |
| 28 | A | B | B | elute II | deposit | elute I | regenerate |
| 32 | B | B | A | regenerate | elute I | elute II | deposit |
| ... | ... | ... | ... | ... | ... | ... | ... |
| 96 | B | B | A | regenerate | elute I | elute II | deposit |

Table 5.5 Column operational parameters indicating valve positions and reversed-phase column iteration procedure for the 2D-HPLC system.

Three of the ten-port valves are integrated in the Integral™ 100QWorkstation, pneumatically operated and made of PEEK (Rheodyne, Rhonert Park, CA, USA). Two external electrically driven ten-port valves (Valco Instruments Co. Inc, Houston, TX, USA) were controlled by electrical contact closures from the Integral™ 100Q workstation. Home made electronics converted TTL or 12 V pulses from the workstation into contact closures. Two individual high-pressure gradient systems were used for the second dimension. One system consisted of two HPLC pumps model 2200 and a Central Processor model 7110 for gradient control (Bischoff Analysentechnik, Leonberg, Germany). The second pump set consisted of two LC-10 AD pumps (Shimadzu, Kyoto, Japan). Both reversed-phase gradient systems performed individual gradient control while the start signal was triggered by an electrical contact closure from the workstation. Gradient mixing was performed using two dynamic low void volume mixing chambers (Bischoff Analysentechnik). An isocratic pump (LKB 2150, Pharmacia, Uppsala, Sweden) was used for column regeneration. To minimise void volume, tubing lengths were kept to a minimum and an inner diameter of 0.127 mm for the PEEK tubing was used (Upchurch Scientific, Oak Harbor, WA, USA). One UV-detector was part of the workstation and equipped with a 1.2 µl flow cell, while the second detector was a Lambda 1000 (Bischoff Analysentechnik) equipped with a 0.8 µl flow cell. Both detectors were operated at a wavelength of 215 nm. Data from the second detector were imported as an analogue auxiliary detector signal into the software. The complete procedure to control the 2D-HPLC system was programmed in the method editor software of the workstation. The samples were stored in 1.2 ml vials at 3º C in the temperature controlled autosampler tray. Injections were automatically performed by filling a 100 µl sample loop. Real-time monitoring the UV-absorption after the first dimension during a multidimensional run was not possible, as the pressure drop between the columns of the first and the second dimension, which are linked through a valve, would have destroyed the detector cell. The chromatogram after the first dimension was made in a single column mode.

A photograph of the entire separation platform and a magnification of the column and switching valve arrangement is shown in Figure 5.20.

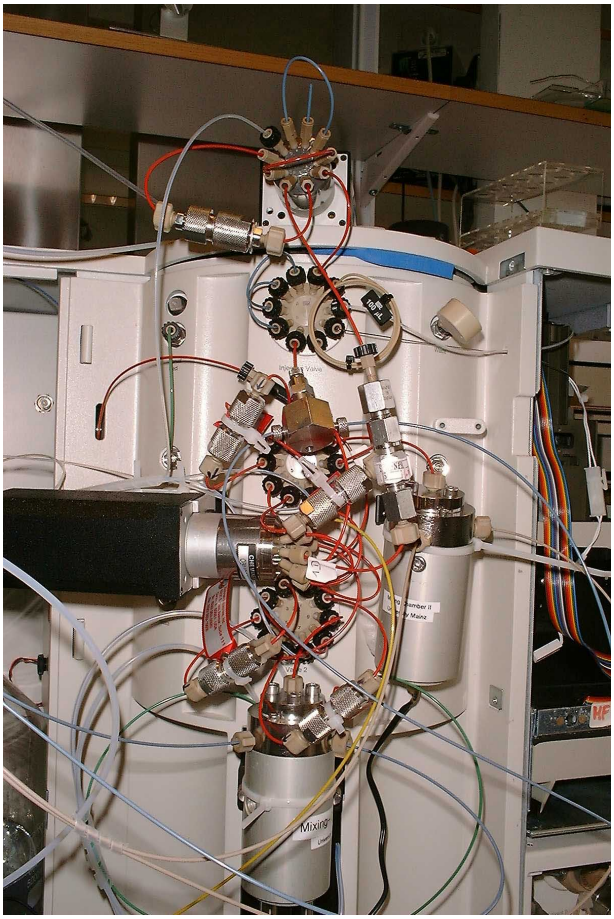

Figure 5.20 Photograph of the 2D-HPLC set-up using four parallel RP columns and two detectors and a sample fractionation step. The second picture is a magnification of the column and switching valve arrangement.

### 5.6.2 First dimension columns and operation parameters

The analytical ion exchange column was TSKgel SP-NPR or TSKgel DEAE-NPR providing either DEAE or $SO_3H$ functionality like in the previous set-up. The column flow rate was 0.5 ml/min and the column was always operated in-series with the corresponding ion exchange restricted access column.

The linear gradient in the first dimension ran from 10 mM phosphate buffer to 1.0 M phosphate buffer in 96 min. Afterwards, the first dimension was washed with 1.0 M phosphate buffer for 8 min, followed by 8 min column regeneration using buffer A prior to the next 2D-analysis.

### 5.6.3 Second dimension columns and operation parameters

The four similar reversed-phase columns were MICRA ODS I of 14 mm x 4.6 mm I.D. dimensions. The eluents for RP separations were A = 0.1 % trifluoroacetic acid (TFA) in water and B = 0.1 % TFA in acetonitrile. The gradient cycle for the reversed-phase columns started with 4 % B, which was increased to 40 % B within 6 min and further increased to 100 % B within 0.66 min, then maintained for 0.15 min. Initial column regeneration and tube flushing was performed at 4 % B for 1.17 min using a flow rate of 2 ml/min. Additional reversed-phase column regeneration was performed with water at a flow rate of 0.5 ml/min prior to new sample enrichment.

### 5.6.4 Cation exchange / reversed-phase separation of human hemofiltrate including sample fractionation

The cation- or anion exchange RAM column was loaded with 100 µl (50 µg protein/µl) human hemofiltrate at a flow rate of 0.2 ml/min applying 100 % buffer A as described previously. The column was washed for 12 min. After valve switching, elution was performed in a backflush mode in-series with the analytical ion exchange column.

Figure 5.21 shows the cation exchange separation of a fractionated human hemofiltrate sample at pH = 3.0. The chromatogram shows an incomplete separation of the molecular weight fraction below 15 kDa within the 96 min analysis time. Approximately 25 peaks were visible but not baseline resolved. Each of the 24 fractions of 4 min duration (2 ml eluent) was transferred on-line to the second dimension for subsequent reversed-phase chromatography on MICRA ODS I columns.

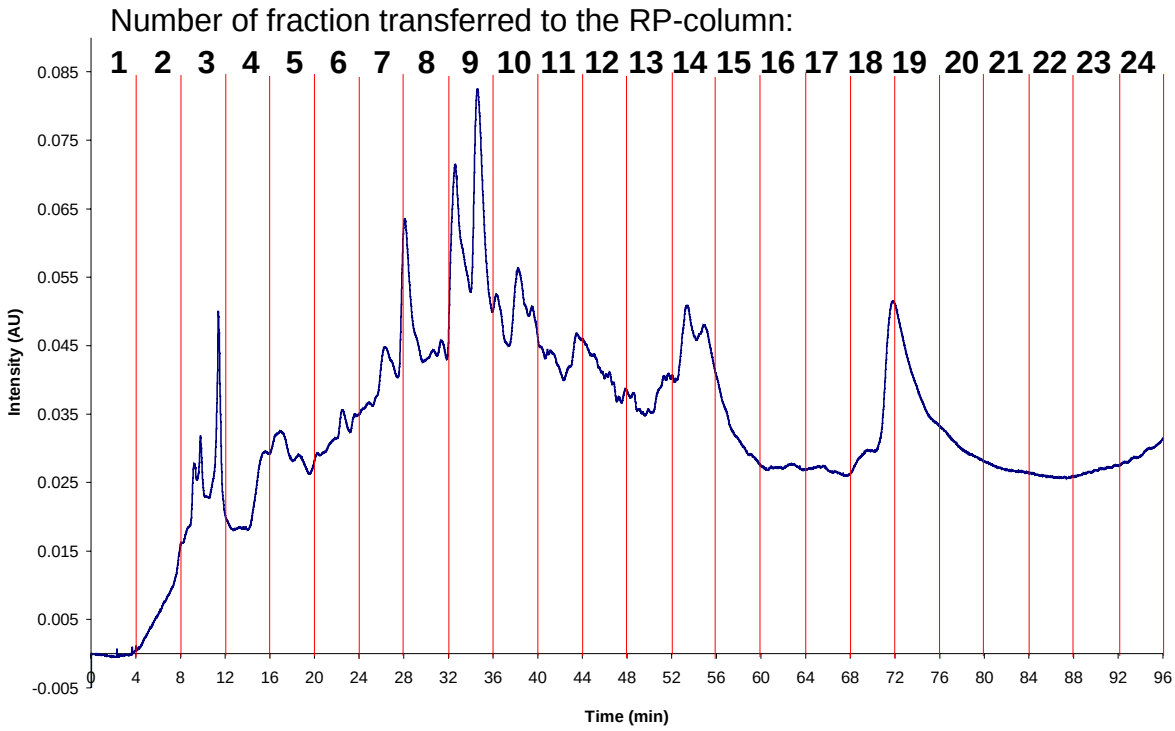


Figure 5.21 The chromatogram illustrates the separation of human hemofiltrate on the analytical cation exchange column in the first dimension after being subjected to selective enrichment on a cationic RAM. The fractions (24 in total) were continuously transferred to the second dimension in four minute intervals for subsequent analysis by reversed-phase chromatography.

Figure 5.21 shows 22 typical consecutive reversed-phase chromatograms (fractions 1-22) generated during a complete two-dimensional (RAM/cation exchange/RP) run. More than 1000 peaks were resolved in all 24 chromatograms within the total analysis time of 96 min.

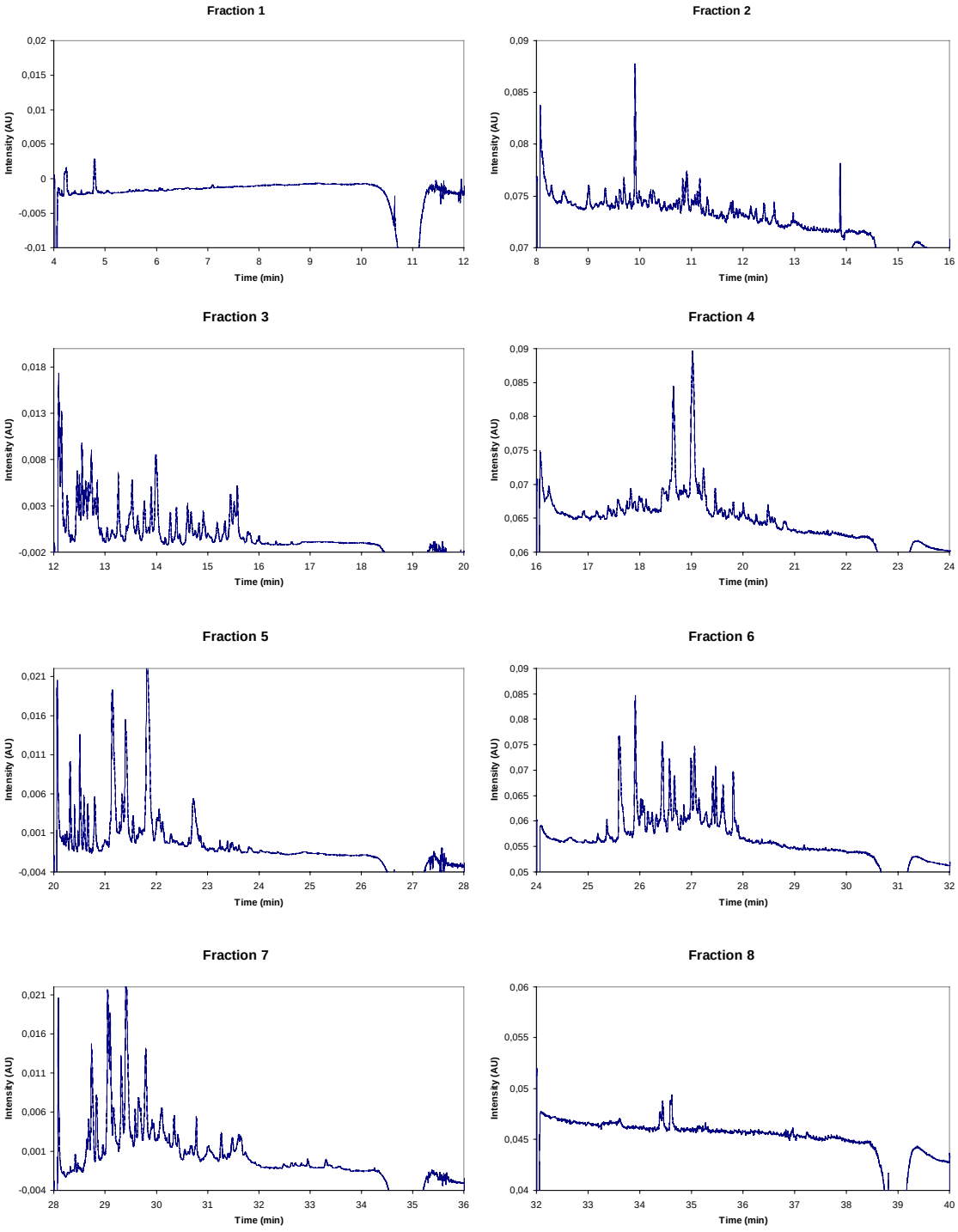
Fraction 1
Intensity (AU)
Time (min)
Fraction 2
Intensity (AU)
Time (min)
Fraction 3
Intensity (AU)
Time (min)
Fraction 4
Intensity (AU)
Time (min)
Fraction 5
Intensity (AU)
Time (min)
Fraction 6
Intensity (AU)
Time (min)
Fraction 7
Intensity (AU)
Time (min)
Fraction 8
Intensity (AU)
Time (min)

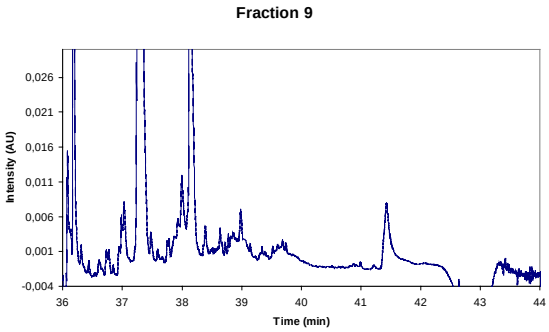
Fraction 9
Intensity (AU)
Time (min)

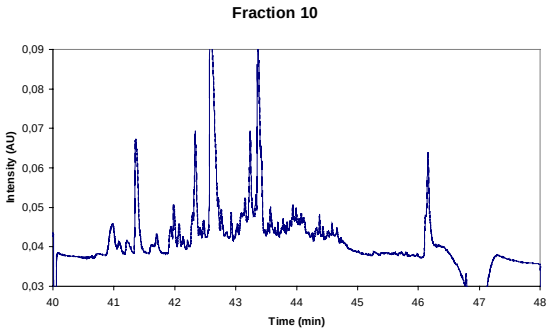
Fraction 10
Intensity (AU)
Time (min)

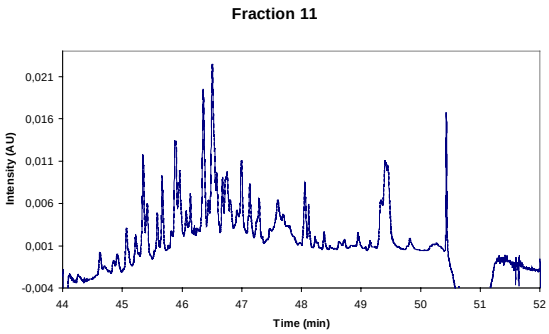
Fraction 11
Intensity (AU)
Time (min)

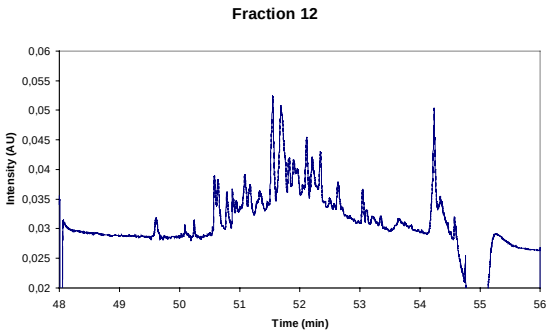
Fraction 12
Intensity (AU)
Time (min)

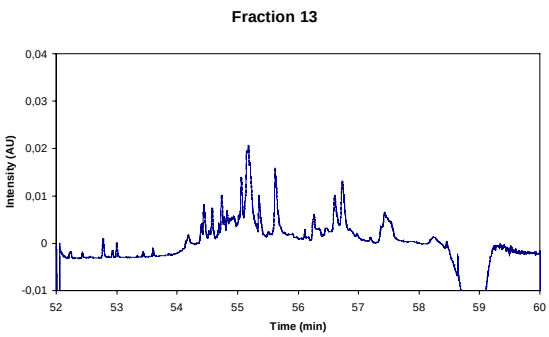
Fraction 13
Intensity (AU)
Time (min)

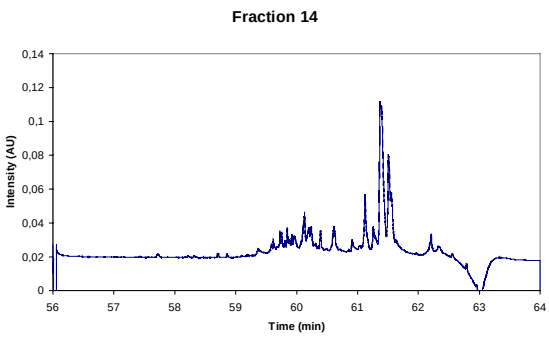
Fraction 14
Intensity (AU)
Time (min)

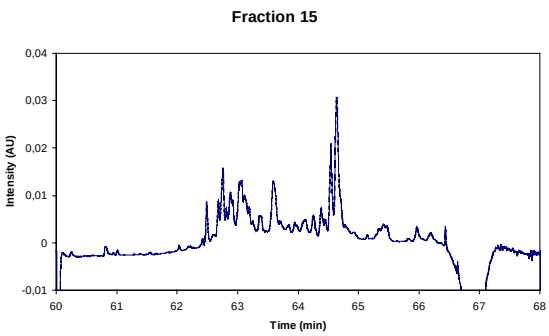
Fraction 15
Intensity (AU)
Time (min)

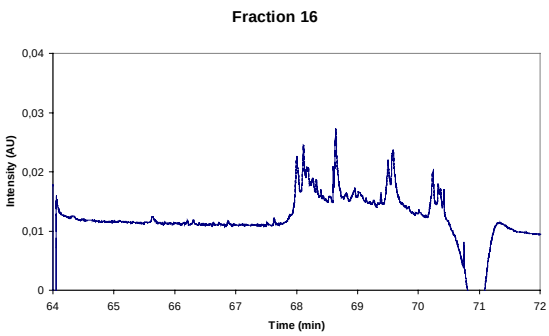
Fraction 16
Intensity (AU)
Time (min)

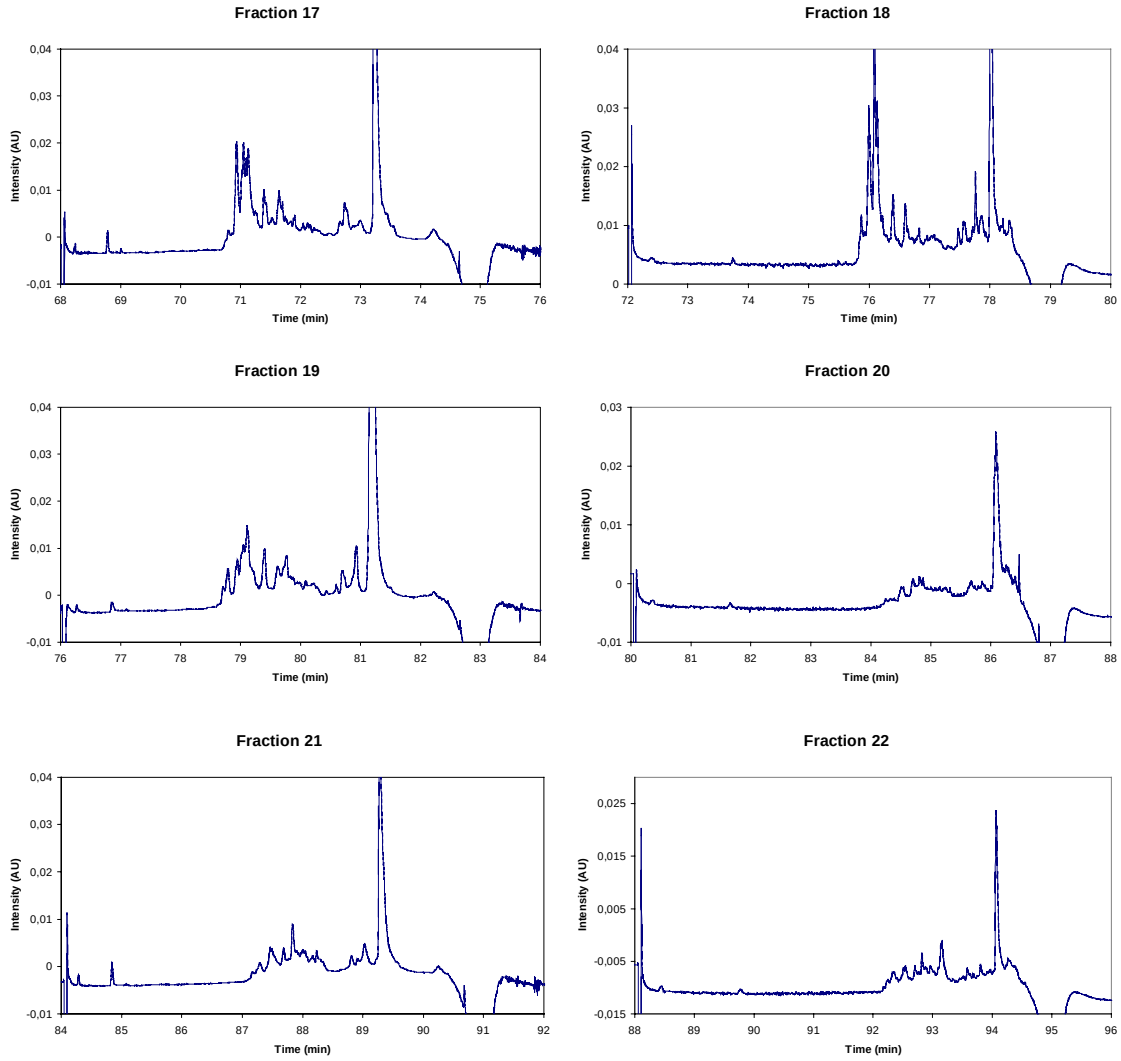


Figure 5.22 Selected reversed-phase chromatograms corresponding to a two-dimensional RAM / cation exchange / reversed-phase separation of human hemofiltrate

The fraction number mentioned on the reversed-phase chromatogram corresponds to the labelled intervals in the ion exchange chromatogram. Automatic fractionation of equidistant intervals, regardless of the first dimension separation pattern, was applied for sample transfer due to the automated system. The number of first dimension peaks roughly equals the number of fractions transferred to the RP-columns. The peak capacity was inversely proportional to the retention factors, a problem which could be circumvented by using a non-linear gradient for optimisation. R. Murphy [67] investigated the effect of sampling rate on resolution in comprehensive two-dimensional gel-permeation/RP-chromatography of copolymers claiming that each peak in the first dimension should be sampled at least three times into the second dimension. However,

previous investigations using standard proteins demonstrated a large number of redundant peaks in the second dimension at high sampling rates due to a low efficiency in the ion exchange mode. Even when the peak in the ion exchange chromatogram seems to reach the baseline again, there are still small amounts of protein eluting from the column. This seems to be an additional specific problem in ion exchange chromatography, limiting the resolution. Adding low amounts of organic modifier (4 % methanol) to the ion exchange mobile phase for suppressing any hydrophobic interaction did not result in a remarkable improvement of the ion exchange separation. However, the amount that can be added is limited to approximately 5 % of methanol due to the enrichment of the analytes on the reversed-phase column. The use of other cation exchanger columns in the first dimension like Mini S or Mono S from Pharmacia Biotech, Uppsala, Sweden did not result in a considerable improvement.

A total number of 24 RP-chromatograms were generated in the second dimension. Every second chromatogram was produced with the additional external UV-detector. The start time of each chromatogram must be deducted to compare the absolute retention times in the RP-mode.

More than 60 peaks were resolved in some RP-chromatograms, clearly demonstrating the resolving power for small proteins and peptides. Comparison of two consecutive RP-chromatograms from a single first dimension run showed the orthogonal separation power of the system. The chromatograms are different, with only few peaks appearing in two adjacent chromatograms. However, despite a total number of 1000 resolved peaks in the 2D-system, it does not necessarily signify that 1000 different components are resolved, as would be expected in a single mode run. This is an intrinsic feature of the column coupling approach. One peak of a single component can appear in two or more consecutive chromatograms due to partial separation in the ion exchanger mode or from splitting a first-dimension peak into two adjacent fractions.

The identification of redundant peaks to get information on the number of resolved components can either be done by an overlay of two consecutive chromatograms or by converting the first and second dimension chromatograms into a 3D-display. The data calculated from the cation exchange and 23 reversed-phase chromatograms were displayed in a 3D-diagram, shown in Figure 5.23.

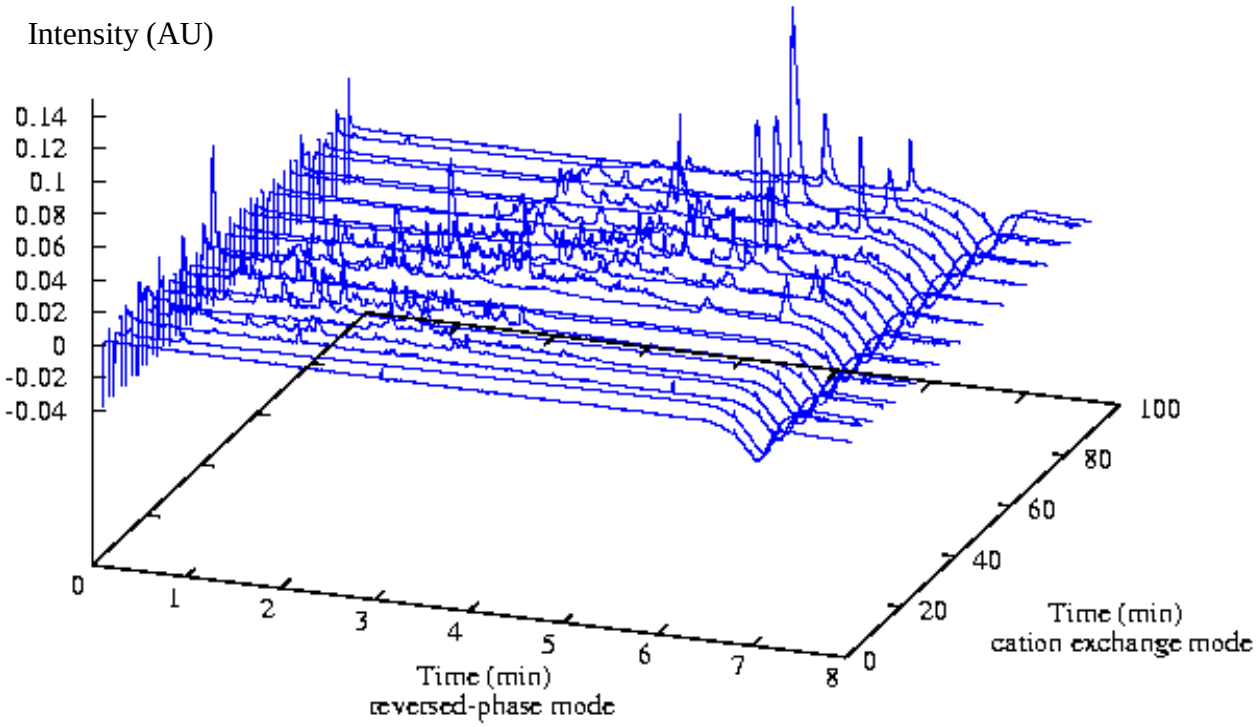


Figure 5.23 3D-display of the RAM / cation exchange / reversed-phase separation of human hemofiltrate

The 3D-display indicating the retention times in either separation mode and the UV-intensity confirms the orthogonal separation power. Only a limited number of redundant peaks, appearing in two or more adjacent fractions, are visible. The peak capacity in the second dimension can be calculated to approximately 130 per column. Considering the 24 fractions from the first dimension as the first dimension peak capacity, the total theoretical peak capacity can be calculated to be as high as 3000.

Figure 5.24 is a zoom of the RP chromatogram corresponding to fraction 10 clearly demonstrating the high separation performance.

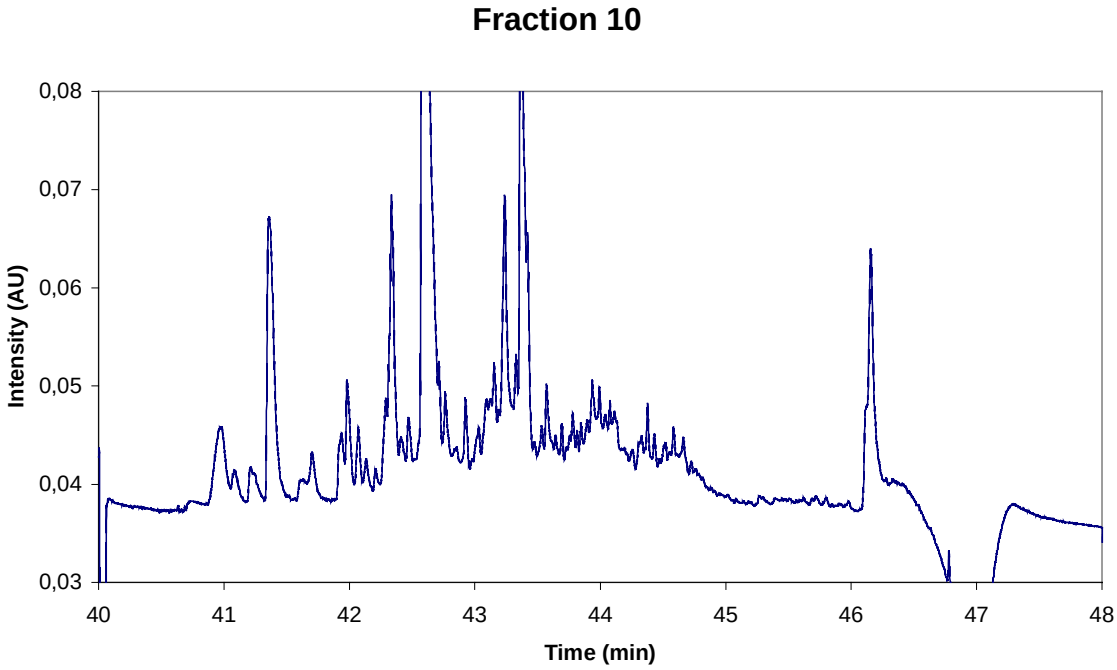


Figure 5.24 Magnification of the reversed-phase chromatogram corresponding to fraction 10, exemplifying the high resolving power within 8 min of analysis time

### 5.6.5 Repeatability of the integrated 2D-HPLC platform

The repeatability of the cation exchange/reversed-phase system was investigated by assessing the relative standard deviations of the retention time, peak height and peak area. Fifteen randomly selected peaks generated from six consecutive runs of human hemofiltrate were chosen for computation. The repeatability data are shown in Table 5.6.

| Peak number | 1 | 2 | 3 | 4 | 5 |
|---|---|---|---|---|---|
| Average Retention Time [min] | 21.19 | 21.80 | 22.74 | 28.67 | 29.42 |
| RSD Retention Time [%] | 0.34 | 2.41 | 0.20 | 0.18 | 0.16 |
| RSD Peak Area [%] | 14.8 | 17.6 | 19.3 | 13.1 | 21.1 |
| RSD Peak Height [%] | 16.5 | 7.4 | 25.6 | 12.9 | 29.3 |

| Peak number | 6 | 7 | 8 | 9 | 10 |
|---|---|---|---|---|---|
| Average Retention Time [min] | 37.38 | 38.18 | 41.44 | 45.78 | 55.66 |
| RSD Retention Time [%] | 0.21 | 0.15 | 0.13 | 0.70 | 0.08 |
| RSD Peak Area [%] | 6.6 | 7.4 | 16.9 | 13.2 | 22.0 |
| RSD Peak Height [%] | 4.4 | 2.9 | 17.8 | 6.1 | 10.2 |

| Peak number | 11 | 12 | 13 | 14 | 15 |
|---|---|---|---|---|---|
| Average Retention Time [min] | 56.72 | 63.37 | 64.64 | 81.17 | 89.31 |
| RSD Retention Time [%] | 0.03 | 0.50 | 0.05 | 0.05 | 0.04 |
| RSD Peak Area [%] | 35.6 | 15.7 | 12.5 | 18.2 | 29.8 |
| RSD Peak Height [%] | 15.4 | 11.9 | 13.4 | 8.6 | 20.5 |

Table 5.6 Repeatability data from six consecutive runs of the two-dimensional system

The RSD of the retention times was less than 0.5 % on average. The peak areas and peak heights were determined by employing automatic integration; the RSD values ranged between 5-25 % with a few exceptions. Hence, the obtained RSD values were better than or in the same range as the repeatability of 2D-gel electrophoresis. The on-line column coupling approach, which automatically desalts the samples, easily allows the detection of proteins and peptides in the deep ultraviolet region at 215 nm, providing a high sensitivity absorption in peptide bonds. The limit of detection which was determined to approximately 50 ng using the previous set-up and standard proteins is in the same order of magnitude as the sensitivity of silver stains.

### 5.6.6 Cation exchange / reversed-phase separation of a human fetal fibroblast cell-line sample including sample fractionation

Human lung fibroblasts (CCL-153) were obtained from the American Type Culture Collection (ATCC, Rockville, MD, USA). The cells were grown to confluence for 48 h in T 75 flasks and harvested by scraping the cells. The cell layer was washed three times with 3 ml cold PBS and centrifuged (40,000 g, 4° C, 20 min). The pellet was resuspended in 2.5 ml PBS buffer containing 7 M urea, 2 M thiourea and 4 % CHAPS and sonicated for 40 s. A second centrifugation was performed (40,000 g, 4° C, 30 min). The fibroblast sample was adjusted to pH 3 for subsequent loading onto the cation exchange RAM column.

2 ml fibroblast sample were loaded onto the RAM column in four consecutive steps each of 500 µl at a flow rate of 0.2 ml/min applying 100 % buffer A. The column was washed for 12 min after each injection. Elution was performed in a backflush mode in-line with the analytical cation exchange column applying exactly the same conditions as used for the hemofiltrate separation. Figure 5.25 demonstrates the separation power of the 2D-HPLC system for the cell sample derived from a human fibroblast cell culture.

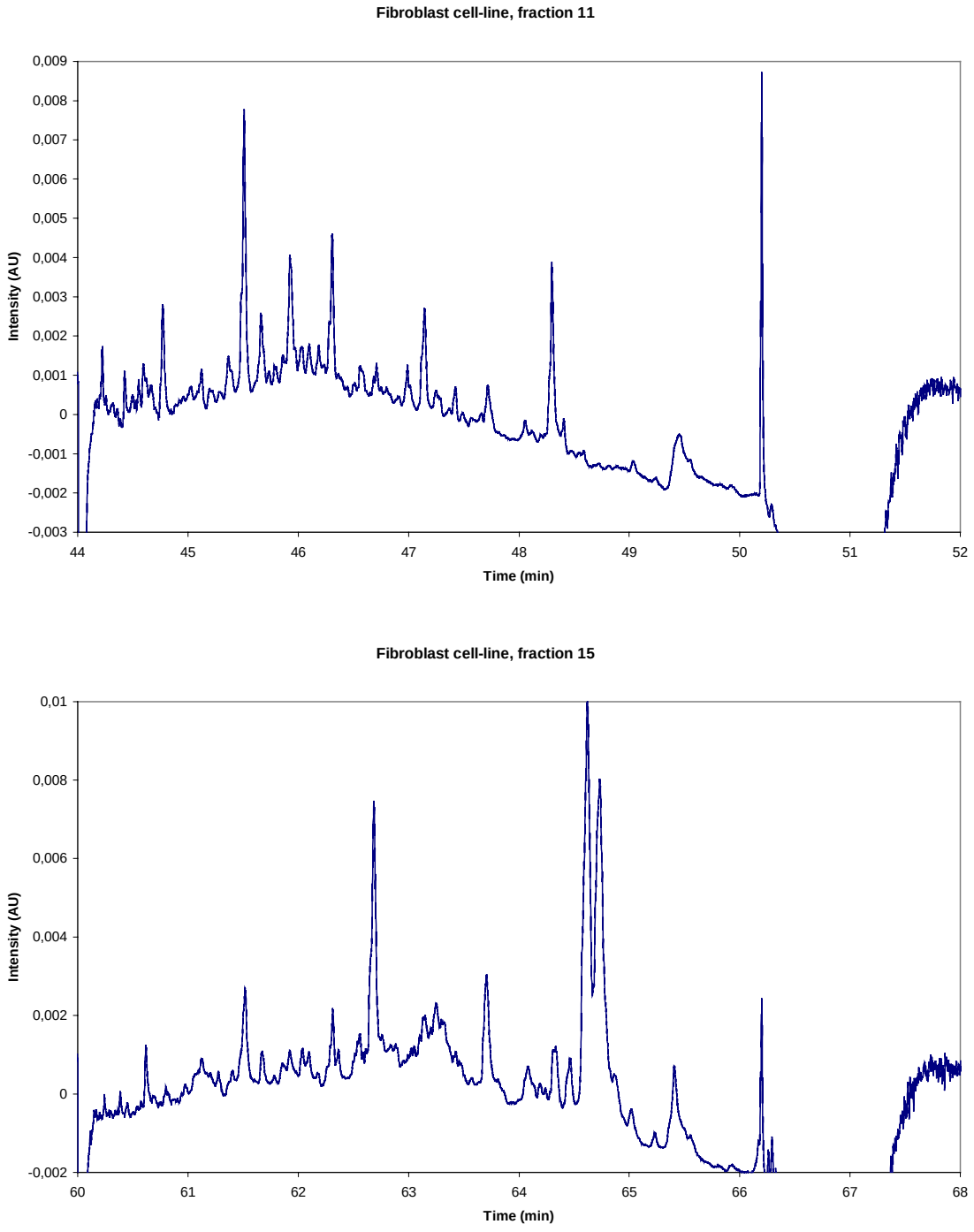


Figure 5.25 Two out of 24 reversed-phase chromatograms originating from the direct injection of the human fetal fibroblast cell-line.

Fraction 11 and fraction 15 were chosen as examples out of 24 chromatograms generated. It should be emphasised that no special pre-treatment of the sample was necessary prior to sample injection into the multidimensional system, although 7 M urea, 2 M thiourea and 4 % CHAPS 8 M were used to solubilise the proteins from the primary cells. The separation efficiency was found to be similar to that of the hemofiltrate separation. The total protein amount of the sample was determined by a protein assay to be about 0.5 mg/ml, which required a total sample loading of 2 ml onto the RAM column for sufficient enrichment of the low molecular mass analytes. It was demonstrated that high-resolution power with minimal sample preparation can be achieved at a concentration level which is accessible by UV detection. This offers the potential to map expression differences (up-and down regulations) by comparing the UV traces. The applicability for mapping small sized proteins and peptides from primary cells is limited by the high amount of sample needed, thus a large number of cells must be available.

### 5.6.7 Cation exchange / reversed-phase separation for the isolation of synthetic peptides from their by-products

The suitability of the 2D-HPLC system for the isolation of synthetic peptides from a complex mixture of by-products was investigated. Two different crude peptides were provided by the University of Ioannina, Ioannina, Greece. The sequences are given in Figure 5.26.

Peptide 1: (12p-peptide):

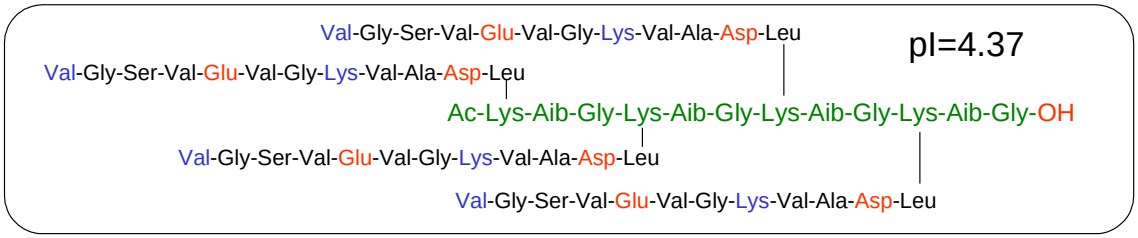


Peptide 2: (7p-peptide):

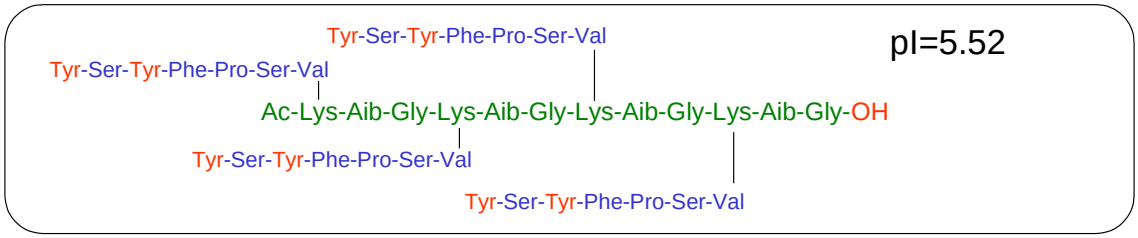


Figure 5.26 Sequence of synthetic peptides subjected to 2D-HPLC for separation from their side-products

The peptides consist of the same main chain of 13 amino acids but differ in the side chains. The so called 12p-peptide (pI=4.37, mw=5758 g/mol) consists of four similar side chains of 12 amino acids while the so called 7p-peptide (pI=5.52, mw=4517 g/mol) consists of four similar side chains of seven amino acids.

100 µl sample at a concentration of 1 mg/ml were loaded onto the $SO_3H$-RAM column at a pH of 3.0 and transferred to the 2D-system. The chromatographic conditions were exactly the same compared to the hemofiltrate separation. Due to the low molecular weight of the target analytes, the use of the RAM column is only necessary for the isolation of by-products above 15 kDa, thus the fraction in the void volume of the RAM was negligible (data not shown). The cation exchange chromatogram of the 7p-peptide and the relevant corresponding RP-chromatograms can be found in Figure 5.27.

CIX-separation of the 7p-peptide after the first dimension:

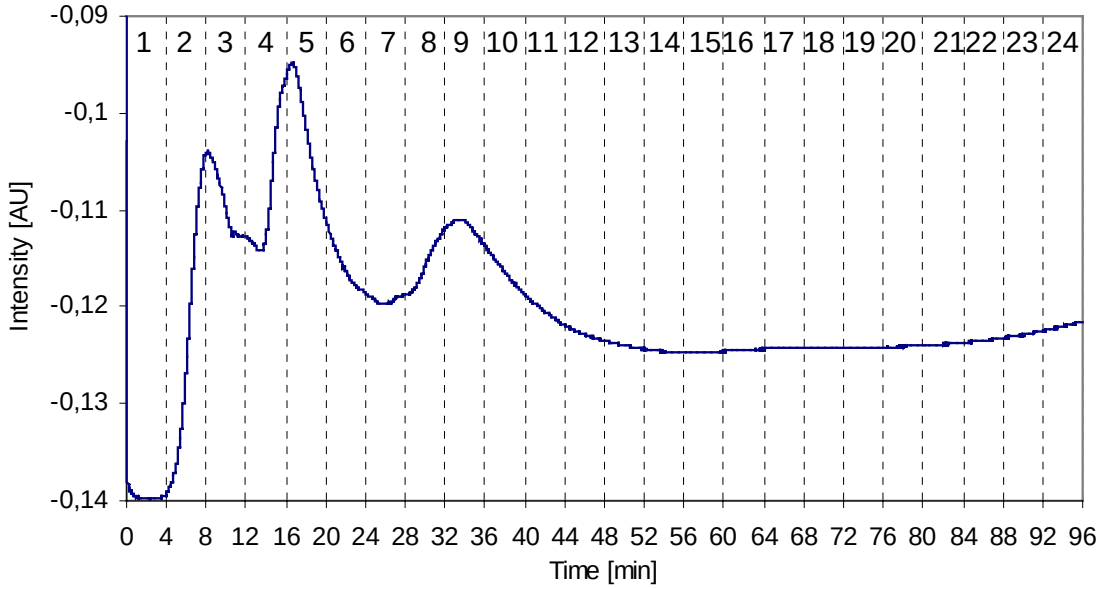


RP-chromatograms of the 7p-peptide in the second dimension:

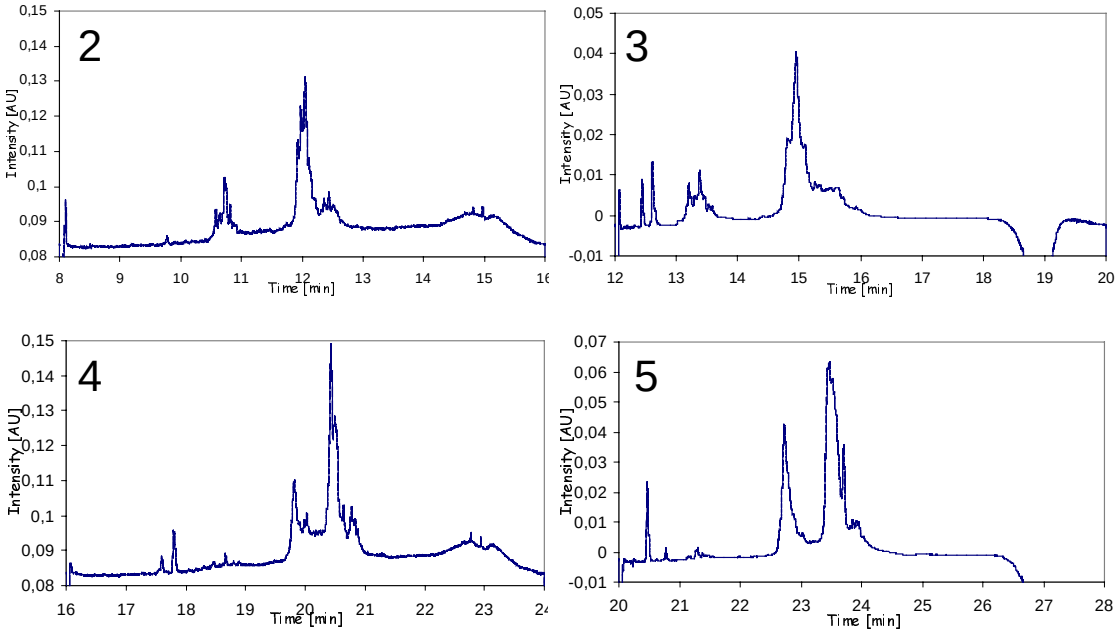

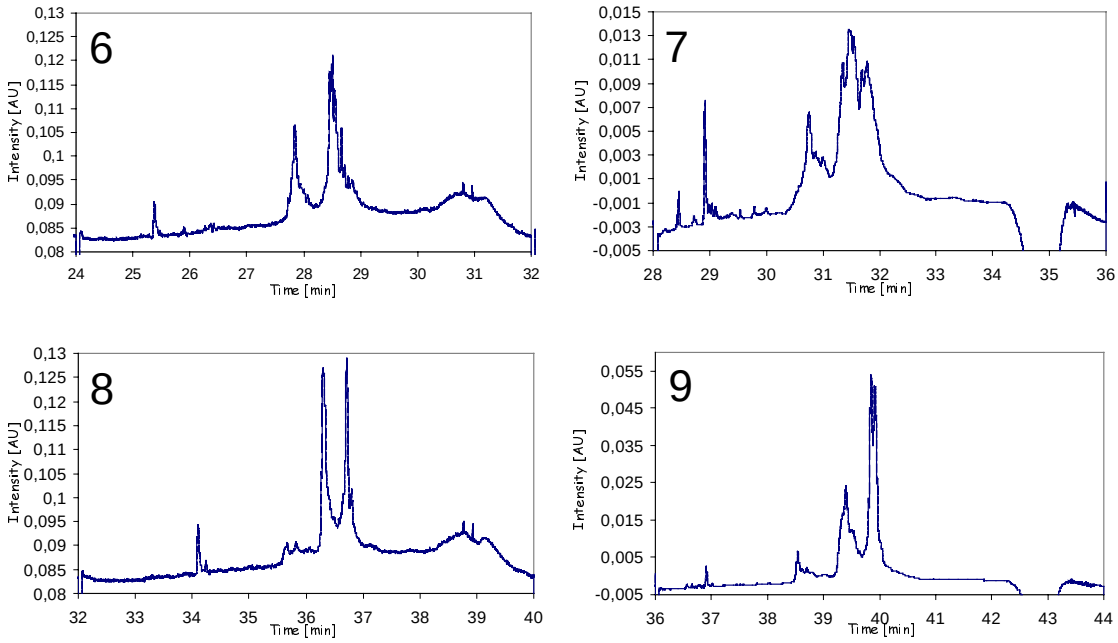


Figure 5.27 Cation exchange / reversed-phase separation of 7p-peptide and by-products

The cation exchange chromatogram and the subsequent relevant RP-chromatograms for the 12p-peptide are displayed in Figure 5.28.

CIX-separation of the 12p-peptide after the first dimension:

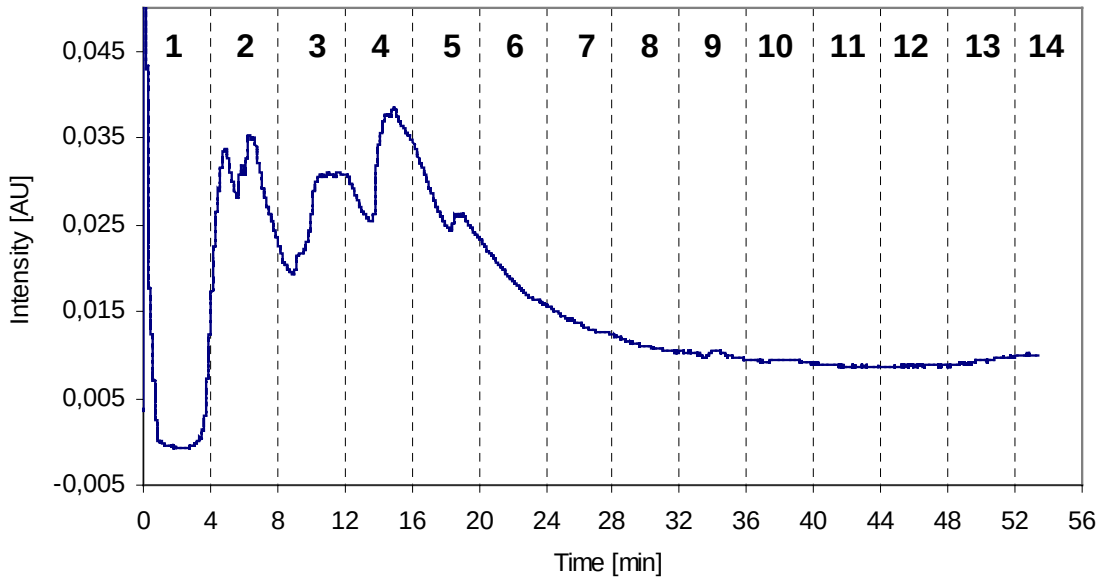

RP-chromatograms of the 12p-peptide in the second dimension:

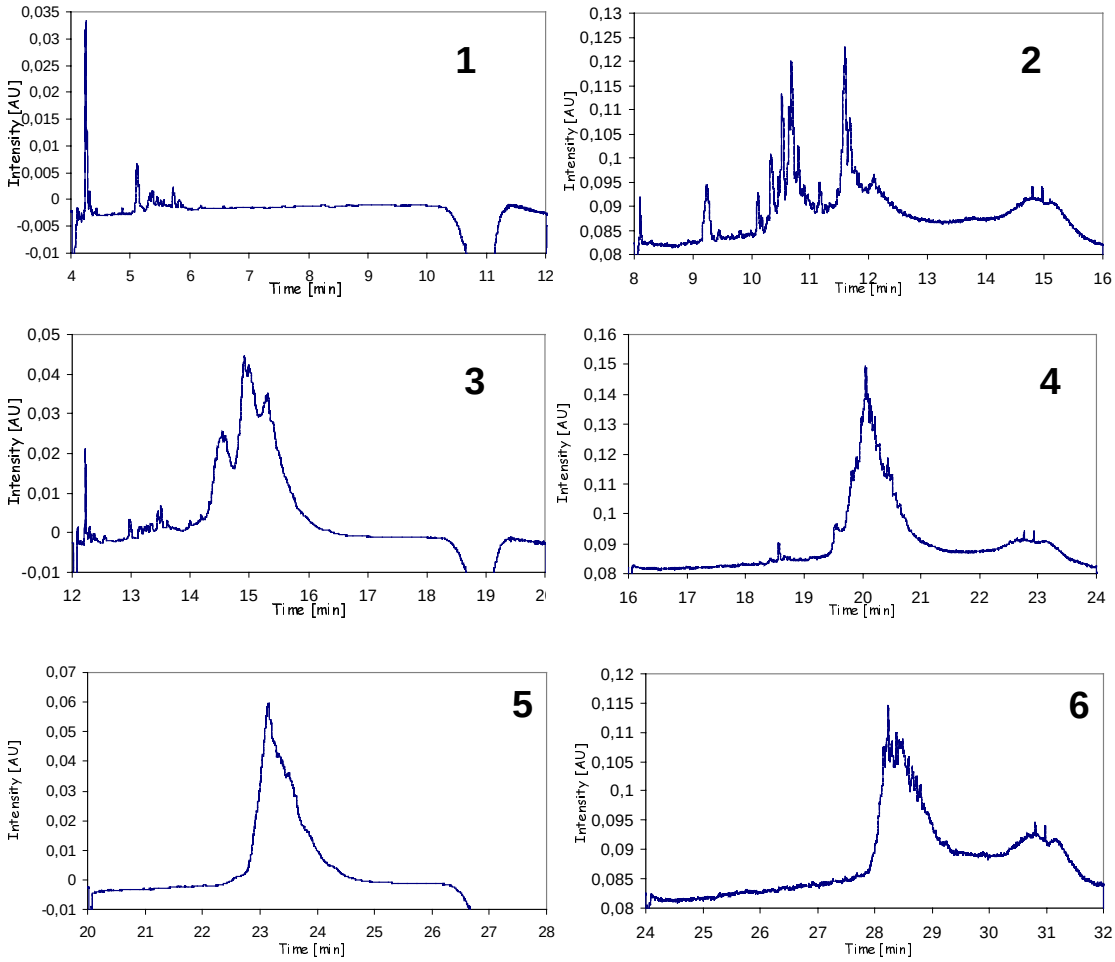


Figure 5.28 Cation exchange / reversed-phase separation of 12p-peptide and by-products

Due to low pI-values of the peptides as the main component, the non optimised cation exchange separation did not fill in the maximal available space in the chromatogram. Thus only the RP chromatograms of the first fractions are relevant and displayed. Three peaks were partly separated in the ion exchange mode and further resolved according to hydrophobicity. It is evident, that the peak for the target compound appears in approximately three consecutive RP chromatograms but well separated from the by-products.

Although the 2D-HPLC system is especially designed for protein and peptide mapping over a wide range of isoelectric points and hydrophobicities of a complex sample, it can also successfully be applied for isolation of a target compound. The multidimensional system provided much higher separation power compared to a single high resolution separation in the RP-mode [102]. The automated system can also be used for preparative isolation of compounds especially when the non-porous columns in the second dimension are replaced by porous ones (*e.g.* Chromolith$^{TM}$) providing a higher loadability.

### 5.6.8 Anion exchange / reversed-phase separation of a human hemofiltrate sample including sample fractionation

The separation of the human hemofiltrate sample was performed at pH = 7.0 by coupling the DEAE-RAM column and the analytical anion exchange column. The size selective sample is characterised by the elution profile from the DEAE-RAM column, shown in Figure 5.29. After 6 min run time, the RAM column was loaded with 100 µl (50 µg protein/µl) of human hemofiltrate at a flow rate of 0.2 ml/min applying buffer A. After 12 min elution of the matrix a linear gradient from 0 to 100 % B within 16 min was started to elute the low molecular weight target analytes from the RAM column.

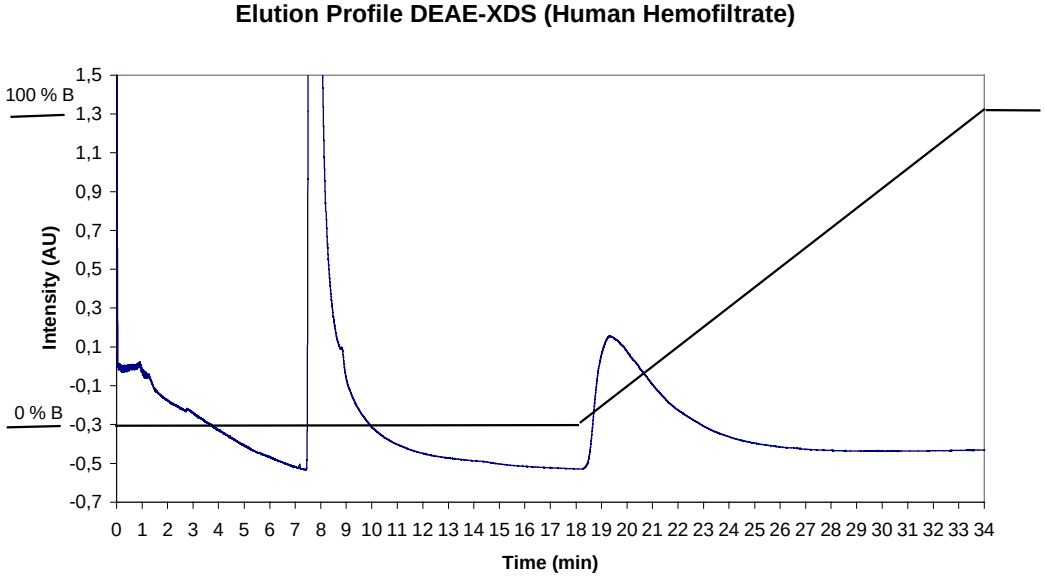


Figure 5.29 Elution profile of the human hemofiltrate sample from the DEAE-RAM column

The two peaks obtained are characteristic for the high molecular weight fraction in the inter particle volume of the column and the low molecular weight fraction retained on the inner surface of the RAM particles.

Figure 5.30 displays the separation after the RAM column coupled in-series with the anion exchange column. The operational parameters were exactly the same as used for the previous separations applying cation exchange chromatography. The eluents for the anion exchange RAM column and the analytical anion exchanger consisted of A = 10 mM phosphate buffer at pH = 7.0 and B = 0.5 M phosphate buffer at pH = 7.0. The linear gradient ran from 0 to 100 % B within 96 min.

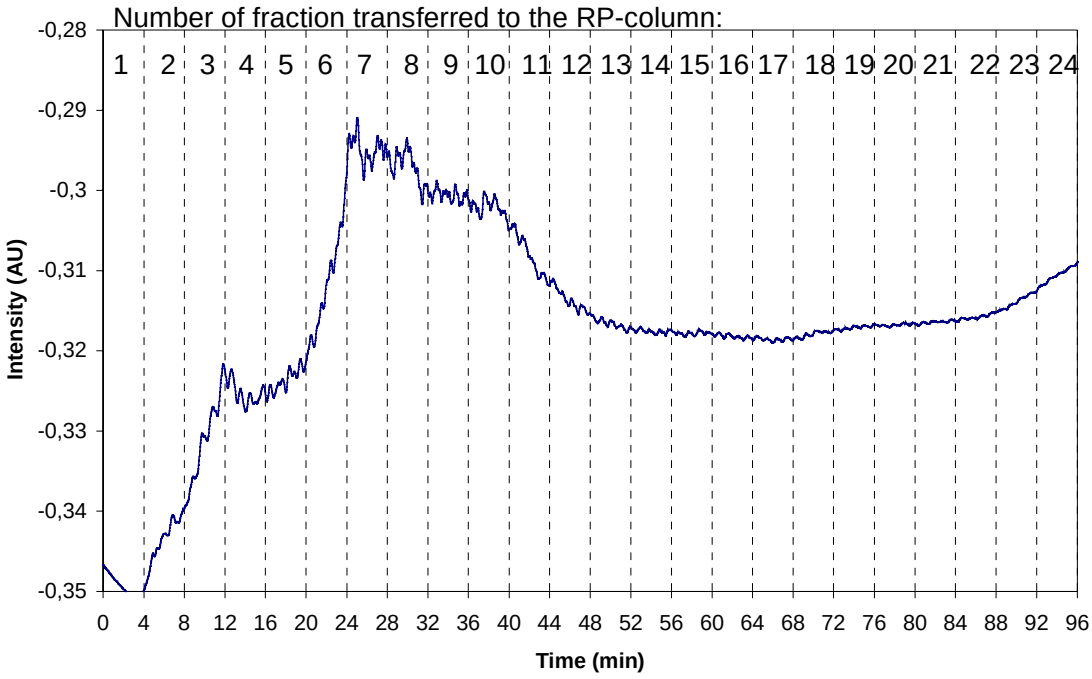


Figure 5.30 Anion exchange separation of human hemofiltrate at pH=7.0 including size selective sample fractionation

Using the anion exchange mode in the first dimension led principally to the same findings compared to the application of the cation exchange mode as discussed previously. However, the anion exchange separation in the first dimension produced fewer and wider peaks compared to the cation exchange mode. Due to the pH value limitation of pH = 7.0, only the small fraction exhibiting isoelectric points below approximately pI = 6 was retained on the DEAE-RAM column, thus fewer components

were resolved in the RP mode. Figure 5.31 exhibits the first six fractions resolved in the reversed-phase mode.

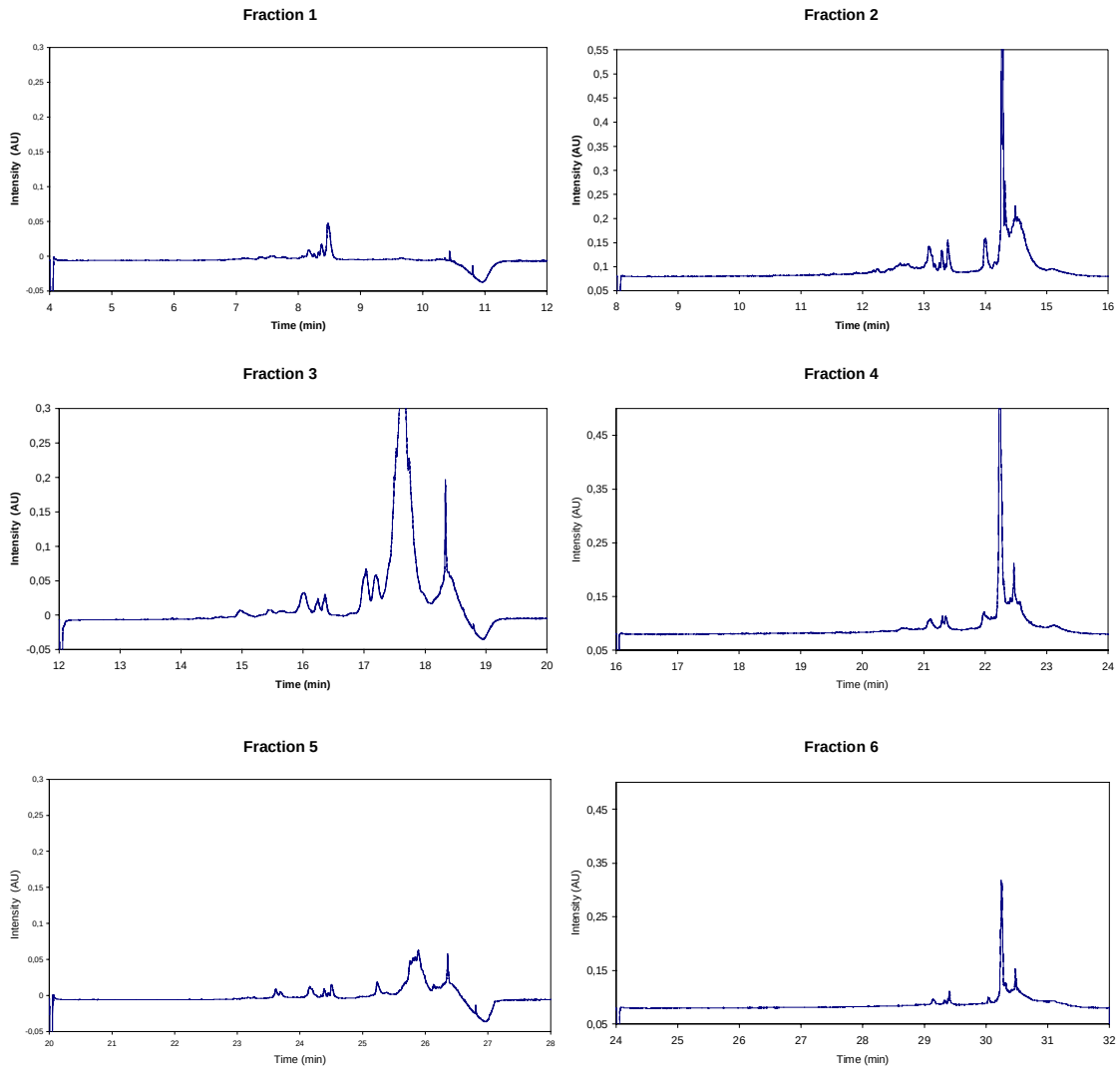


Figure 5.31 Selected RP-chromatograms from an anion exchange / RP-separation of human hemofiltrate

The separation power was inferior compared to the use of the cation exchange column in the first dimension at pH = 3.0 as expected from the separation after the first dimension. However, the general applicability for focusing on a special range of pI values was demonstrated.

### 5.6.9 Mass mapping by MALDI-TOF MS

The mass determination was made using a previous state of the cation exchange / RP column system with integrated sample fractionation using four parallel RP columns but only one UV detector. The resolution power in the RP dimension was inferior due to reduction of the gradient time by a factor of almost two. The advantage was a less complex experimental design, the handling of only one data channel and easy fraction collection from only one detector outlet. A schematic of this approach is shown in Figure 5.32. The RP column outlets were connected with the detector via the outer and the central ten-port valve. The experimental condition were the same as for the separations previously described with exception of the gradient in the RP mode. The gradient ran from 4 % to 40 % B in 3.8 min and was further increased from 40 % to 100 % B in 0.4 min followed by column regeneration applying 4 % B for 3.2 min. Further regeneration was performed with water for 4 min at a flow rate of 0.5 ml/min.

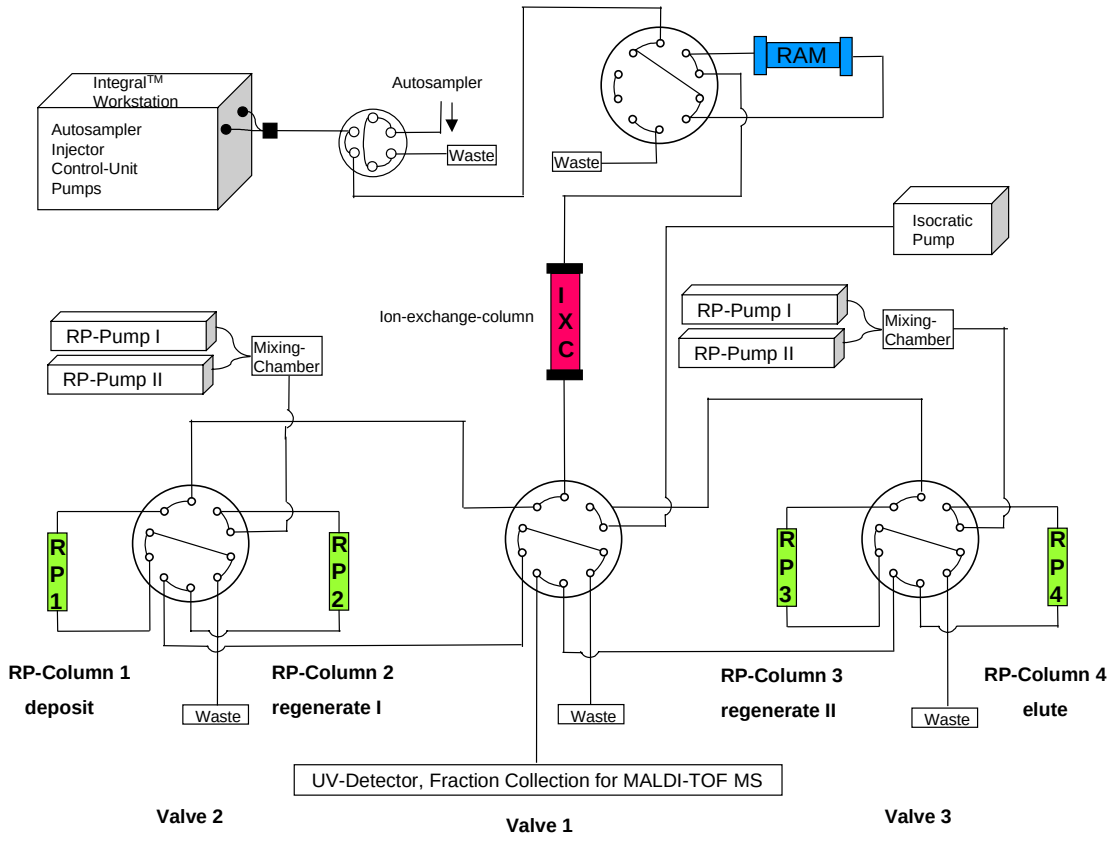


Figure 5.32 Schematic of the 2D-HPLC system with integrated sample fractionation using four parallel RP columns but only one UV detector.

The system did not apply parallel gradient elution and detection, thus the separation in the RP-mode can easily be displayed in one single continuos chromatogram shown in Figure 5.33. Despite of the lower separation power compared to the two detector system, using a more shallow gradient, approximately 600 peaks are resolved.

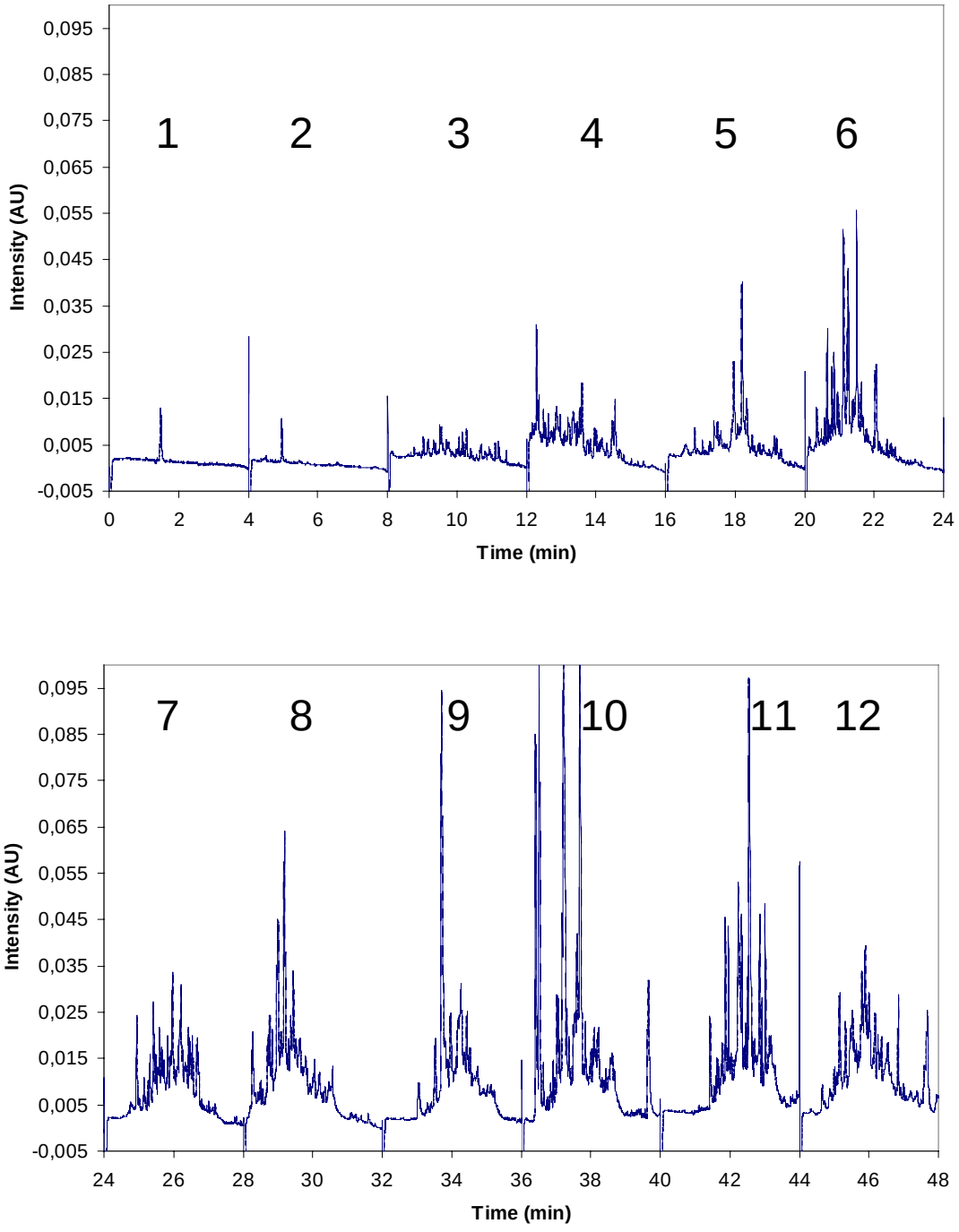

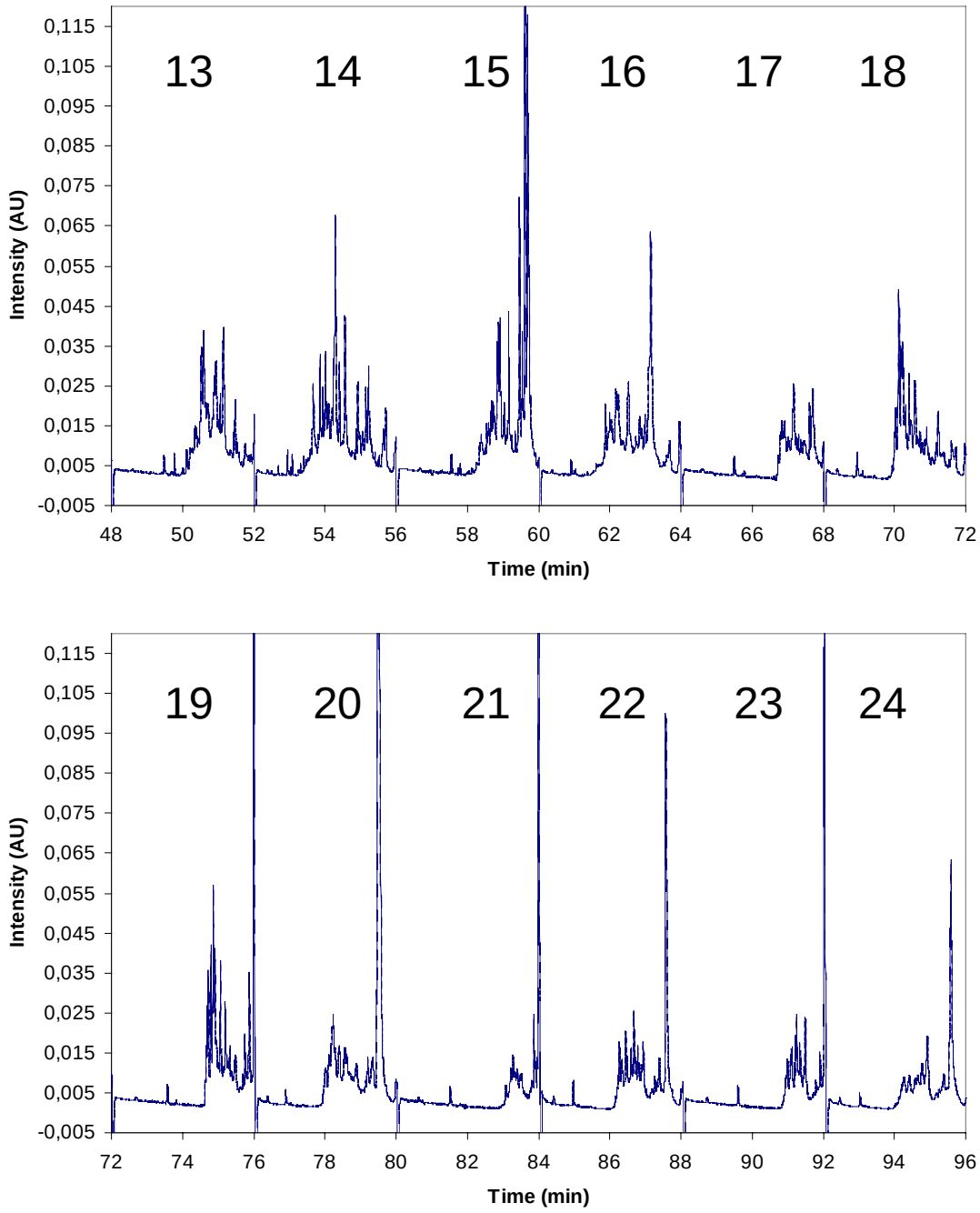


Figure 5.33 24 RP-chromatograms of the cation exchange / RP-separation of human hemofiltrate displayed in one chromatogram over 96 min total analysis time

A comparison of the chromatographic resolution in the RP-mode of the two different set-ups is shown in Figure 5.34. In the one detector set-up, the gradient ran from 4 % B to 40 % B within 3.8 min and within 6.0 min for the two parallel detector set-up.

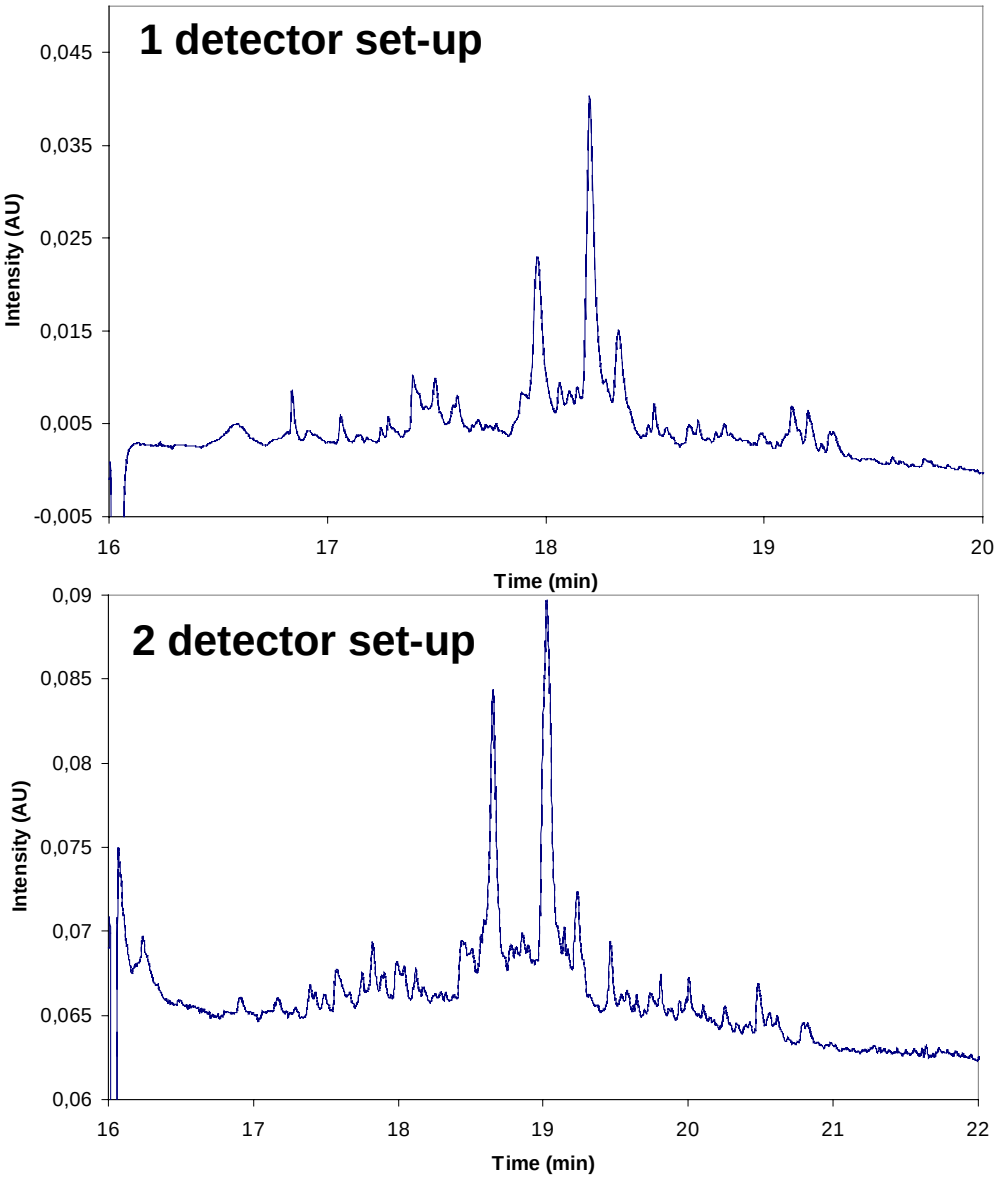


Figure 5.34 Comparison of two RP-chromatograms, both corresponding to fraction 5, applying different gradient times

In the first chromatogram applying the short gradient time, 30 peaks are detectable while 50 peaks are resolved in the second chromatogram using the longer gradient time. This experimentally confirms the demand to modify the separation platform. The theoretical background has already been discussed in Chapter 4.6.3.3.

Effluent fractions (approximately 20 µl) corresponding to selected peaks from the second dimension were manually collected from the detector outlet and used for MALDI-TOF MS analysis according to a seed layer technique [103].

The targets were manually prepared on polished stainless steel plates measuring 45 x 47 mm. A diluted matrix solution (either α-cyano-4-hydroxycinnamonic acid or sinapinic acid, 2 mg/ml in acetonitrile) was applied (0.5 µl) on the target plate. Then the sample was mixed 1:1 with either saturated matrix solution (15 mg/ml of α-cyano-4-hydroxycinnamonic acid or sinapinic in acetonitrile, 0.2 % TFA) and applied (0.5 µl) on the same spot. The MALDI-TOF MS instrument was a Voyager DE-PRO (Applied Biosystems) with built-in delayed extraction and a linear path of 1.1 m. It is equipped with a video camera system to ensure precise focusing of the 337 nm nitrogen laser, having a focused laser spot diameter of approximately 100 µm. The mass spectra were acquired both in the reflector and linear mode at an accelerating voltage of 20 kV and a delay time of 150 ns. Internal mass calibration with a standard peptide mixture from Applied Biosystems was used.

Figure 5.35 shows a RP chromatogram originating from fraction 6 of the cation exchange separation of human hemofiltrate. The arrow indicates the peak which was subjected to MALDI-TOF analysis. A mass spectrum corresponding to a selected peak from fraction 7 is displayed in Figure 5.36, from fraction 9 in Figure 5.37 and from fraction 10 in Figure 5.38.

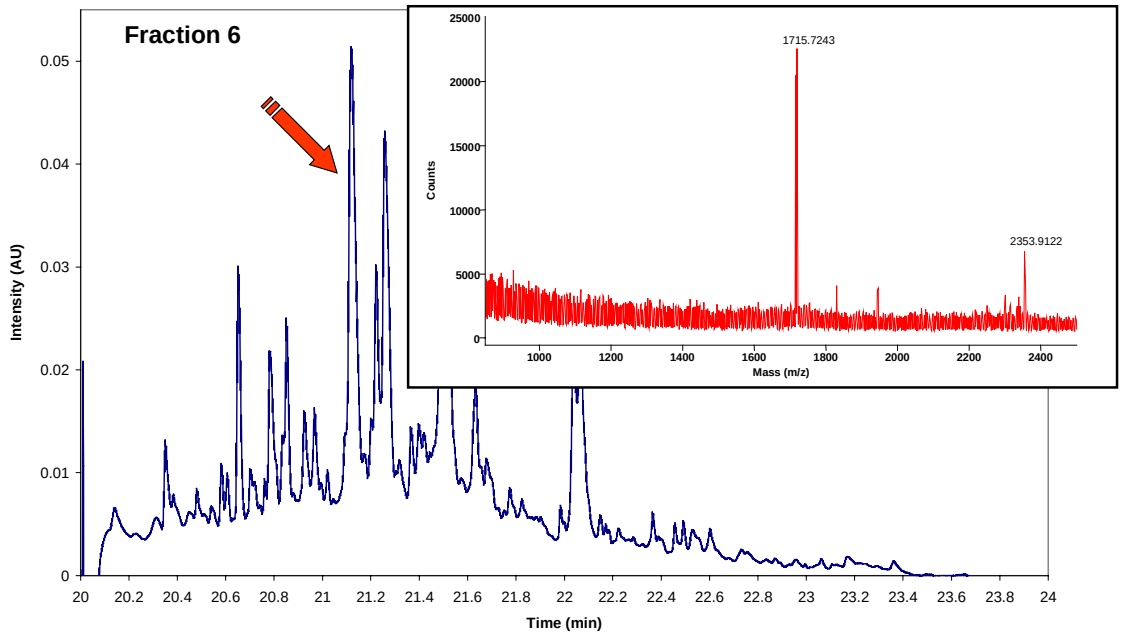


Figure 5.35 Typical MALDI spectrum corresponding to the peak (arrow) in the chromatogram which shows fraction 6 of a human hemofiltrate sample. In this case two masses were observed from a single UV peak

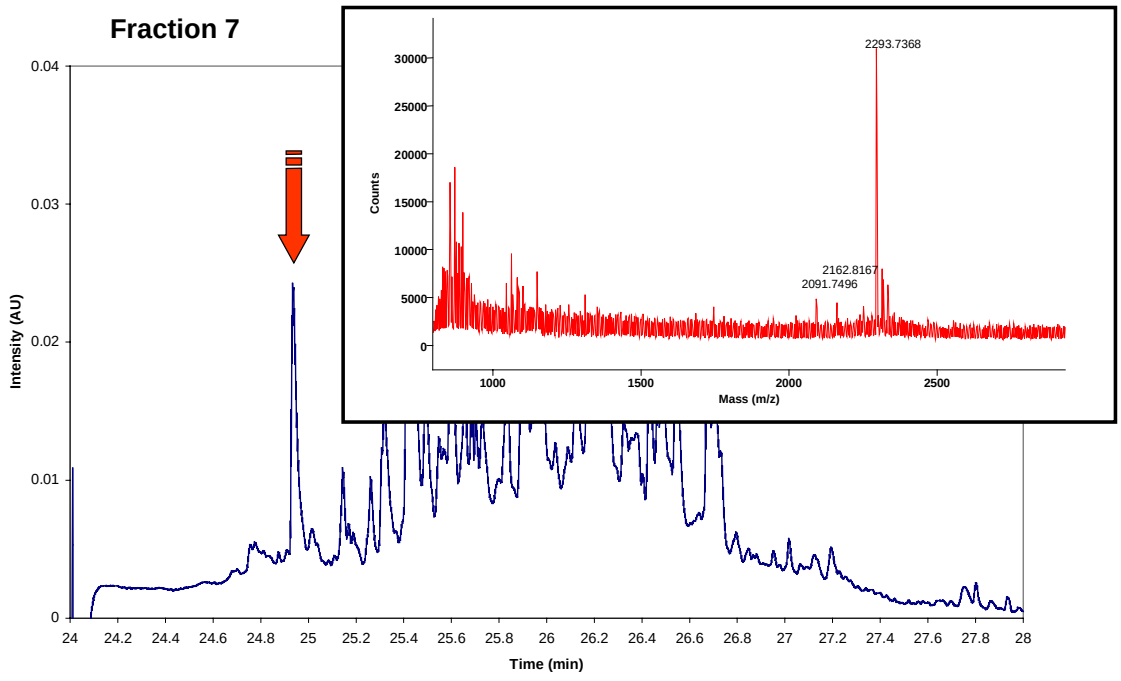


Figure 5.36 Typical MALDI spectrum corresponding to the peak (arrow) in the chromatogram which shows fraction 7 of a human hemofiltrate sample. In this case three masses were observed from a single UV peak

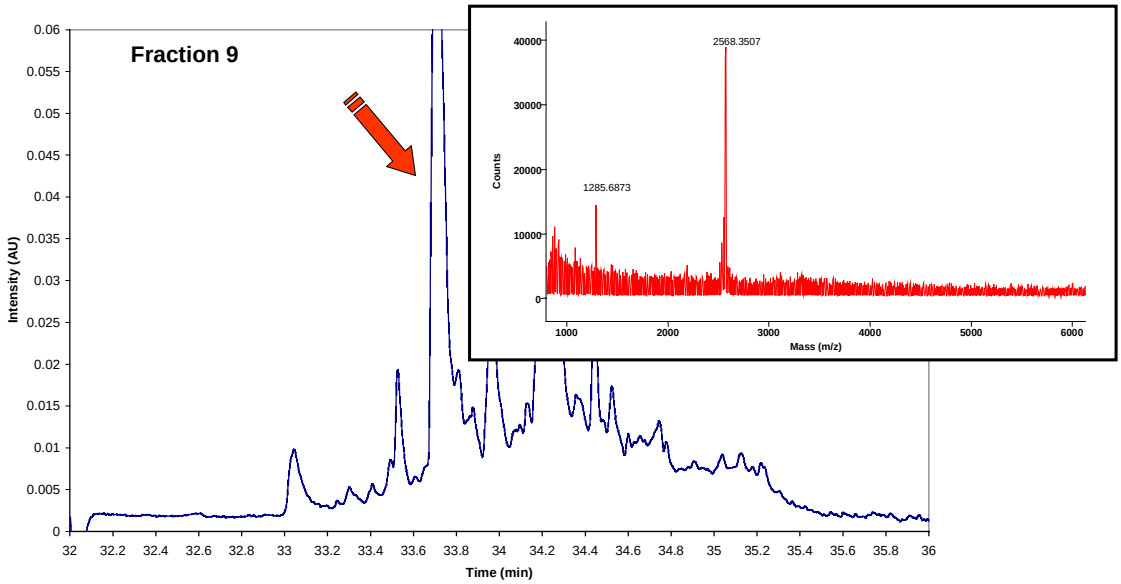


Figure 5.37 Typical MALDI spectrum corresponding to the peak (arrow) in the chromatogram which shows fraction 9 of a human hemofiltrate sample.

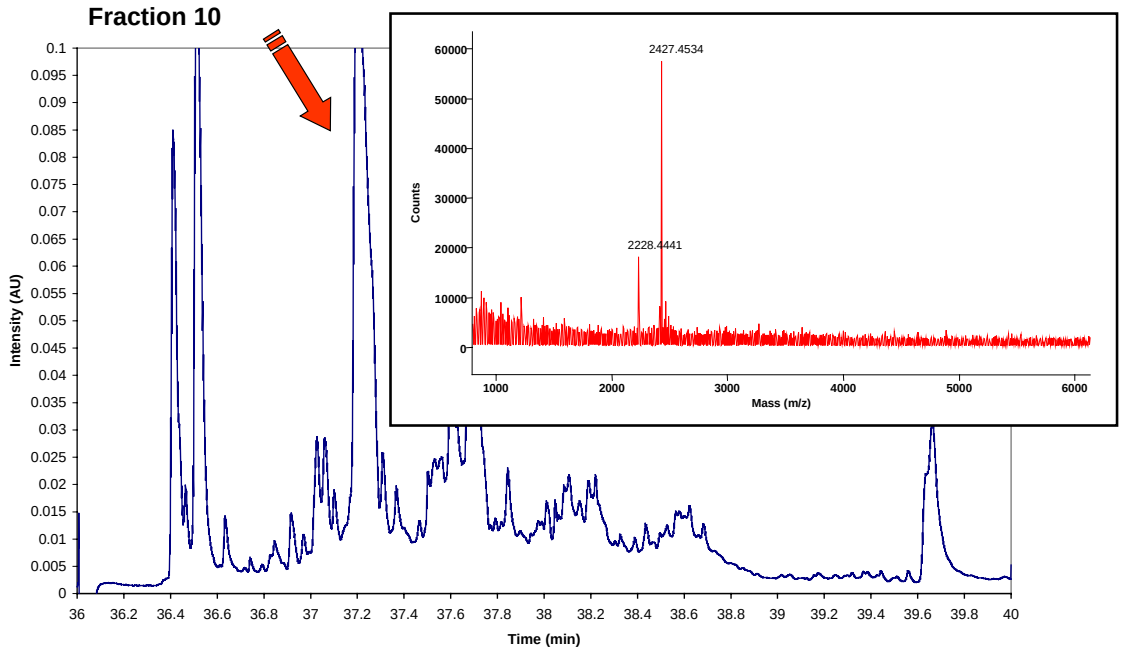


Figure 5.38 Typical MALDI spectrum corresponding to the peak (arrow) in the chromatogram which shows fraction 10 of a human hemofiltrate sample.

For most of the chromatographic peaks that have been analysed by MALDI-TOF-MS only one mass was visible, indicating the high resolving power of the 2D-HPLC system. Some collected peaks contained up to three different components, *i.e.* mass spectrometry provides a third dimension to the system. Although not used in this case,

sequencing of the resolved peptides by tandem mass spectrometry (*e.g.* static nano-ESI) may be an additional option to ascertain identity by database searching. The mass measurements by MALDI-TOF-MS revealed that the molecular mass range of the peptides were between 800-5,000 Da. Fractions which have been collected from human hemofiltrate separation using the latest set-up with two parallel detector outlets are currently used for peptide identification applying Edmann degradation, MALDI-TOF MS and database search. This is an ongoing work at IPF PharmaCeuticals, Hannover, Germany.

The essential need of a high resolving separation system prior to mass spectrometric detection was demonstrated by the analysis of the crude hemofiltrate sample and the low molecular weight fraction achieved using the $SO_3H$-RAM column. The MALDI-targets were prepared by the seed layer technique applying α-cyano-4-hydroxycinnamonic acid as described before. A diluted hemofiltrate sample (10 µg/ml) in 10 mM phosphate buffer was used for target preparation. The corresponding mass spectrum is shown in Figure 5.39. The low molecular weight fraction from 5 mg human hemofiltrate eluted with 2.5 ml of 1 M phosphate buffer from the $SO_3H$-RAM column was also subjected to mass analysis as shown in Figure 5.40.

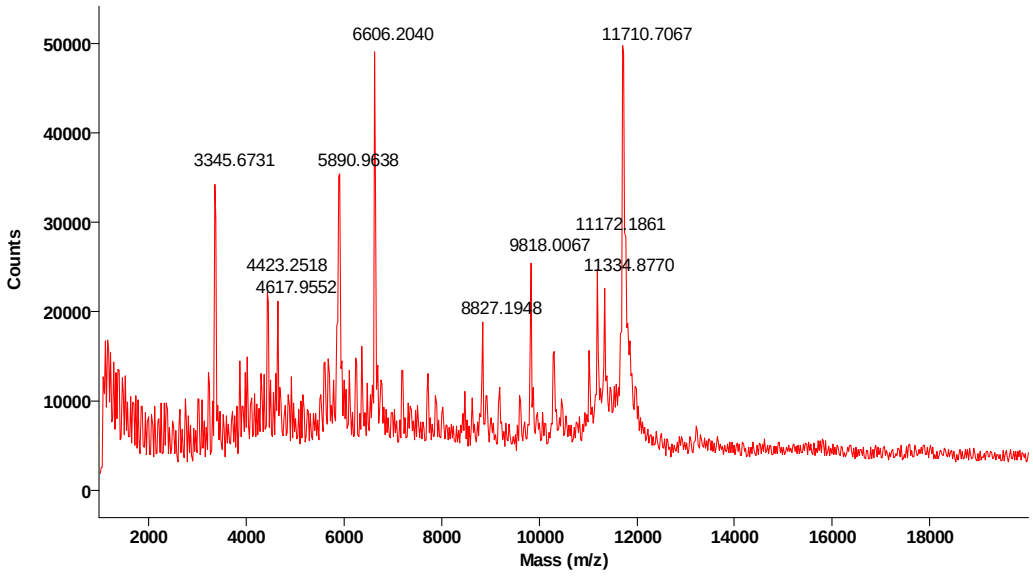


Figure 5.39 MALDI-TOF spectrum corresponding to a diluted sample of crude human hemofiltrate

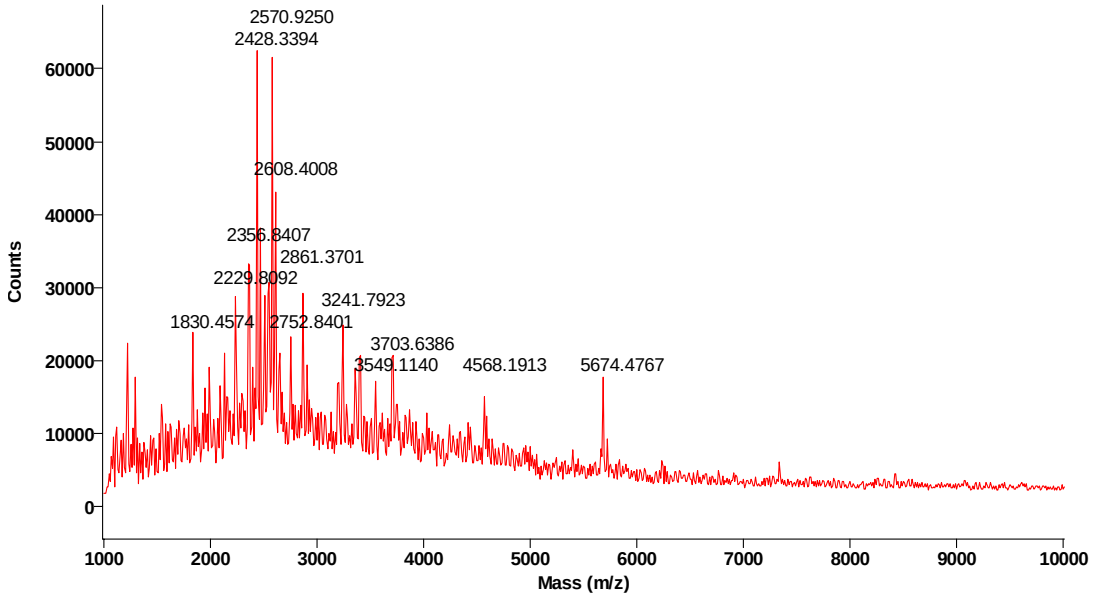


Figure 5.40 MALDI-TOF spectrum corresponding to the low molecular weight fraction of human hemofiltrate achieved by the $SO_3H$-RAM column

Despite of the unsurpassed mass accuracy in MALDI-TOF MS it can definitely not replace a high resolution separation. The complexity of the hemofiltrate sample was clearly demonstrated by the 2D-HPLC system resolving more than 1000 peaks. The number of components which can be detected in parallel is inferior to the chromatographic system due to ion suppression effects in a complex sample. High abundant molecules can mask low abundant once leading tosevere losses of information of sample complexity.

However, it is obvious that the size selective sample fractionation step has an influence on the mass spectrum. The mass spectrum of the crude hemofiltrate sample indicates masses up to 12,000 g/mol while the masses did not exceed 5,000 g/mol in the low molecular weight fraction. It has to be considered that the method using α-cyano-4-hydroxycinnamonic acid as matrix is only optimised for small proteins and peptides up to approximately 10 kDa. For that reason higher molecular weight components were not detectable. For the ionisation of higher molecular weight molecules other matrices have to be applied.

## 5.7 Micro-HPLC for high resolution separations at low concentration levels

The general applicability of micro-HPLC for protein and peptide mapping at a low concentration level was demonstrated. The miniaturisation of the on-line 2D-HPLC platform puts high demands on the technical details especially on the low void volume plumbing and switching valves. Furthermore, the realisation of high speed separations in an on-line coupled column system is difficult especially with regard to system stability and robustness. Thus, the low molecular weight fraction was analysed in only one dimension by micro reversed-phase HPLC, after the size selective fractionation step using the RAM columns had been performed.

The equipment was a Ultimate capillary HPLC system providing a gradient system based on flow splitting and an UV detector with Z-shaped capillary flow cell of 45 nl volume and 10 mm path length from LC Packings, Amsterdam, The Netherlands. The column was a Grom-SIL 120, ODS-4 HE 3µm of 15 cm x 180 µm I.D. supplied by Grom Analytik, Herrenberg, Germany. The flow rate was 2 µl/min. The eluents were A = 0.1% trifluoroacetic acid (TFA) in water containing 5 % acetonitrile and B = 0.1% TFA in acetonitrile containing 5 % water. The gradient ran from 0 % to 100 % B in 80 min.

Figure 5.41 shows a micro-HPLC reversed-phase separation of the low molecular weight fraction achieved by fractionation using the C-18 ADS RAM column. The fraction below 15 kDa starting with 5 mg human hemofiltrate was isolated applying the same procedure as described for the SDS-PAGE analysis. The fraction was lyophilised to evaporate the acetonitrile and the TFA. The dry sample was dissolved in 1.2 ml 10 mM $KH_2PO_4$ buffer at pH = 3.0 and 5 µl were injected leading to a well resolved chromatogram at high absorption units.

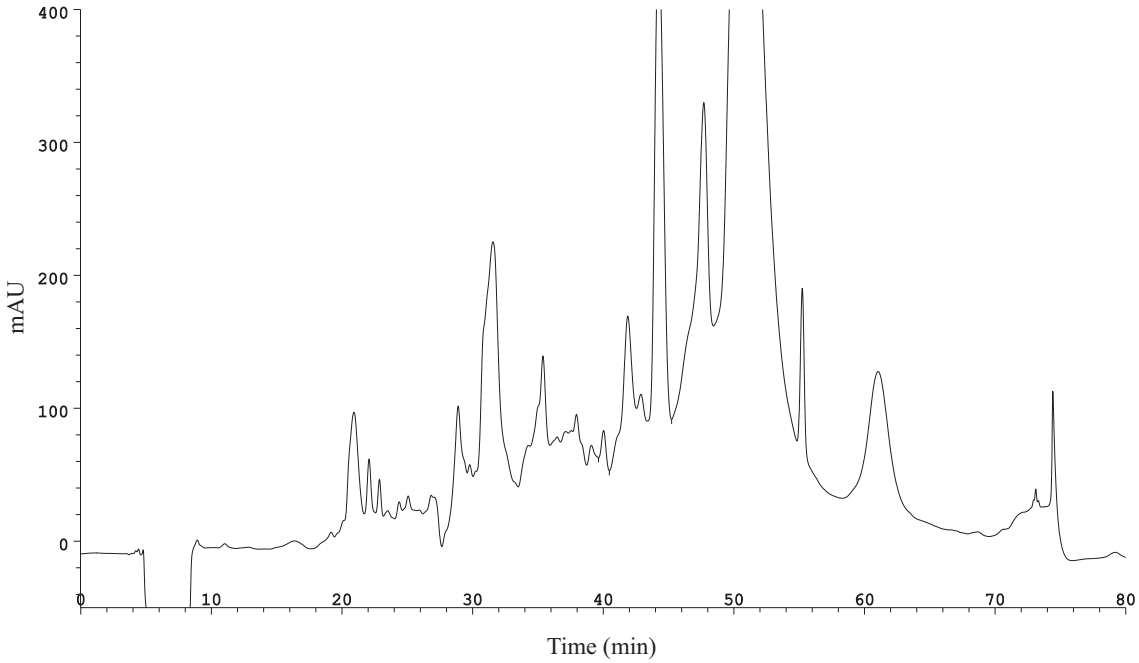


Figure 5.41 Micro-HPLC reversed-phase separation of the low molecular weight fraction of a human hemofiltrate sample in one dimension

The chromatogram clearly demonstrates the high sensitivity of the system. The protein and peptide amount injected was 240 times lower as compared to the 2D-separations of < 15 kDa fraction from human hemofiltrate. Long analysis times as well as long column regeneration times are limitations for the use in an on-line 2D-separation platform.

## 5.8 Chromolith$^{TM}$ columns for high-speed separations in the reverse-phase mode

Silica rod columns are favourable to use in the high-speed reversed-phase mode since they generate a considerable reduced pressure drop as compared to particulate columns. This offers the potential to use longer columns to increase the number of theoretical plates, thus improving the separation performance. Chromolith$^{TM}$ columns were tested with regard to column length, flow rate and gradient time. The results were compared to MICRA ODS I columns (14 mm x 4.6 mm I.D. or 30 mm x 3.0 mm I.D.), TSK Super ODS (100 mm x 4.6 mm I.D., TosoHaas, Stuttgart, Germany) and Zorbax SB-C 18 (150 mm x 2.1 mm I.D., Agilent Technologies, Waldbronn, Germany).

The chromatographic equipment was a HP 1090 (Agilent Technologies, Waldbronn, Germany). The column performance was investigated by injecting 10 µl crude human hemofiltrate at a concentration of 1 mg/ml. The number of resolved peaks by either automated or manual peak detection was assigned as a measure of separation performance. UV detection was performed at a wavelength of 215 nm. The eluents were A = 0.1% trifluoroacetic acid (TFA) in water containing 5 % acetonitrile and B = 0.1% TFA in acetonitrile containing 10 % water.

### 5.8.1 Comparison of MICRA ODS I and Chromolith™ columns

The performance of MICRA ODS I (30 mm x 3.0 mm I.D) and Chromolith™ columns (25 mm x 4.6 mm I.D.) were investigated. The flow rate was 1 ml/min for the Chromolith™ and 0.5 ml/min for the MICRA ODS I column. The gradient ran from 10 % B to 40 % B in 10 min before coming back to 10 % B in 12 min.

An overlay of the two chromatograms and a comparison of the number of resolved peaks is shown in Figure 5.42.

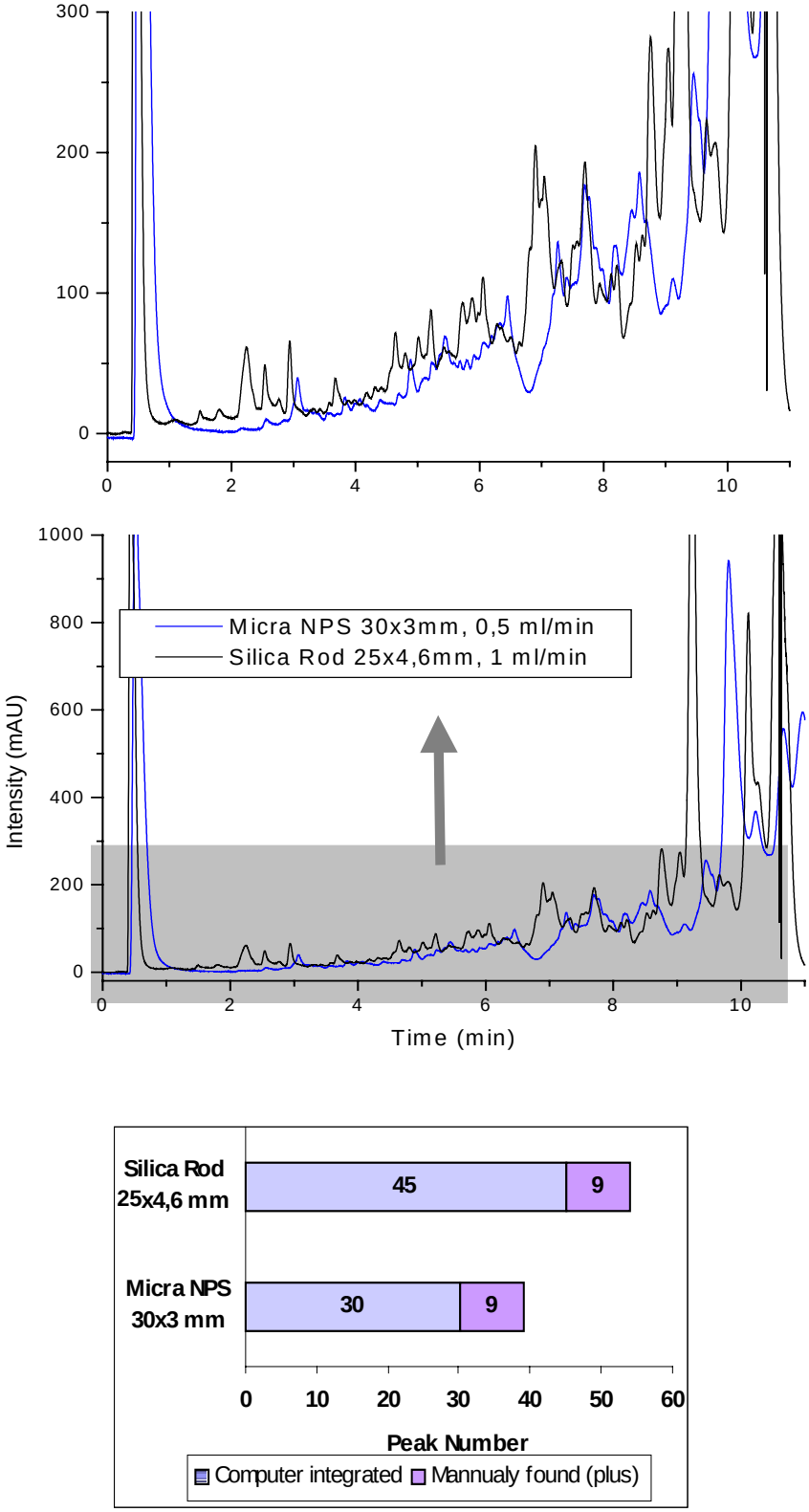


Figure 5.42 Comparison of Chromolith™ and MICRA ODS I columns each of approximately 30 mm length for the separation of a human hemofiltrate sample. The column performance was determined by measuring the number of resolved peaks

It is obvious, that the Chromolith™ columns resolved a higher number of compounds at a low column back pressure, thus showing higher efficiencies and peak capacities at the same column length. Additionally, the number of theoretical plates can be further increased by increasing the column length. Due to pressure restrictions the use of longer columns is only possible for the monolithic type.

### 5.8.2 Comparison of different column length using Chromolith™ columns

When the flow rate is reduced to a sufficiently small value, and the gradient time is optimised, the best strategy is to increase column length for further increase in the number of theoretical plates N and resolution. Chromolith™ columns of 25 mm x 4.6 mm I.D., 50 mm x 4.6 mm I.D., 100 mm x 4.6 mm I.D. were tested at a flow rate of 1 ml/min. The gradient ran from 10 % B to 40 % B in 10 min before coming back to 10 % B in 12 min. An overlay of the three chromatograms and a comparison of the number of detected peaks is shown in Figure 5.43.

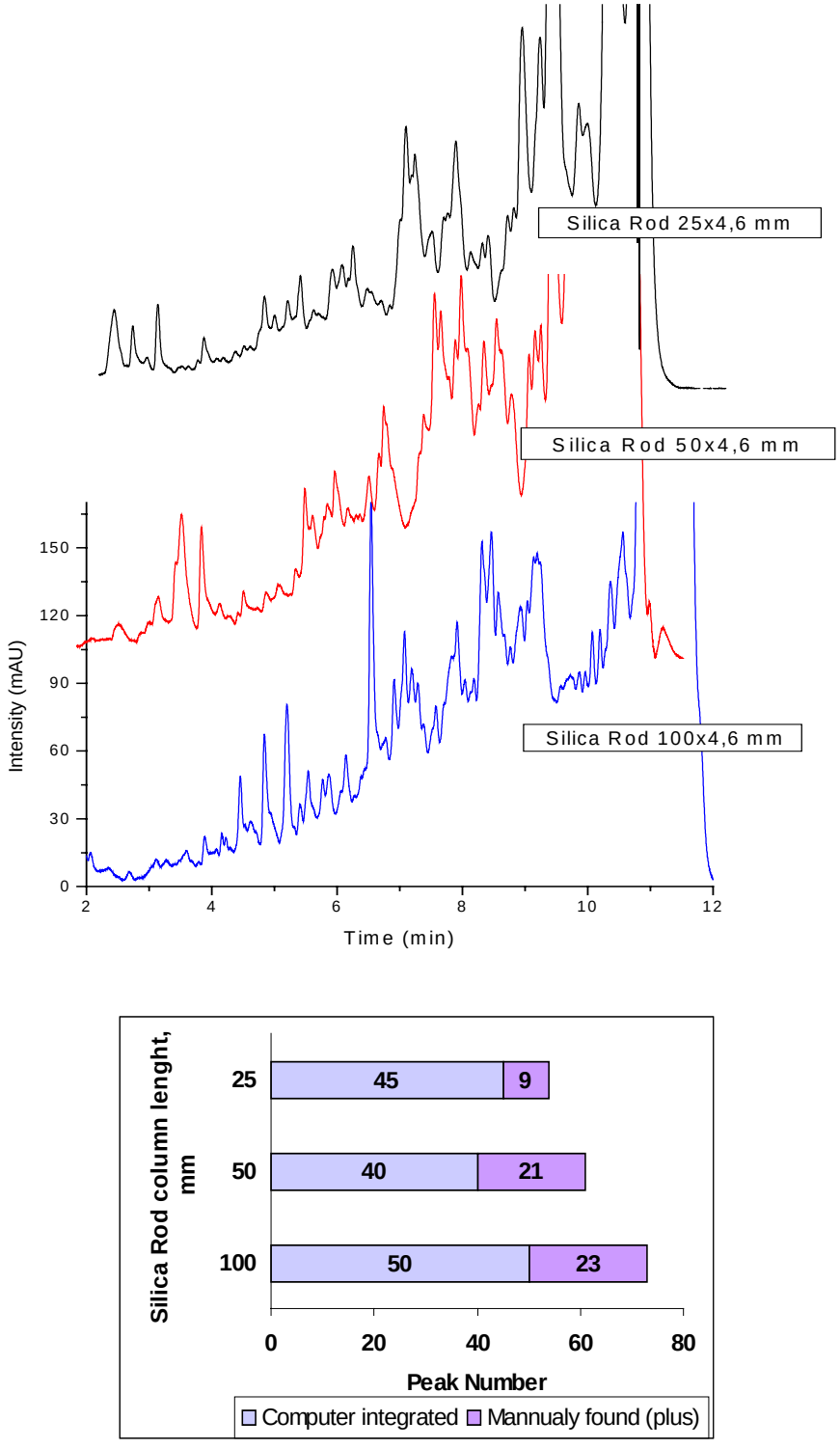


Figure 5.43 Comparison of Chromolith$^{TM}$ columns at different column lengths

It is evident that the peak capacity and the chromatographic resolution increased by using longer columns. These experimental data were expected by the theory discussed in Chapter 4.6.3.3, where the resolution increases with the square root of the number of

theoretical plates, which is proportional to column length. The use of long monolithic columns is generally not restricted by the instrumental set-up.

### 5.8.3 Influence of the gradient time for Chromolith™ columns

The influence of the gradient time was investigated using the 100 mm x 4.6 mm I.D. column at a flow rate of 1 ml/min. A linear gradient from 0 % to 40 % B was used varying the gradient times. Figure 5.44 shows a comparison of the number of resolved peaks for the crude hemofiltrate sample.

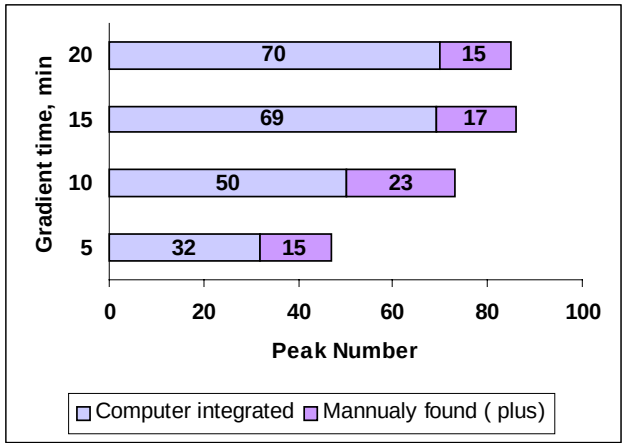


Figure 5.44 Influence of the gradient time on the number of resolved peaks

Figure 5.44 demonstrates an increase in the peak capacity approximated by the number of resolved peaks by using longer gradient times until reaching a maximum, which is according to theory. Very long gradient times lead to band broadening due to longitudinal diffusion. The ideal gradient time for the specific separation problem was investigated to be approximately 15 min.

### 5.8.4 Optimisation of the flow-rate for Chromolith™ columns

The published H(u)-curve for Chromolith™ columns determined by injecting *e.g.* toluene in an isocratic mode indicates a minimum plate height at a flow rate of approximately 1.5 ml/min but a very shallow slope towards higher flow rates.

This is confirmed by experiments at a constant gradient time of 12 min running a linear gradient from 0 % to 40 % B at different flow rates varying between 0.5 ml/min and 3.0 ml/min. As indicated in Figure 5.45, the number of resolved peaks was almost constant between a flow rate of 1 ml/min and 3 ml/min.

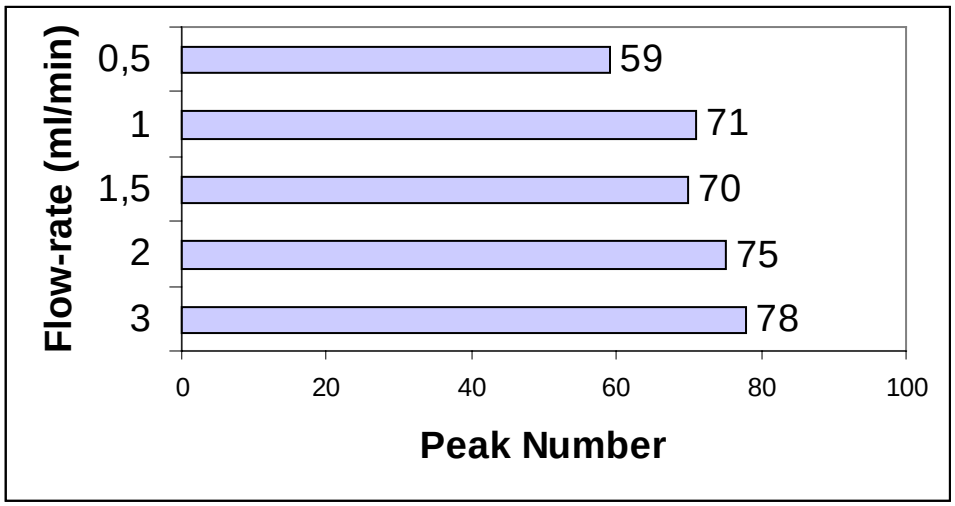


Figure 5.45 Influence of column flow rate at constant gradient time on the number of resolved peaks using crude human hemofiltrate as sample

The experimental data demonstrates a rather constant number of resolved peaks. It has to be mentioned that the chromatograms at a higher flow rate provided shorter retention times, thus shorter chromatograms. In order to maintain the retention coefficients $\bar{k}$ constant, the gradient volume $t_g F$ has to be maintained constant.

### 5.8.5 Influence of gradient time for 14 mm MICRA ODS I columns

The influence of gradient time on the number of resolved peaks for the MICRA ODS I column was investigated at a constant flow rate of 1 ml/min, thus the gradient volume $V_G$ was not maintained constant. A linear gradient from 0 % to 40 % B was applied varying from 5 min to 20 min. Figure 5.46 displays two chromatograms, the first using a gradient time of 5 min and the second applying a gradient time of 20 min. The comparison of the number of resolved peaks is also shown in Figure 5.46. An additional experiment was used for the evaluation of the optimum flow rate, the gradient time was

constant at 10 min and the flow rate varied between 0.5 ml/min and 3.0 ml/min these data are also displayed in Figure 5.46.

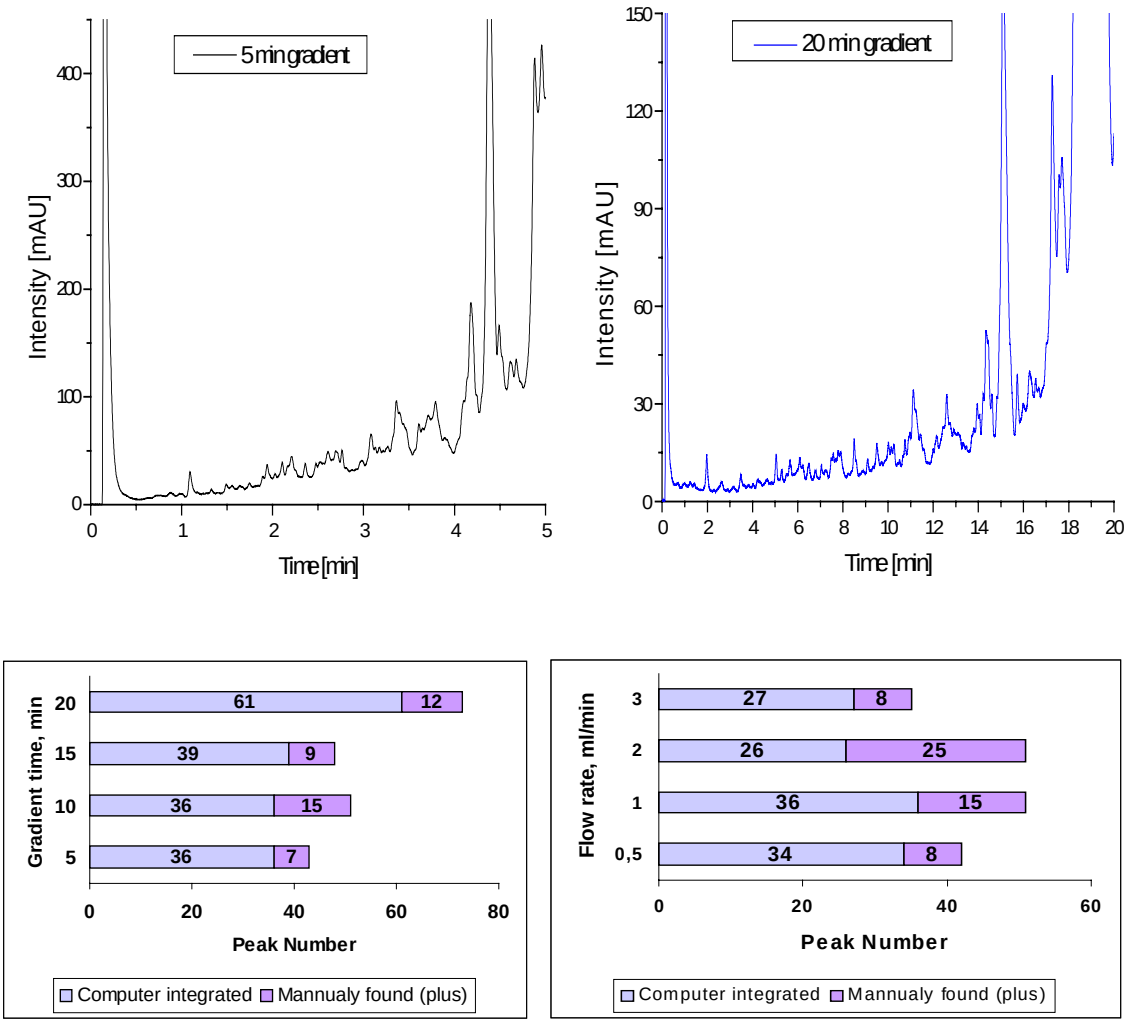


Figure 5.46 Comparison of different gradient times and flow rates using the 14 mm MICRA ODS I column

The data clearly confirm the improvement in column performance at shallow gradients and an optimum flow rate between 1 ml/min and 2 ml/min for the 14 mm MICRA ODS I column. The experimental data are predicted by the theoretical considerations already discussed in Chapter 4.6.3.3.

### 5.8.6 Comparison of different column types for human hemofiltrate separation

MICRA ODS I columns (30 mm x 3.0 mm I.D), TSK Super ODS (100 mm x 4.6 mm I.D.), Zorbax SB-C 18 (150 mm x 2.1 mm I.D.) and Chromolith™ (100 mm x 4.6 mm I.D.) were tested with regard to highest resolution in terms of number of resolved peaks applying the crude human hemofiltrate sample. The flow rate for the MICRA and Zorbax column was 0.5 ml/min and 1.0 ml/min for the Chromolith™ and the TSK Super ODS column. A linear gradient from 0 % to 40 % B within 12 min was applied. The number of resolved peaks for the different columns is displayed in Figure 5.47.

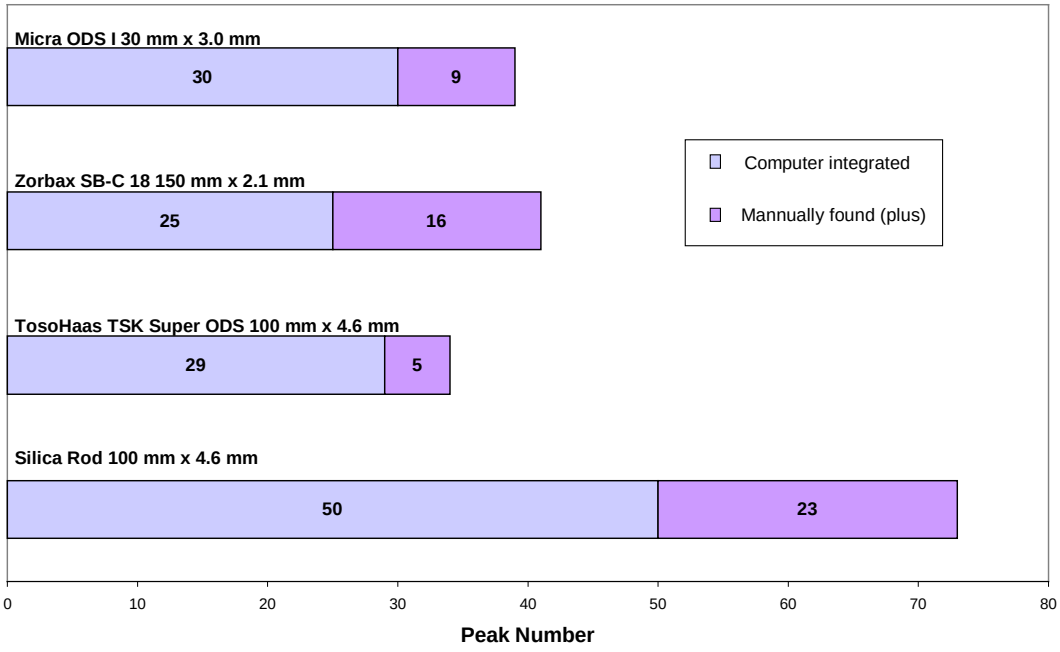


Figure 5.47 Comparison of different column types for the separation of human hemofiltrate

The data clearly demonstrates the superior separation power of the Chromolith™ column under the conditions applied.

## 5.9 Attachment to the experimental part

All buffers (Merck Darmstadt, Germany) and TFA (Fluka Chemika, Buchs, Switzerland) were of analytical grade while eluents were of HPLC gradient grade (Merck Darmstadt, Germany). Pure water was produced using a Milli-Q device (Millipore Bedford, MA, USA). All separations were performed at room temperature. The standard proteins were all purchased from Sigma (Deisenhofen, Germany).

# 6 Conclusions and perspectives

Reversed-phase HPLC is a favourable technique for resolving low molecular weight proteins and peptides. The chromatographic resolution and sensitivity are inversely proportional to the molecular weight of the protein while, for a gel, resolution and sensitivity are proportional to the molecular weight of the protein. Ion exchange and reversed-phase chromatography were chosen as orthogonal separation modes, while size-exclusion chromatography was integrated in the sample fractionation step using the RAM columns.

The unrivalled separation power of the latest 2D-HPLC separation platform for the specific molecular weight range was demonstrated with complex samples of human hemofiltrate and human fetal fibroblast cell-line. The total analysis time of less than two hours and fully automated performance are additional advantages to the excellent separation power.

More than 60 peaks were resolved in some of the 24 RP-chromatograms, clearly demonstrating the resolving power for small proteins and peptides. However, despite a total number of 1000 resolved peaks in the 2D-system, it does not necessarily signify that 1000 different components are resolved, as would be expected in a single mode run. One peak of a single component can appear in two or more consecutive chromatograms due to partial separation in the ion exchanger mode or from splitting a first-dimension peak into two adjacent fractions. The comparison of consecutive RP-chromatograms in a three dimensional display proved the orthogonal separation power of the system.

For most of the chromatographic peaks that were analysed by MALDI-TOF-MS only one mass was visible, indicating the high resolving power of the 2D-HPLC system. Some collected peaks contained up to three different components, *i.e.* mass spectrometry provides a third dimension to the system. Mass mapping of the crude hemofiltrate sample and the low molecular weight fraction after the RAM column demonstrated the need for the high resolving separation platform. Despite of the unrivalled mass accuracy of the MALDI-TOF technique, the number of compounds

which can be determined in parallel is limited. The repeatability of different ion exchange / reversed-phase systems was investigated by assessing the relative standard deviations of the retention time, peak height and peak area. The RSD of the retention times was less than 0.5 % on average. The peak areas and peak heights were determined by employing automatic integration; the RSD values ranged between 5-25 % with a few exceptions. Hence, the obtained RSD values were better than or in the same range as the repeatability of 2D-gel electrophoresis. The limit of detection was determined without the sample preparation step using standard proteins. The on-line column coupling approach, which automatically desalts the samples, easily allows the detection of proteins and peptides in the deep ultraviolet region at 215 nm, providing a highly sensitive absorption of peptide bonds. The limit of detection (*e.g.* 50 ng for ovalbumin) is in the same order of magnitude as the sensitivity of silver stains.

Coupling a size-selective fractionation step on-line with a continuous 2D-HPLC system is a new straightforward procedure. RAM columns are ideally suited for sample preparation of small sized biopolymers since they enable one to boost the sensitivity for low abundant sample components by loading high amounts of sample and allow one to exclude the higher molecular weight fraction. They allow the direct and repetitive injection of untreated biofluids.

Even though the human hemofiltrate had been filtered through a 30 kDa membrane during the dialysis of patients suffering from chronic renal disease, the major component was still human serum albumin with a molecular weight of 66 kDa.

By the use of ultrafiltration (10 kDa membrane), human serum albumin was almost completely eliminated, while proteins and peptides below approximately 30 kDa were able to migrate through the membrane. All RAM columns tested, also showed an enrichment of lower molecular mass components and a reduction in the high molecular mass fraction of the sample. Although human albumin was not completely eliminated the general applicability for size selective fractionation and enrichment was demonstrated. Quantification of the non-specific protein binding on the RAM columns showed a dependency on the amount of loaded protein most probably due to protein binding sites on the outside surface.

The RAM column was eluted in a backflush-mode, in-series with the analytical ion exchange column which is susceptible to band broadening. Comparison to the direct injection onto the cation exchange column proved that band broadening was negligible and alternative approaches for sample transfer like post column dilution, proved to be not realisable.

Even though ion exchange chromatography does not provide the highest resolution power, it gives the best possible orthogonality to the reversed-phase separation. Cation exchange chromatography as the first dimension has significant advantages, especially when silica based stationary phases are used. In order to achieve positively charged solutes in an unknown mixture with randomly differing pI-values, the pH-value must be set to a very acidic value (*e.g.* pH = 2). This pH-value is favourable for silica based support which is stable up to a maximum pH of 8. For achieving a complete negatively charged sample, the pH-value has to be set to a high value (*e.g.* pH = 11) whereby the stationary phase has no long term stability. Furthermore, proteins are generally more stable at acidic than basic environments. The use of anion exchange chromatography is still useful when focusing on a specific part of the pI-range. The short elution times in the RP mode will probably cause less denaturation of the proteins compared to 2D-gel electrophoresis or SDS-page. This offers the chance to run bio-assays to screen the fractions.

Non-porous resins were chosen as packing material for quantitative recoveries without adding an organic modifier, which is a prerequisite for enrichment of fractions on a reversed-phase column. High loading capacities, in the milligram range for both ion exchange columns, are favourable for their use in the first dimension. N-octadecyl bonded non-porous silica particles with an average diameter of 1.5 µm proved to have the required characteristics for the second dimension, due to their high mechanical stability, fast mass transfer kinetics due to a lack of pore diffusion and high recoveries. Short columns packed with these particles allow short analysis and reconditioning times at peak capacities of approximately 250-300. Monolithic silica based columns (Chromolith$^{TM}$) showed similar or even better performance in single column mode tests and there are no restrictions in column length due to the low pressure drop. The four MICRA ODS I RP columns used alternatively in the second dimension of the latest

system set-up showed an almost identical resolution pattern with reproducible retention data. The valve positions and the consecutive column usage were identical from run to run. This enabled the direct comparison and correlation of consecutive chromatographic runs despite slight variations in the performance of the four columns. The columns were used for more than 1500 single runs over two years showing high robustness combined with a long lifetime. The use of non-porous MICRA ODS I columns especially designed for high-speed HPLC still required shallow gradients and, thus, long analysis times. The extension of the gradient time to approximately 8 min led to a large increase in the number of resolved peaks for complex protein and peptide mixtures as compared to lower gradient times.

The basic idea of an on-line comprehensive 2D-HPLC system is the use of a slow separation in the first dimension followed by a fast separation in the second dimension. In order to match the requirements for high resolution in the second dimension without reducing the sampling rate or slowing down the first dimension, at least two second dimension columns need to be eluted in parallel. The second criterion for economising analysis time and achieving reproducible results is to allow sufficient time for column regeneration between the gradient elutions. This can be done by regenerating an additional column in parallel to the elutions in the second dimension. The latest set-up using four parallel columns in the second dimension satisfies the requirements with respect to speed, resolution, reproducibility and recovery. On-column-focusing for fraction transfer to the second dimension has considerable advantages. Enrichment of the fractions directly on top of the column does not require any sample storage, hence there is no vial contamination or sample loss due to other sample handling procedures, such as fraction collection and reinjection. It was proved that all polypeptides were strongly adsorbed to the microparticulate reversed-phase packing materials when applied to strictly aqueous eluents, thus no analytes were lost. The procedure avoids sample dilutions and automatically desalts the analytes, thus preventing eluent incompatibilities.

Miniaturisation is an option for a further increase in sensitivity and possibly in resolution and will be necessary in cases where there is only a limited amount of sample available. The new method providing high-resolution power within the short analysis

time of less than two hours with a single injection onto the RAM column can easily be used in high-throughput applications. Although not used in this case, sequencing of the resolved peptides by tandem mass spectrometry (*e.g.* static nano-ESI) may be an additional option to ascertain identity by database searching. Direct coupling to ESI-MS is straightforward since the analytes stay in a desalted liquid phase all the time. One further option would be to couple the second dimension to a piezoelectric flow-through microdispenser for on-line array fractionation onto targets for MALDI-TOF MS [104].

While 2D-gel electrophoresis provides extremely high resolution separations for proteins, this technique has also intrinsic properties that can limit and complicate the resolution and detection of small and low abundant proteins. For these reasons, both academic and commercial interests are currently developing alternatives or complementary methods to 2D-gels such as 2D-HPLC MS/MS. The commercialisation of an automated miniaturised multidimensional liquid chromatography system interfaced to mass spectrometric detection have a great potential to provide a viable alternative to traditional 2D-gels in proteomics.

The separation platform described in this thesis already proved to be an excellent complementary method to 2D-gel electrophoresis for mapping peptides and small proteins.

# 7 List of figures

# 8 List of tables

# 9 Literature


1 Hochstrasser, D.F. in Proteome research (Eds: Wilkins, M.R., Williams, K.L., Appel, R.D., Hochstrasser, D.F.), Springer, Berlin 1997

2 Wilkins, M.R., Sanchez, J.-C., Gooley, A.A., Appel, R.D., Humphery-Smith, I., Hochstrasser, D.F., Williams, K.L., Biotechnol. Genet. Eng. Rev., 1996, 13, 19-50

3 Wasinger, V.C., Cordwell, S.J., Cerpa-Poljak, A., Electrophoresis, 1995, 16, 1090-1094

4 Anderson, L., Seilhamer, J. Electrophoresis 1997, 18, 533-537

5 Quadroni, M., James, P., Electrophoresis, 1999, 20, 664-667

6 Lottspeich, F., Angew. Chem., Int. Ed. Engl. 1999, 38, 2476.

7 Abbott, A., Nature 2001, 409, 747

8 Sperling, K., Electrophoresis 2001, 22, 2835-2837

9 O'Farrell, P.H., J. Biol. Chem. 1975, 250, 4007.

10 Görg, A., Postel, W., Gunther, S., Electrophoresis, 1988, 9, 531

11 Tomer, K.B., Chem. Rev. 2001, 101, 297-238

12 Beckey, H.D., Int. J. Mass Spectrom. Ion Phys. 1969, 2, 500

13 Morris, H.R., Panico, M., Barber, M., Bordoli, R.S., Sedgwick and Tyler, A., Biochem. Biophys. Res. Commun. 1981, 101, 623

14 Fenn, J.B., Mann, M., Meng, C.K., Wong, S.F., Whitehouse, C.M., Science 1989, 246, 64-71

15 Karras, M., Bachmann, D., Bahr, U., Hillemkamp, F., Int. J. Mass Spectrom. Ion Proc. 1987, 78, 53-68

16 Tanaka, K., Waki, H., Ido, Y., Akita, S., Yoshida, Y., Yoshida, T., Rapid Commun. Mass Spec. 1988, 2, 151-153

17 Johnson, K., Presentation on the IBC conference on Technical Advances and Applications of Proteomics, London, 1998

18 Persidis, A. Nature Biotechnology 1998, 16, 981

19 Figeys, D., Pinto, D., Electrophoresis 2001, 22, 208-216

20 Schena, M., Shalon, D., Davis, R.W., Brown, P.O., Science 1995, 270, 467-470

21 Tswett, M.S., Ber. Dtsch. Bot. Ges., 1906, 24, 316

22 Martin, A.J.P., Synge, R.L.M., Biochem J. 1941, 35, 1358

23 Hanson, M., Unger, K.K., LC˙GC Int. 1996, 9, 650

24 Snyder, L., Anal. Chem., 2000, 72, 412

25 Janzen, R., Unger, K.K., Giesche, H. Kinkel, N., Hearn, M.T.W., J. Chromatogr., 1987, 397, 81

26 Karlsson, E., Ryden, L., in Protein Purification Principles, High Resolution Methods and Applications, Janson, J.-C, Ryden, L.G. (Eds.), VCH, New York 1989

27 Hearn, M.T.W., in Protein Purification Principles, High Resolution Methods and Applications, Janson, J.-C, Ryden, L.G. (Eds.), VCH, New York 1989

28 Geng, X. and Regnier, F.E., J. Chromatogr., 1984, 296, 15-30

29 Snyder, L.R., in High Performance Liquid Chromatography, Hórvath, C.G. (Ed.), Acadenic Press, New York, 1980 1980, Vol 1, 208

30 van Deemter, J.J., Zuiderweg, F.J., Klinkenberg, A., Chem. Eng. Sci., 1956, 5, 271

31 Kennedy, G.J., Knox, J.H., J. Chromatogr. Sci., 1972, 10, 549

32 Stadalius, M.A.,Gold, H.S., Snyder, L.R., J.Chromatogr., 1984, 296, 31-59

33 Snyder, L.R., Stadalius, M.A., Quarry, M.A., Anal. Chem., 1983, 55, 14, 1412-1430

34 Stadalius, M.A., Quarry, M.A., Snyder, L.R., J.Chromatogr., 1985, 327, 93-113

35 Vissers, J.P.C. J. Chromatogr. 1999, 856 117

36 Golay, M.J.E., in Desty, D.H. (Ed.) Gas Chromatography, Butterworth, London, 1958, page 36

37 Hórvath, C.G., Preiss, B.A. and Lipsky, S.R., Anal.Chem, 1967, 39, 1422

38 Chervet, J.P., Ursem, M., Salzmann, J.P., Anal. Chem, 1996, 68, 1507

39 Vissers, J.P.C., J. Chromatogr., 1999, 856, 117

40 Cabera, K., Lubda, D., Eggenweiler, H.-M., Minakuchi, H., Nakanishi, K., J. High Resol. Chromatogr. 2000, 23, 93-99

41 Chervet, J.P., Ursem, M., Salzmann, J.P., Vannoort, R.W., J. High Resol. Chromatogr. 1989, 12, 278

42 Stöber, W., Fink, E., Bohn, E., J. Colloid Interf. Sci., 1968, 26, 62-69

43 Issaeva, T.; Kourganov, A.; Unger, K.K., J. Chromatogr. A, 1999, 846, 13.

44 Lamotte, S., PhD thesis, University of the Saarland, Saarbrücken 1998

45 Poppe, H., J. Chromatogr. A, 1997, 778, 3-21

46 MacNair, J.E., Patel, K.D. and Jorgenson, J.W., Anal.Chem 1999, 71, 700-708

47 Dittmann, M.M., Rozing, G.P., J. Chromatogr. A, 1996, 744, 63-74

48 Tanaka, N., Nagayama, H., Kobayashi, H., Ikegami, T., Hosoya, K., Ishizuka, N., Minakuchi, H., Nakanishi, K., Cabrera, K., Lubda, D., J. High Resol. Chromatogr. 2000, 23, (1) 111-116

49 Minakuchi, H., Nakanishi, K., Soga, N., Ishizuka, N., Tanaka, N., Anal.Chem., 1996, 68, 3498-3501

50 Ericson, C., Liao, J.-L., Nakazato, K., Hjertén, S., J. Chromatogr. A, 1997, 767, 33-41

51 Majors, R.E., LC-GC Intl. (1991) 4, 10-14

52 Kallweit, U, Börnsen, K.O., Kresbach, G.M.K. and Widmer, H.M. Rapid Commun. Mass Spectrom., 1996, 10, 845

53 Boos, K.-S. and Rudolphi, A. LC-GC 1997, 15, 814-823

54 van der Hoeven, R.A.M., Hofte, A.J.P., Frenay, M., Irth, H., Tjaden, U.R., van der Greef, J., Rudolfi, A., Boos, K.-S., Marko-Varga, G., Edholm, L.-E. J. Chromatogr. A, 1997, 762, 193-200

55 Hagestam, I.H., Pinkerton, T.C., Anal. Chem., 1985, 57, 1757-1763

56 Cook, S.E. and Pinkerton, T.C., 1986, 368, 223

57 Pinkerton, T.C. and Koeplinger, K.A. Anal. Chem. 1990, 62, 2121

58 Desilets, C.P., Rounds, M.A. and Regnier, F.E. J. Chromatogr. 1991, 544, 25

59 Boos, K.-S.; Grimm, C.-H., TrAC, 1999, 18.175-180

60 Boos, K.-S. and Rudolphi, A. LC-GC 1997, 15 602-611

61 Racaityte, K., Lutz, E.S.M.; Unger, K.K.; Lubda, D.; Boos, K.-S., J. Chromatogr. A 2000, 890, 135f.

62 Grimm, C.H.; Boos, K.-S.; Apel, C.; Unger, K.K.; Önnerfjord, P.; Heintz, L.; Edholm, L.E.; Marko-Varga, G., Chromatographia 2000, 52, 703

63 Cortes, H.J., J. Chromatogr., 1992, 626, 3-23

64 Davis, J.M., Giddings, J. C. Anal. Chem. 1983, 55, 418

65 Giddings J.C. in Cortes, H.J. (Ed.), Multidimensional Chromatography, Marcel Dekker, New York, 1990

66 Giddings, J.C., J. Chromatogr. A, 1995, 703, 3-15

67 Murphy, R. E.; Schure, M. R.; Foley, J. P. Anal. Chem., 1998, 70, 1585-1594

68 Phillips, J.B. and Beens, J., J. Chromatogr. A, 1999, 856, 331

69 Majors, R., J. Chromatogr. Sci., 19980, 18, 571

70 Lemmo, A.V., Jorgenson, J.W., Anal. Chem., 1993, 70, 1576

71 Schure, M.R., Anal. Chem., 1999, 62, 161

72 Bushey, M. M.; Jorgenson, J. W. Anal. Chem. 1990, 62, 161

73 Opiteck, G.J.; Jorgenson, J. W.; Anderegg, R. J. Anal. Chem. 1997, 69, 2283-2291

74 Heine, G., Raida, M.; Forssmann, W. G. J. Chromatogr. A 1997, 776, 117

75 Schrader, M.; Jürgens, M.; Hess, R.; Schulz-Knappe, P.; Raida, M.; Forssmann, W. G. J. Chromatogr. A 1997, 776, 139

76 Richter, R.; Schulz-Knappe, P.; Schrader, M.; Ständker, L.; Jürgens, M.; Tammen, H.; Forssmann, W. G. J. Chromatogr. B, 1999, 726, 25-35

77 Udiavar, S; Apffel, A.; Chakel, J., Hancock, W.S.; Pungor, E., Jr. Anal. Chem., 1998, 70, 3572-3578.

78 Wall, D. B.; Kachman, M. T.; Gong, S.; Hinderer, R.; Parus, S.; Miek, D. E.; Hanash, S. M. and Lubman, D. M. Anal. Chem., 2000, 72, 1099

79 Vissers, J. P. C., Van Soest, R. E. J.; Chervet, J.-P.; Cramers, C. A. J. Microcolumn Separations, 1999, 11 (4), 277-286.

80 Link, J.; Eng, J.; Schielz, D. M.; Charmack, E.; Mize, G. J.; Morris, D. R.; Garvik, B. M.;Yates, J. R. Nat. Biotechnol., 1999, 17, 676

81 Davis, M. T.; Beierle, J.; Bures, E. T.; McGinley, M.D.; Mort, J.; Robinson, J. H.; Spahr, C. S.; Yu, W.; Luethy, R.; Patterson, S. D. J. Chromatogr. B, 2001, 752, 281-291

82 Holland, L.A. and Jorgenson, J.W., Anal.Chem., 1995, 67, 3275

83 Opiteck, G.J.; Jorgenson, J. W.; Anderegg, R. J. Anal. Chem., 1997, 69, 1518-1524

84 Köhne, A.P., Welsch, T., J. Chromatogr. A, 1999, 845, 463-469

85 Opiteck, G.J.; Jorgenson, J.W.; Anderegg, R.J. Anal. Chem., 1997, 69, 2283-2291

86 Wagner, K., Racaityte, K., Unger, K.K.; Miliotis, T., Edholm, L. E., Bischoff, R., Marko-Varga, G., J. Chromatogr., A, 2000, 893, 293.

87 Gygi, S.P.; Corthals, G.L.; Zhang, Y.; Rochon, Y.; Aebersold R. Proc. Natl. Acad. Sci., 2000, 97, 9390

88 Mann, M., Højrup, P. and Roepsdorff, P., Biol. Mass Spectrom., 1993, 22, 338

89 Yates, J.R., J. Mass Spectrom., 1998, 33, 1

90 McCormack, A.L., Schieltz, D.M., Goode, B., Yang, S., Barnes, G., Drubin, D. and Yates, J.R. Anal. Chem., 1997, 69, 767

91 de Frutos, M. and Regnier, F, Anal. Chem., 1993, 65, 17

92 Nadler, T.K., Palival, S.K. and Regnier, F.E., J. Chromatogr. A, 1994, 676, 331

93 Regnier, F.; Huang, G., J. Chrom. A, 1996, 750, 3

94 Lundell, N. and Markides, K., Chromatographia, 1992, 34, 369-375

95 Wall, D.B.; Kachman, M.T.; Gong, S.; Hinderer, R.; Parus, S.; Miek, D.E.; Hanash, S. M. and Lubman, D.M., Anal. Chem., 2000, 72, 1099

96 Opiteck, G.J., Ramirez, S.M., Jorgenson, J.W. and Moseley, A.M., Analytical Biochemistry, 1998, 258, 349-361

97 Opiteck, G.J., Jorgenson, J.W., Moseley, A.M., Anderegg, R.J., J. Microcolumn Separations, 1998, 10(4), 365-375

98 Lahm, H.W. and Langen, Electrophoresis, 2000, 21, 2105

99 Gygi, S. P.; Rist, B.,Greber, S.A., Turecek, F., Gelb, M.H. and Aebersold R., Nature Biotechnology, 1999, 17, 994-999

100 Geng, M., Ji, J. and Regnier, F.E., J. Chromatogr. A, 2000, 870, 295

101 Wagner, K., Diploma thesis, J. Gutenberg University Mainz, Germany, 1998

102 Huber, M. PhD thesis, J. Gutenberg University Mainz, Germany, in preparation

103 Önnerfjord, P.; Ekström, S.; Bergquist, J.; Nilsson, J.; Laurell, T.; Marko-Varga, G. Rapid Commun. Mass Spectrom. 1999, 13, 315

104 Miliotis, T., Kjellström, S., Önnerfjord, P., Nilsson, J., Laurell, T., Edholm, L.-E., Marko-Varga, G., J. Chromatogr. A, 2000, 886, 99-110